Life Cycle Design and Assessment of an Algal Biofuel that is Sustainable, Scalable, and Salable

by

Nolan D. Orfield

A dissertation submitted in partial fulfillment
of the requirements for the degree of
Doctor of Philosophy
(Natural Resources and Environment)
in the University of Michigan
2013

Doctoral Committee:

Professor Gregory A. Keoleian, Chair
Professor Nancy G. Love
Associate Professor Shelie A. Miller
Research Scientist Jarod C. Kelly

For Cara & Calvin

ACKNOWLEDGEMENTS

I would like to thank Cara for her loving and unflinching support over the past several years. Her gracious accommodation of my academic pursuits despite her own graduate school, full-time work, and motherhood underscore how lucky I am to be her husband.

I would like to thank my committee chair, Greg Keoleian, for creating this research opportunity, providing me with the tools to complete the tasks, and keeping me focused throughout the entire journey. His conscientious but firm mentorship kept me on track during periods when I became distracted, and for that I am grateful. I would like to thank Nancy Love for helping to extend my mechanical engineering training into the realm of environmental engineering as required to conduct this research. Thank you to Shelie Miller for making the subject of bioenergy exciting and for teaching me how to approach design trade-offs in environmental systems analyses. Also, I would like to thank Jarod Kelly for demonstrating that the utility of design optimization lies in how one defines the research question.

This dissertation was made possible through financial support provide by the National Science Foundation, Emerging Frontiers in Research and Innovation (EFRI), Hydrocarbons from Biomass (HyBi) program (Grant No. 0937992). I would like to thank the members of the HyBi team (Phillip Savage, PI) for your direct contributions to my research and for tolerating my lack of Chemical Engineering knowledge these past four years. Thank you to Bobby Levine for keeping me in step with private sector practices

and for helping me devise appropriate research questions. Also, thank you to Peter Valdez and Mike Nelson for their excellent laboratory research which provided the foundation for my life cycle modeling.

Thank you to Helaine Hunscher for being a thoughtful officemate and for keeping me paid and insured during my time at SNRE, and to the rest of the CSS for providing an engaging environment in which to work. In particular I would like to thank Andrew Fang for his modeling contributions.

Lastly I would like to thank the rest of my family for their unwavering encouragement, including Calvin for being a receptive audience during my dissertation defense preparation.

TABLE OF CONTENTS

LIST OF FIGURES

LIST OF TABLES

LIST OF APPENDICES

LIST OF ACRONYMS

ANL	Argonne National Laboratory
BOD	Biological Oxygen Demand
CARB	California Air Resources Board
CHG	Catalytic Hydrothermal Gasification
EISA	Energy Independence and Security Act
EPA	Environmental Protection Agency
FAPRI-CARD	Food and Agricultural Policy and Research Institute in the Center for Agricultural and Rural Development
FER	Fossil Energy Ratio
FWC	Flue Gas and Wastewater Co-Utilization
GHG	Greenhouse Gas
GIS	Geographic Information Sciences
GREET	Greenhouse Gases, Regulated Emissions, and Energy Use in Transportation
GTAP	Global Trade Analysis Project
GWP	Global Warming Potential
HRP	High Rate Pond
HRT	Hydraulic Residence Time
HTL	Hydrothermal Liquefaction
ILUC	Indirect Land Use Change
LCA	Life Cycle Assessment
LCD	Life Cycle Design
LEA	Lipid Extracted Algae
LUC	Land Use Change
NASS	National Agricultural Statistics Service
NER	Net Energy Ratio
NOAA	National Oceanic and Atmospheric Administration
NREL	National Renewable Energy Laboratory
TFF	Tangential Flow Filtration
TKN	Total Kjeldahl Nitrogen
US	United States
WSI	Water Stress Index

ABSTRACT

Algae are an appealing source of bioenergy due to their high yields relative to terrestrial energy crops. The high cost of production, however, has prohibited commercialization despite significant investment by the private sector. Three novel strategies and technologies encompassing algae production and conversion have been examined in terms of their life cycle environmental impacts and potential to achieve large scale production.

Coupling algae cultivation ponds with flue gas emissions from power utilities to provide carbon dioxide and municipal wastewater to provide nutrients not only reduces the upstream impacts and costs associated with providing inputs, but also provides a credit for wastewater treatment. A geospatial economic overlay analysis was conducted to evaluate the abundance and relative location of the input resources of this co-utilization strategy. Results of the analysis highlight the inability to scale beyond 1.7 billion liters annually due primarily to the limited availability of nutrients in wastewater.

Growing heterotrophic algae in fermenters with sugar as the energy and carbon source rather than sunlight and carbon dioxide is an approach being pursued in the private sector. Results of this study indicate that a reduction in the global warming potential and an improvement in the fossil energy ratio for algal biodiesel could be possible for the heterotrophic pathway relative to the phototrophic, but only if fermentation can be performed efficiently. The sugar crops used as feedstocks for

heterotrophic cultivation require more land, however, and introduce concerns about land constraints.

Lastly, a life cycle assessment of an algal biorefinery featuring hydrothermal liquefaction is conducted. Recent experimental work providing insight into the HTL reaction networks is incorporated into an analysis that models the performance of an algal biorefinery. Results demonstrate a design trade-off, as the reaction conditions for minimizing the carbon footprint (0.74 kg CO_2e at 250 °C, 60 minutes) are different than those found for minimizing cost ($\$1.72 \cdot L^{-1}$ at 400 °C, 5 minutes). A novel regrowth pathway featuring utilization of *E. coli* to boost oil yields is also explored. It was found that the pathway could further reduce costs but comes with an increased carbon footprint and reduced net energy ratio.

CHAPTER 1. INTRODUCTION

1.1 Overview

This dissertation explores three key life-cycle design opportunities to address challenges related to the production and conversion of algae into biofuel. The first opportunity relates to utilizing waste materials for input resources, the second includes alternative cultivation strategies that require less sophisticated technology, and the third features a novel biomass conversion strategy that produces more fuel per unit of algal biomass thereby reducing costs.

The United States intends to increase domestic biofuel production in an effort to reduce dependence on imported petroleum and mitigate the impacts of global warming[1]. Since carbon dioxide from the atmosphere is sequestered via photosynthesis during feedstock production, biofuels have the potential to reduce the life-cycle emissions of greenhouse gases (GHGs) and the overall global warming potential (GWP) relative to conventional fossil fuels. However, life-cycle analyses (LCAs) of first-generation biofuels such as corn ethanol and soy biodiesel indicate that these benefits can be greatly reduced by the impacts associated with the production of these energy crops and their conversion into liquid fuels[2–4]. Furthermore, the land required to

produce these crops could displace agricultural operations, negatively impacting the global food market[5].

Algae have been proposed as an alternative bioenergy feedstock because of their high growth rate and aerial productivity[6]. Estimates indicate that transport fuel needs for the United States could be met by algal bio-oil using 1/20th of current agricultural land area, whereas the equivalent yield from corn or soybean would be impossible to achieve due to land area constraints[7]. By growing algae in open ponds, biomass can be produced on marginal, non-arable lands that are not currently used for farming[8]. Studies indicate that producing bio-oil from algae with current technology has a low life cycle net energy ratio (NER), however, and sequesters less net greenhouse gases than biofuels produced with other crops [9–11]. These findings are due partly to the carbon dioxide and fertilizer input requirements.

Coupling algae cultivation ponds with flue gas emissions from power utilities to provide a source of carbon dioxide and municipal wastewater to provide a source of nutrients has been recommended in several studies[12–18]. This flue gas and wastewater co-utilization (FWC) strategy not only reduces the upstream impacts and costs of supplying carbon dioxide and nutrients, but also creates environmental and economic credits by offsetting the aeration and nutrient removal impacts from wastewater treatment. Pilot facilities have demonstrated that algae are capable of growth in systems with concurrent removal of high levels of biological oxygen demand and with reduced aeration energy requirements [19,20]. An analysis by Lundquist et al. (2010)

demonstrates that the economic credit for such a service is also a necessary revenue stream to bring production costs to a reasonable level [21].

Regardless of whether or not FWC is implemented, achieving large-scale production of phototrophic algae has proven difficult due to the high capital and operational costs of open ponds[21–25]. Additionally, the relatively low biomass concentration requires significant energy inputs to circulate the large volumes of water and to concentrate the harvested biomass[26]. These challenges have prompted exploration of an alternative approach to growing algae: heterotrophic cultivation. Unlike phototrophic algae, the metabolism of heterotrophic algae facilitates fast growth in unlit fermenters whereby energy is derived from an organic carbon source rather than sunlight[27]. Mixotrophic species of algae, which can use either sunlight or organic carbon for energy depending on their environment, have also been proposed as an option to be pursued within a hybrid pathway[28–30].

In addition to the need for reducing infrastructure costs, another looming technical hurdle is a means to convert the algal biomass into a usable transport fuel[26,31]. A technology called hydrothermal liquefaction (HTL) could address both of these obstacles by providing a means to convert wet algal biomass to biocrude oil while reducing the amount of pond infrastructure required to produce a given quantity of algal biofuel.

A life cycle assessment (LCA) by Lardon et al. (2009) illustrated that the solvent-based oil extraction technologies used for other energy crops such as soybean cannot be relied upon for algae; the amount of energy required to dry the biomass to levels typical

of terrestrial crops would exceed the energy content in the algal oil[9]. Several studies have examined the viability of "wet" solvent extraction strategies to separate the lipid fraction of the algal biomass as an oil that can be upgraded via transesterification to a biodiesel product[9,32]. This approach still has not been implemented at commercial scale, however, and efficient recovery of the solvent has proven to be a challenge[31]. Another limitation of solvent extraction is that the yield of oil per unit of biomass is limited to the fraction of the biomass that is lipid. Currently the most economical strategy for cultivating phototrophic algae is an open, paddle-wheel mixed pond, and the species grown in these ponds typically have just 10-25% lipid content[33].

By contrast, HTL converts a portion of the carbohydrate and protein fractions of the algal biomass into oil in addition to the lipid fraction[34]. This process works by converting a wet algal slurry under high temperature and pressure into a variety of products including a biocrude oil. In addition to the oil that is formed, HTL produces solids, gas, and soluble products remaining in the water, or the "aqueous phase". Nelson et al. (2013) demonstrated that *E. coli* can be grown on the aqueous phase products from HTL and Valdez et al. (2013) demonstrated recovery of crude bio-oil from *E. coli* biomass via HTL with yields similar to those of algae[35]. Therefore the proposed regrowth pathway could incorporate cultivation of microbial biomass such as *E. coli* to recycle carbon and thereby yield more oil per unit of initial algal biomass.

1.2 Life Cycle Design Framework

LCA has emerged as a critical tool for evaluating a product's environmental impact. By evaluating the inputs and outputs associated with each step of a product's life from acquisition of the material through end-of-life disposal, metrics can be implemented to evaluate its sustainability. Life cycle design (LCD), then, is the process of incorporating these LCA metrics into a framework for developing products that are optimized for objectives that extend beyond traditional metrics to include sustainability[36]. LCD is a complex process requiring systems-wide analysis and, ideally, interdisciplinary collaboration throughout the research and development process.

In practice design iterations generally happen at the product release cycle; an LCA is not performed (if at all) until the product has been released and in use, and results are incorporated into a redesign only when the subsequent product development cycle is initiated. By integrating LCD directly into the product conception stage rather than on the product release cycle time frame, considerable impact can be reduced in the avoidance of initial releases that are poorly optimized, particularly for products with complex environmental implications[37].

Biofuels are sufficiently complex to necessitate engaging in the LCD process early in the design process. The algal biofuel industry is striving to develop a cost-competitive product devoid of the indirect negative impacts associated with first generation biofuels. Preliminary LCAs have yielded widely varied results; the inconsistency in these results has provided a poor platform for decision-makers in both the private and public

sector to decide how and where funding should be allocated and, generally speaking, whether or not the technology is worth pursuing. This variability has emerged due to the huge uncertainties regarding operating assumptions, cultivation and harvesting methods used, processing technologies employed, geographic resource constraints, and the species of algae selected as the biomass feedstock. Even the ideal metabolism of the organism, phototrophic or heterotrophic, has yet to be settled upon. In terms of the design process, then, this indeed represents a scenario with a high number of design degrees of freedom.

The research conducted for this dissertation provided a unique opportunity to work collaboratively with research scientists to both guide experimental work toward development of the optimal process design as well as to produce a well-informed life cycle assessment framework to realistically assess the practicality of algal biofuels.

1.3 Research Objectives

1.3.1 Algal bio-oil production potential through flue gas and wastewater co-utilization

While there is a substantial body of literature exploring methods to improve cultivation and processing such that algal bio-oil production could eventually thrive in a stand-alone facility, no comprehensive assessment has been done to assess the feasibility of large-scale bio-oil production using the FWC approach. This dissertation provides the first national assessment, which requires integration of spatial-temporal climate data with carbon dioxide and wastewater constraints.

This research aims to address the following questions on the topic:

Q1. What quantity of algal biofuel could be produced using FWC in a manner that is cost-competitive with fossil fuel?
Q2. Which resource constraint will become limiting (if any) as production scales?
Q3. Which cost constraints are most significant?
Q4. Where are the best locations for producing algal biofuel using FWC?

1.3.2 Growing algae for biofuel on direct sunlight vs. sugars

This dissertation features a comparative LCA evaluating algal biofuel production pathways featuring photo-, mixo-, and heterotrophic metabolisms. This is the first such analysis of its kind outside of private sector studies which have not been made public. This gap in the literature is noteworthy given that several of the leading private firms in the algae industry, as well as numerous academic groups, are currently pursuing these approaches.

This research aims to address the following questions on the topic:

Q5. How do the life-cycle impacts of algal biodiesel produced heterotrophically compare to a phototrophic pathway featuring algae grown in ponds.
Q6. Could a hybrid approach featuring mixotrophic algae provide relative benefits?
Q7. How do the life cycle impacts of the heterotrophic/hybrid pathways vary depending on the sugar feedstock (i.e. sugar from sugarcane vs. sugar from sugar beet)?

1.3.3 The effect of hydrothermal liquefaction (HTL) reaction conditions and an alternative pathway featuring microbial regrowth on the life cycle and economic performance of an algal biorefinery

Recent research has enabled a more thorough understanding of HTL rooted in experimental results[45]. This dissertation will incorporate the reaction network model developed by Valdez et al. (2013) into an LCA that evaluates the life cycle impacts of an algal biocrude oil from HTL across a range of reaction conditions[46]. Given the

importance of reducing costs to enable commercialization of algal biofuels, this analysis will evaluate an economic metric in addition to the life cycle metrics of net energy ratio (NER) global warming potential (GWP), and occupied land.

In addition to being the first study to analyze the sensitivity of LCA performance to the HTL reaction conditions, this dissertation will examine the viability of a novel pathway for boosting oil yields proposed by Nelson et al. (2013)[35]. The proposed regrowth pathway incorporates cultivation of microbial biomass such as *E. coli* on the aqueous phase products of HTL to recover carbon and thereby boost oil yields.

This research aims to address the following questions on the topic:

Q8. How would varying the reaction conditions affect the system's performance in terms of environmental impacts and economics?
Q9. If a secondary biomass such as *E. Coli* were to be grown on the nutrients remaining in the aqueous phase, how would this affect the system's performance in terms of environmental impacts and economics?

1.4 Organization of Dissertation

In addition to the specific research questions mentioned in the previous section, the overarching theme of the dissertation will focus on life cycle modeling strategies in pursuit of an algal biofuel that is sustainable, scalable, and salable. Simple metrics for these criteria are defined as follows:

Sustainable: NER is greater than 1.0 and GWP is less than half that of conventional fuel.

Scalable: Could theoretically meet the Energy Independence and Security Act (EISA) Renewable Fuel Standards (RFS) , requiring production of advanced biofuels on the order of billions of gallons annually[1].

Salable: Can compete with fossil fuels, so a total cost of less than less than $\$1\cdot^{-L}$.

These metrics will be revisited in the final chapter of the dissertation. To guide research and development toward a biofuel that achieves these objectives, the life cycle design process outlined in this dissertation will begin by analyzing the resource constraints upstream of algae cultivation. The analysis will then incorporate these results into a review of pathways for producing algal biomass. Once these processes have been well characterized a pathway will be selected and adapted into an overarching LCA of a biorefinery featuring HTL. This final analysis includes a more detailed investigation into the sensitivity of results to design variables. A summary of this dissertation structure and general design framework is shown in Figure 1.1.

Chapter 2 addresses questions 1-4 by examining the abundance and location of the two key input resources (flue gas and wastewater) on a broad, national basis. Preliminary techno-economic and energy balance calculations look promising, but the geographic information systems (GIS) economic overlay analysis indicates that resource constraints (nutrients in wastewater, specifically) are significantly limiting so scalability criteria fails. The dissertation moves forward with analysis of an alternative strategy that also boasts the potential to compete with fossil fuel prices.

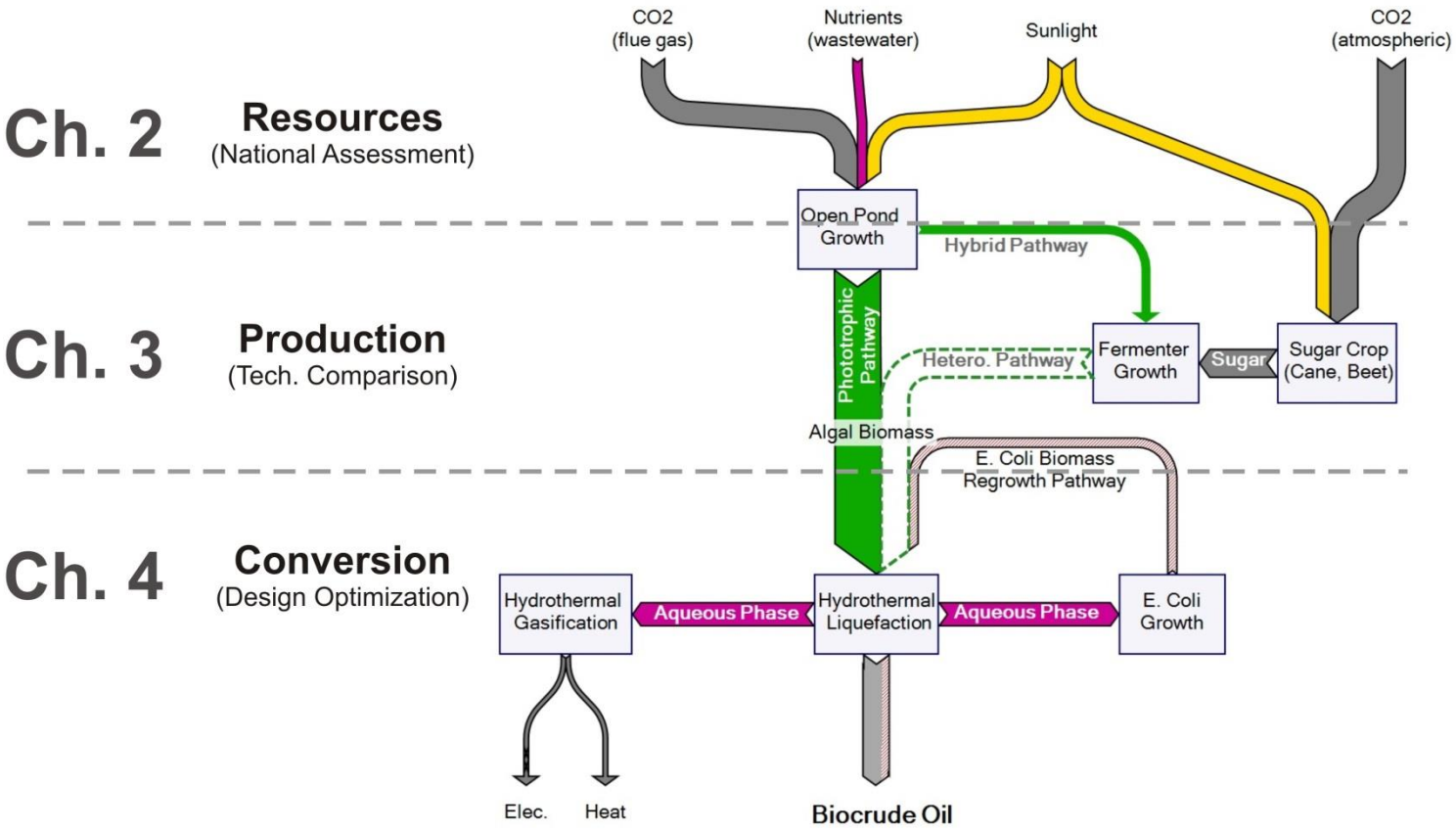

Figure 1.1 - Dissertation structure and research framework.

Chapter 3 addresses questions 5-7 by evaluating an approach that has proven to be appealing within the private sector: use of heterotrophic algae rather than phototrophic. This strategy was investigated as a means to cultivate a biomass feedstock to eventually be fed to through HTL for biomass conversion. The low cost of sugar signals the benefits of such an approach from the perspective of salability, but a more thorough LCA demonstrates that the strategy comes with drawbacks typical of first generation biofuels which suggest that use of terrestrial energy crops might not be sustainable. A GIS-based impact assessment was performed and concerns regarding indirect land use change (iLUC) and land footprint are brought into the fray. Growth

modeling results from Chapter 2 are incorporated to help identify the water stress and land footprint of the phototrophic and hybrid pathway. The dissertation moves forward using the assumption of phototrophic algae grown in open ponds as the feedstock most likely to meet the overarching objectives.

Chapter 4 addresses questions 8 and 9 by incorporating the results of phototrophic pathway modeling with experimental data provided by collaborators exploring HTL. The benefits of the phototrophic pathway in terms of LCA metrics is confirmed in Chapters 2 and 3, but the high costs of production remain an obstacle to commercialization. Varying the HTL reaction conditions and incorporating secondary biomass as a means to boost yields of biocrude oil yield is explored as a means to address these concerns.

Key findings from each of the three studies will be highlighted in Chapter 5. Results will be interpreted in relation to the dissertation's overarching themes of sustainability, scalability, and salability.

1.5 Journal Submissions from Chapters

Chapters 2, 3, and 4 each represent unique bodies of research that have been submitted to academic journals for publication. Chapter 2 was submitted to *Biomass & Bioenergy* in May of 2011, revised and resubmitted in April 2012, and revised again in December 2012. Additional collaborators on this article included Gregory Keoleian and Nancy Love.

Chapter 3 was submitted to *Environmental Science& Technology* in April of 2013 and is in the process of being revised based on reviewer comments in addition to feedback

from this dissertation committee. Additional collaborators on this article included Robert Levine, Gregory Keoleian, Shelie Miller, and Phillip Savage.

Chapter 4 was submitted to the journal *Algal Research* in September of 2013. Additional collaborators on this article included Andrew Fang, Gregory Keoleian, Peter Valdez, Michael Nelson, Xiaoxi (Nina) Lin, and Phillip Savage. The three bodies of research mentioned above are included in their complete form so some content included in this introductory section of the dissertation will be duplicated in Chapters 2-4.

1.6 Chapter 1 References

(1) Energy Independence and Security Act of 2007. **2007**, *Public Law*, 1–311.

(2) Farrell, A. E.; Plevin, R. J.; Turner, B. T.; Jones, A. D.; O'Hare, M.; Kammen, D. M. Ethanol can contribute to energy and environmental goals. *Science* **2006**, *311*, 506–508.

(3) Wang, M.; Wu, M.; Huo, H. Life-cycle energy and greenhouse gas emission impacts of different corn ethanol plant types. *Environmental Research Letters* **2007**, *2*, 024001.

(4) Wang, M.; Han, J.; Dunn, J. B.; Cai, H.; Elgowainy, A. Well-to-wheels energy use and greenhouse gas emissions of ethanol from corn, sugarcane and cellulosic biomass for US use. *Environmental Research Letters* **2012**, *7*, 045905.

(5) Pimentel, D.; Marklein, A.; Toth, M. A.; Karpoff, M. N.; Paul, G. S.; McCormack, R.; Kyriazis, J.; Krueger, T. Food Versus Biofuels: Environmental and Economic Costs. *Human Ecology* **2009**, *37*, 1–12.

(6) Sheehan, J.; Dunahay, T.; Benemann, J.; Roessler, P. Look Back at the U.S. Department of Energy's Aquatic Species Program: Biodiesel from Algae; Close-Out Report. **1998**.

(7) Chisti, Y. Biodiesel from microalgae. *Biotechnology Advances* **2007**, *25*, 294–306.

(8) Chisti, Y. Biodiesel from microalgae beats bioethanol. *Trends in biotechnology* **2008**, *26*, 126–131.

(9) Lardon, L.; Hélias, A.; Sialve, B.; Steyer, J.-P.; Bernard, O. Life-Cycle Assessment of Biodiesel Production from Microalgae. *Environmental Science & Technology* **2009**, *43*, 6475–6481.

(10) Clarens, A. F.; Resurreccion, E. P.; White, M. A.; Colosi, L. M. Environmental life cycle comparison of algae to other bioenergy feedstocks. *Environmental science & technology* **2010**, *44*, 1813–9.

(11) Liu, X.; Clarens, A. F.; Colosi, L. M. Algae biodiesel has potential despite inconclusive results to date. *Bioresource technology* **2012**, *104*, 803–6.

(12) Kadam, K. L. Power plant flue gas as a source of CO2 for microalgae cultivation: economic impact of different process options. *Energy Conversion and Management* **1997**, *38*, 505–10.

(13) Benemann, J. R. Utilization of carbon dioxide from fossil fuel-burning power plants with biological systems. *Energy Conversion and Management* **1993**, *34*, 999–1004.

(14) Zeiler, K. G.; Heacox, D. A.; Toon, S. T.; Kadam, K. L.; Brown, L. M. The Use of Microalgae for Assimilation and Utilization of Carbon-Dioxide from Fossil Fuel-Fired Power-Plant Flue-Gas. *Energy Conversion and Management* **1995**, *36*, 707–712.

(15) Green, F. B.; Lundquist, T. J.; Oswald, W. J. Advanced integrated wastewater pond systems for nitrogen removal. *Water Science and Technology* **1995**, *31*, 9–20.

(16) Oswald, W. J.; Gotaas, H. B.; Ludwig, H. F.; Lynch, V. Algae Symbiosis in Oxidation Ponds: III. Photosynthetic Oxygenation. *Sewage and Industrial Wastes* **1953**, *25*, 692–705.

(17) Woertz, I.; Feffer, A.; Lundquist, T.; Nelson, Y. Algae Grown on Dairy and Municipal Wastewater for Simultaneous Nutrient Removal and Lipid Production for Biofuel Feedstock. *Journal of Environmental Engineering* **2009**, *135*, 1115.

(18) Clarens, A. F.; Nassau, H.; Resurreccion, E. P.; White, M. A.; Colosi, L. M. Environmental Impacts of Algae-Derived Biodiesel and Bioelectricity for Transportation. *Environmental science & technology* **2011**, *45*, 7554–7560.

(19) Oswald, W. J. Advanced integrated wastewater pond systems. In *Proceedings of the ASCE convention: Supplying water and saving the environment for six billion people.*; 1990; pp. 73–80.

(20) Noüe, J.; Laliberté, G.; Proulx, D. Algae and waste water. *Journal of Applied Phycology* **1992**, *4*, 247–254.

(21) Lundquist, T. J.; Woertz, I. C.; Quinn, N. W. T.; Benemann, J. R. A Realistic Technology and Engineering Assessment of Algae Biofuel Production. *Assessment* **2010**, *October*, 1.

(22) Davis, R.; Aden, A.; Pienkos, P. T. Techno-economic analysis of autotrophic microalgae for fuel production. *Applied Energy* **2011**, *88*, 3524–3531.

(23) Benemann, J. R.; Oswald, W. J. Systems and economic analysis of microalgae ponds for conversion of CO{sub 2} to biomass. Final report. **1996**.

(24) Gallagher, B. J. The economics of producing biodiesel from algae. *Renewable Energy* **2011**, *36*, 158–162.

(25) Sun, A.; Davis, R.; Starbuck, M.; Ben-Amotz, A.; Pate, R.; Pienkos, P. T. Comparative cost analysis of algal oil production for biofuels. *Energy* **2011**, *36*, 5169–5179.

(26) Pienkos, P. T.; Darzins, A. The promise and challenges of microalgal-derived biofuels. *Biofuels Bioproducts and Biorefining* **2009**, *3*, 431–440.

(27) Miao, X.; Wu, Q. Biodiesel production from heterotrophic microalgal oil. *Bioresource Technology* **2006**, *97*, 841–846.

(28) Brennan, L.; Owende, P. Biofuels from microalgae—A review of technologies for production, processing, and extractions of biofuels and co-products. *Renewable and Sustainable Energy Reviews* **2010**, *14*, 557–577.

(29) Heredia-Arroyo, T.; Wei, W.; Hu, B. Oil accumulation via heterotrophic/mixotrophic Chlorella protothecoides. *Applied Biochemistry And Biotechnology* **2010**, *162*, 1978–95.

(30) Xiong, W.; Gao, C.; Yan, D.; Wu, C.; Wu, Q. Double CO(2) fixation in photosynthesis-fermentation model enhances algal lipid synthesis for biodiesel production. *Bioresource Technology* **2010**, *101*, 2287–2293.

(31) Mercer, P.; Armenta, R. E. Developments in oil extraction from microalgae. *European Journal of Lipid Science and Technology* **2011**, *113*, 539–547.

(32) Halim, R.; Gladman, B.; Danquah, M. K.; Webley, P. A. Oil extraction from microalgae for biodiesel production. *Bioresource Technology* **2011**, *102*, 178–85.

(33) Becker, E. W. *Microalgae: biotechnology and microbiology*; Baddiley, J.; Carey, N. H.; Higgins, I. J.; Potter, W. G., Eds.; Cambridge University Press, 1994; Vol. 10, p. 293.

(34) Biller, P.; Ross, A. B. Potential yields and properties of oil from the hydrothermal liquefaction of microalgae with different biochemical content. *Bioresource technology* **2011**, *102*, 215–25.

(35) Nelson, M.; Zhu, L.; Thiel, A.; Wu, Y.; Guan, M.; Minty, J.; Wang, H. Y.; Lin, X. N. Microbial utilization of aqueous co-products from hydrothermal liquefaction of microalgae Nannochloropsis oculata. *Bioresource technology* **2013**, *136*, 522–8.

(36) Keoleian, G. A. The application of life cycle assessment to design. *Journal of Cleaner Production* **1993**, *1*, 143–149.

(37) Maxwell, D.; Van Der Vorst, R. Developing sustainable products and services. *Journal of Cleaner Production* **2003**, *11*, 883–895.

(38) Sander, K.; Murthy, G. S. Life cycle analysis of algae biodiesel. *The International Journal of Life Cycle Assessment* **2010**, *15*, 704–714.

(39) Campbell, P. K.; Beer, T.; Batten, D. Life cycle assessment of biodiesel production from microalgae in ponds. *Bioresource Technology* **2011**, *102*, 50–56.

(40) Collet, P.; Hélias, A.; Lardon, L.; Ras, M.; Goy, R.-A.; Steyer, J.-P. Life-cycle assessment of microalgae culture coupled to biogas production. *Bioresource technology* **2011**, *102*, 207–14.

(41) Batan, L.; Quinn, J.; Willson, B.; Bradley, T. Net energy and greenhouse gas emission evaluation of biodiesel derived from microalgae. *Environmental science technology* **2010**, *44*, 7975–7980.

(42) Stephenson, A. L.; Kazamia, E.; Dennis, J. S.; Howe, C. J.; Scott, S. A.; Smith, A. G. Life-Cycle Assessment of Potential Algal Biodiesel Production in the United Kingdom: A Comparison of Raceways and Air-Lift Tubular Bioreactors. *Energy & Fuels* **2010**, *24*, 4062–4077.

(43) Resurreccion, E. P.; Colosi, L. M.; White, M. A.; Clarens, A. F. Comparison of algae cultivation methods for bioenergy production using a combined life cycle assessment and life cycle costing approach. *Bioresource Technology* **2012**, *126*, 298–306.

(44) Frank, E. D.; Elgowainy, A.; Han, J.; Wang, Z. Life cycle comparison of hydrothermal liquefaction and lipid extraction pathways to renewable diesel from algae. *Mitigation and Adaptation Strategies for Global Change* **2012**.

(45) Valdez, P. J.; Nelson, M. C.; Wang, H. Y.; Lin, X. N.; Savage, P. E. Hydrothermal liquefaction of Nannochloropsis sp.: Systematic study of process variables and analysis of the product fractions. *Biomass and Bioenergy* **2012**, *46*, 317–331.

(46) Valdez, P.; Savage, P. A Reaction Network for the Hydrothermal Liquefaction of Nannochloropsis sp. *Manuscript Submitted, Algal Research* **2013**.

CHAPTER 2. A GIS BASED NATIONAL ASSESSMENT OF ALGAL BIO-OIL PRODUCTION POTENTIAL THROUGH FLUE GAS AND WASTEWATER CO-UTILIZATION

2.1 Abstract

The high theoretical productivity of microalgae makes it a promising energy crop, but economically viable large-scale production facilities have yet to emerge. Coupling algae cultivation ponds with flue gas emissions from power utilities to provide carbon dioxide and municipal wastewater to provide nutrients has been recommended as a solution. This flue gas and wastewater co-utilization (FWC) strategy not only reduces the upstream impacts and costs associated with providing inputs, but also provides a credit for wastewater treatment, a service currently required to reduce production costs to a viable level.

This study provides the first national assessment of the potential for producing algal bio-oil in the United States using FWC. Spatial-temporal algae growth was simulated using solar radiation and temperature data to calculate the average annual algae yield for any location, which significantly impacts the feasibility. The results of this model were integrated into a geospatial overlay analysis which establishes the economically viable bio-oil production potential of FWC by accounting for the relative abundance of

the input resources and their proximity. At most, 1.7 billion liters of bio-oil could be produced annually in a manner economically competitive with crude oil prices of $80 per barrel. The amount of nutrients in wastewater limits yields to 20.5 liters of bio-oil per capita annually, and climatic constraints further reduce this potential by nearly 60%. Carbon dioxide constraints play a negligible role. Although the bio-oil production potential of FWC is relatively small, it does provide an opportunity to increase national biofuel output while providing a needed service.

2.2 Introduction

The high areal productivity of microalgae makes it a promising energy crop. Estimates indicate that transport fuel needs for the United States could be met by algal bio-oil using 1/20th of current agricultural land area, whereas the equivalent yield from corn or soybean would be impossible to achieve due to land area constraints[1]. Despite increased recent investment from the public and private sector, however, economically viable large-scale production facilities have yet to emerge. Furthermore, studies examining life-cycle impacts indicate that producing bio-oil from algae with current technology has a low net energy ratio (NER) and sequesters less net greenhouse gases than biofuels produced with other crops [2–4]. These findings are due partly to the carbon dioxide and fertilizer input requirements. Even so, the dramatically reduced land intensity for production of algal bio-oil makes it an attractive alernative to pursue.

Coupling algae cultivation ponds with flue gas emissions from power utilities to provide a source of carbon dioxide and municipal wastewater to provide a source of

nutrients has been recommended in several studies[5–11]. This flue gas and wastewater co-utilization (FWC) strategy not only reduces the upstream impacts and costs of supplying carbon dioxide and nutrients, but also creates environmental and economic credits by offsetting the aeration and nutrient removal impacts from wastewater treatment. Pilot facilities have demonstrated that algae are capable of growth in systems with concurrent removal of high levels of biological oxygen demand (BOD) and with reduced aeration energy requirements [12,13]. An analysis by Lundquist et al. (2010) demonstrates that the economic credit for such a service is also a necessary revenue stream to bring production costs to a reasonable level [14].

While there is a substantial body of literature exploring methods to improve cultivation and processing such that algal bio-oil production could eventually thrive in a stand-alone facility, no comprehensive assessment has been done to assess the feasibility of large-scale bio-oil production using the FWC approach. This study is the first national assessment, which requires integration of spatial-temporal climate data with carbon dioxide and wastewater constraints. Wigmosta et al. (2011) demonstrated that algal bio-oil could theoretically be produced domestically in volumes sufficient to obviate nearly half of our country's transportation petroleum imports [15]. These findings provide an encouraging upper production limit, but as this study shows, the necessity to collocate with other resources dramatically reduces this production potential.

The United States Department of Energy's 20 + year research project, the Aquatic Species Program, provided a thorough examination of the technical aspects of

cultivating algae for bio-oil production. The project concluded that the most cost-effective method for cultivating algae is the use of a high rate pond (HRP), an approach featuring a raceway configuration circulated via a paddlewheel, sparged with a carbon dioxide source to facilitate maximum growth[16]. A life-cycle assessment (LCA) by Stephenson et al. (2010) also concluded that this open pond strategy has significantly less environmental burden than the typical alternative, a tubular photo-bioreactor[17]. In his comparison of the two approaches, Grobbelaar (2009) acknowledges that while photo-bioreactors have many benefits (such as reduced water loss, less risk of contamination, and higher carbon dioxide use efficiency), open ponds have lower construction costs and are easier to maintain[18]. Given these considerations and the availability of data on the HRP approach, this cultivation strategy was modeled in this study.

Many studies have explored the growth of algae on flue gas[7,19–22]. Weissman and Goebel (1987) showed that there are substantial economic benefits offered by avoiding the purchase of carbon dioxide[23]. Use of wastewater as a nutrient source would not only eliminate fertilizer costs, the treatment services provided yield an economic credit to offset the costs of operating the algae pond. Woertz (2009) demonstrated that algae is an effective means for removing nutrients from wastewater when sparged with carbon dioxide, removing more than 99% of ammonium and orthophosphate[10]. Ironically, the chief motivation for removing such nutrients is to prevent uncontrolled algae growth

that disrupts aquatic ecosystems. Growing algae on these nutrients in a controlled environment, conversely, enables the recovery of a valuable product.

The purpose of this study is to identify the most viable regions for FWC and estimate the amount of algal bio-oil that could theoretically be produced in this manner cost-competitively with fossil fuels. To this end an algae growth simulation is conducted to calculate average annual algae yield across the United States. The results of this model are then incorporated into an integrative climate and resource overlay analysis used to compare the economic viability of using FWC at any location throughout the country.

2.3 Background

Clarens et al. (2010) demonstrated in their LCA that more than half of the total upstream energy required for algal biomass production is from providing carbon dioxide and fertilizer. These inputs could theoretically be eliminated by utilizing anthropogenic resources. The results of an LCA performed by Lardon et al. (2009) emphasized the benefits of wet-harvesting rather than drying the algal biomass prior to conversion, but also clearly indicated the significance of energy burdens from fertilizer production[2]. These studies suggest that to achieve a net energy ratio (NER) greater than one for bio-oil produced from algae grown under normal circumstances (i.e. not nutrient limited), not only would a wet-harvesting strategy be required, but also elimination of upstream energy burdens associated with fertilizer production.

The NER could be further increased by assigning a credit for wastewater treatment services and reducing the amount of aeration energy required for traditional treatment

processes. Algae release oxygen during photosynthesis which is required during treatment to enable growth of heterotrophic bacteria that remove BOD. If the energy input requirement for aeration is assumed to be 0.2 kW·h of energy per cubic meter of wastewater treated, then 0.3 MJ of aeration energy would be offset per MJ of bio-oil produced[24]. An additional 0.5 MJ per MJ of bio-oil credit could also be applied for the service of nutrient removal based on data from Maurer et al. (2003) and assumptions about the composition of algal biomass[25,26]. The total amount of energy offset by providing wastewater treatment is therefore substantial, summing to a value that is nearly 80% of the energy content in the bio-oil produced. Refer to the Supporting Information for further details.

In addition to the benefits observed from a life-cycle perspective, there are economic advantages. From the perspective of wastewater treatment, Downing et al. (2002) found that HRPs provided treatment at a cost that was about 70% less than the conventional activated sludge approach[27]. Compared to algae cultivation without the feedstocks there are also significant savings. Weissman and Goebel (1987) provide a detailed account of the economics of constructing and operating a microalgal open pond[23]. The report included an economic comparison between a 1,000 acre pond base case, assuming a carbon dioxide cost of $\$35 \cdot t^{-1}$, and a scenario featuring free carbon dioxide. It was found that nutrients and carbon dioxide represented nearly half of the total costs. Their analysis assumed an optimistic algae yield of 30 $g \cdot m^{-2} \cdot day^{-1}$, so the cost per acre savings would be less for ponds with lower yields. According to the algae

growth model simulation presented later in this study, most locations will not perform as well.

The costs for transporting these resources were investigated as part of the geospatial analysis presented later in this paper. Also, the opacity of sewage does not allow for deep light penetration and therefore phototrophic algae are photolimited[10]. Diluting the wastewater would not only increase the water input requirements, but in order to maintain the desired hydraulic residence time (HRT) the pond depth would need to be increased thereby increasing both the pond construction and operational expenses. Furthermore, to fully treat the wastewater and obtain the necessary credit the HRP must be integrated into a more extensive process. This study assumes the HRP model configuration shown in Figure 1 which was developed by Lundquist et al. (2010) [14]. In their analysis this configuration is identified as the only approach in which algal bio-oil could be produced in an economically viable manner. This analysis, published by the Energy Biosciences Institute, does not appear in a peer-reviewed publication. It is the only such detailed analysis, however, and the authors are preeminent in the field of wastewater treatment using algae. The authors are the first to explore the techno-economic feasibility of fully integrating wastewater treatment into the process design rather than using algae as a form of tertiary treatment for nutrient removal. Anaerobic digestion is used on site to produce electricity and process heat from the residual (non-lipid) biomass along with solids collected from the wastewater in a primary clarifier

upstream of the cultivation ponds. Permitting and regulatory concerns regarding the capture and transport of flue gas are outside the scope of this analysis.

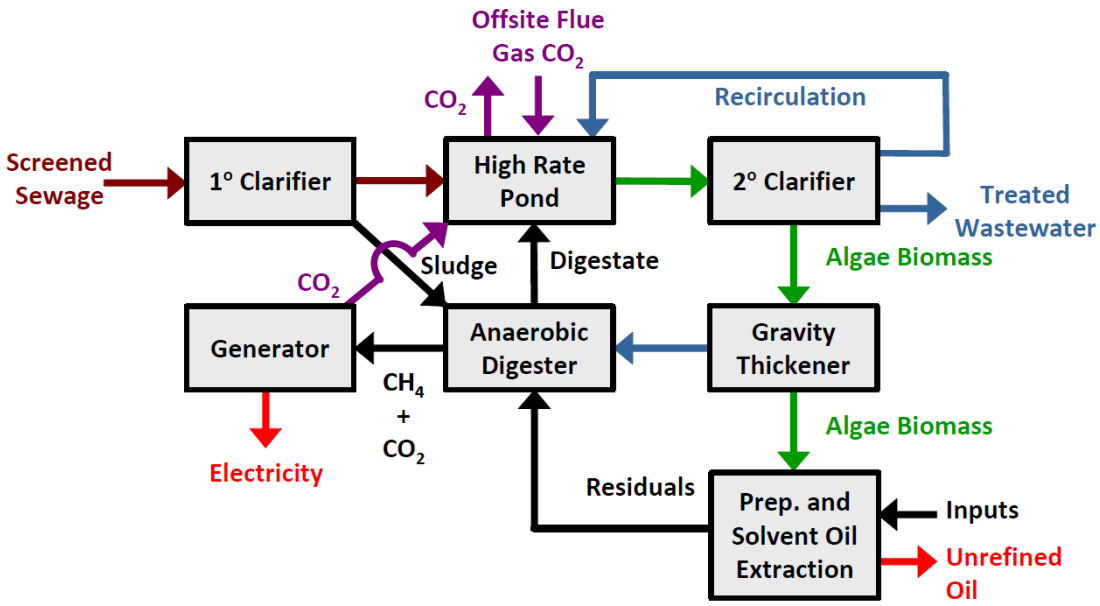

Figure 2.1 - Wastewater treatment & bio-oil production process schematic. Source: Lundquist et al. (2010)[14].

2.4 Methods

The availability of the flue gas and wastewater inputs for algae growth provide an upper limit for how much algae can be cultivated. Conversion factors are therefore determined to establish how the available quantities of these resources translate into bio-oil production. But even locations where these inputs are abundant may not be appropriate for FWC, as not all locations have suitable climates for algae cultivation. Climatic parameters determine pond size requirements and are therefore predominantly responsible for distinguishing economically viable locations from those that are not. A MATLAB® growth model is used to calculate an average annual algae

yield for any location across the contiguous United States based on the spatial-temporal parameters solar radiation and temperature. Finally, a GIS model is used to integrate the locations and quantities of the input resources with the findings of the algae growth model. The results of this overlay analysis are used to establish an estimate for the amount of algal bio-oil production that could be theoretically produced annually using FWC.

2.4.1 Nutrient Availability

The quantity of nutrients required per unit of biomass can be established by the molecular composition of algal biomass. Data from Grobbelaar (2004) suggests a stoichiometry of approximately $C_{100}H_{183}O_{48}N_{11}P$ [26]. Crites and Tchobanoglous (1998) report that the average per capita Total Kjeldahl Nitrogen (TKN, sum of ammonia and organic nitrogen) mass loading rate is 4.85 $kg \cdot person^{-1} \cdot year^{-1}$, while Scheehle & Doorn (2001) estimate a higher value of 9.37 $kg \cdot person^{-1} \cdot year^{-1}$ [28,29]. These values were used as high and low scenarios for a sensitivity analysis and the average was implemented as the baseline. In their meta-analysis, Liu et al. (2012) report lipid contents ranging from 21% to 40% [4], but to be consistent with the Lundquist et al. (2010) techno-economic analysis a lipid content of 25% was used for the baseline [14]. A sensitivity analysis explores a range of values from 20% to 30%. Assuming an annual average nitrogen removal efficiency of 70%, the conversion rate can be established as 20.5 $L\text{-}oil_{algal} \cdot person^{-1} \cdot year^{-1}$. This value determines the theoretical limit for production of bio-oil from algae grown on wastewater, assuming no fraction of the nutrients is recycled.

Considering that the United States consumes 1.4 billion liters of motor gasoline daily[30], if wastewater from all of the 226 million residents served by central facilities [31] could be captured and used for algae cultivation, only about 1% of this transport fuel demand could be met. This provides an upper limit on the FWC scenario proposed.

Based on the biomass composition assumptions, 1.88 kg of carbon dioxide is required per every kilogram of algal biomass grown. A substantial amount of carbon is delivered with the wastewater, however, and much of this material could be collected in the primary clarifier and processed in the anaerobic digester along with the non-lipid portions of the algal biomass. The carbon dioxide recycled from the combustion of biogas is sufficient to meet the algal growth requirements for much of the year, though during periods of high growth some carbon dioxide will need to be imported from an external source such as power utility flue gas [14]. Based on approximations by Lundquist et al. (2010), this analysis assumes that an annual average of 8% of the carbon in the algal biomass will need to be supplemented by flue gas imports. Most of the carbon dioxide emitted from power utilities, however, will not be converted into biomass. It is assumed that no gas storage scheme is utilized and only 30% of the carbon dioxide is assimilated into biomass because the operating schedule of these facilities does not align with the algae growth profile within the ponds[6]. This parameter will be explored as part of a sensitivity analysis performed later in this study with values ranging from 20% to 40%. Maintaining the assumption of 25% lipid content the conversion rate can then be established as 540 L-Oil_{algal} per tonne CO_2. This value compared to the nitrogen

limited conversion rate reveals that availability of carbon dioxide from flue gas is significantly less constraining than the availability of nutrients. The United States emitted more than two billion tonnes of carbon dioxide for energy from combustion of coal alone in 2008, indicating that nearly a fifth of our motor gasoline demand could be met from this supply alone, excluding the carbon available in wastewater, if there were no other limiting factors[32].

The GIS analysis implemented uses a dataset containing populations of "urban areas" from the 2000 United States Census[33]. Clusters of cities often containing surrounding suburbs are lumped into a single region, with boundaries of polygons designating the extent of the area with a sufficiently high population density. Only polygons with large populations (defined here as those containing more than 100,000 people) were considered. These 254 regions included more than 180 million people, or approximately 60% of the total population. A dataset including point locations of power utilities and their carbon dioxide emissions as reported under the EPA's Acid Rain legislation was obtained from Purdue University's Vulcan Project[34]. Only facilities that produce enough carbon dioxide to meet the equivalent bio-oil production from the population cutoff of 100,000 people were considered. A total of 948 power utilities matched this criterion, producing a total of more than 2.4 billion tonnes of carbon dioxide per year, or approximately 40% of total anthropogenic carbon dioxide emissions in the United States.

The GIS modeling assumes that at any point in the United States, wastewater will be transported from the edge of the nearest urban area polygon and carbon dioxide from the point of the nearest power utility. With this assumption, the zone assigned to each resource can be defined using Theissen polygons, which divide the terrain into regions such that any location within the polygon is closer to its associated point than to any other point. The urban area polygons were first converted to points prior to Theissen polygons. The total amount of bio-oil that can be produced based on these inputs can then be established by multiplying the conversion ratios from the previous section with the respective nutrient availability within each of the sets of zones. It will be the lesser of these two quantities that determines how much bio-oil can be produced at that point.

The annualized cost for constructing and maintaining a pipe for carbon dioxide transport is included in Table 2. The annualized cost for constructing and maintaining a trunk sewer for wastewater transport is also included in Table 2. The fact that the cost is proportional to the square root of the flow rate implies economies of scale. In this model it is assumed that only the amount of nutrient required to produce the bio-oil will be transported. So, for example, in a location that is limited by wastewater availability rather than carbon dioxide, all of the wastewater will be transported to that location but only the required fraction of the available flue gas.

2.4.2 Spatial-Temporal Algae Growth Model

Because algae are photosynthetic organisms, biomass production is limited by the exposure to sunlight and hence the area of the cultivation pond. Factoring climatic conditions and amount of solar radiation, the amount of algal biomass that can be cultivated per surface area of the pond, or areal yield, varies significantly by region. Predicting this areal yield, typically expressed in terms of $g \cdot m^{-2} \cdot day^{-1}$ or $L \cdot ha^{-1} \cdot year^{-1}$, is therefore a key aspect of locating optimal algae cultivation sites. Previous research has either compared a small sample of sites or distinguished preferred regions as those exceeding a particular average temperature and/or solar radiation threshold. Given non-linear dependency of algae growth on temperature and insolation, however, using such approaches is an oversimplification.

Tamiya et al. (1953) focus on the growth kinetics of a species of *Chlorella* and investigate the dependence on temperature and light[35]. In this study an equation to describe the areal algae yield, Y_a (measured in $g \cdot m^{-2} \cdot day^{-1}$) is empirically derived and reported to be

$$Y_a = \left(\frac{10}{2}\right) \cdot \left(5.3 \frac{k_G}{\varepsilon}\right) \log\left(1 + \frac{\alpha \gamma L}{H k_G}\right) \cdot C. \quad (1)$$

The parameters used in this formula along with their descriptions, units, and empirically derived values are included in Table 1.

Table 2.1 - Growth formula inputs [35].

Parameter	Description	Units	Value
L	Solar radiation	kilolux-hour·day^{-1} ·m^{-2}	Input, measured in field
KG	Kinetic parameter	day^{-1}·m^{-2}	0.07·Temp - 0.44
γ	Light intensity correction factor	dimensionless	0.64
ε	Extinction coefficient	ml^{-1}	0.41
α	Rectangular hyperbola shape parameter	day^{-1}·kilolux^{-1}	0.45
H	Duration of sunlight	hours·day^{-1}	12
C	Dry weight conversion	g·ml^{-1}	0.25

It is currently more common to report solar irradiance in the flux density units of kW·m^{-2} rather than Kilolux (lux = lumen·m^{-2}). Here it is assumed that the average sun and sky luminous efficiency is 108 lumens per watt[36]. The *H* parameter is used to convert daily quantities of sunlight to an average intensity; by assuming a constant value some error is introduced, particularly at higher latitudes where seasonal variation is more pronounced. This model assumes the culture is maintained with high population densities in the linear phase of growth (i.e. the biomass is harvested in an optimal fashion).

The National Renewable Energy Laboratory (NREL) provides a GIS dataset containing average daily global horizontal insolation in the United States for each month[37]. This data was converted into a grid format with a resolution of approximately 1/10 of a decimal degree using ArcGIS® software and then imported into twelve 250×574

matrices within MATLAB®. The twelve values for each of the grid cells were then linearly interpolated to approximate values for the 365 days of the year. The result is a 250×574×365 matrix containing the estimated $kW \cdot hr \cdot m^{-2}$ for each gridded region of the United States and for each day.

The PRISM Climate Group at Oregon State University provides a dataset containing average daily maximum temperature for each month[38]. Using the same procedure described for the NREL data, a 250×574×365 matrix containing the estimated maximum temperature for each gridded region of the United States and for each day was established. It is assumed that the temperature of the water within the pond matches that of the ambient atmosphere. Heat transfer dynamics are neglected due to the relatively shallow depth of the pond. Average maximum temperatures were chosen because the majority of algae growth occurs during the periods of peak solar radiation which typically coincides with the warmest period of the day. The growth model therefore presents an upper limit on algae yield. The results of a more conservative growth model, which uses the average of the daily maximum and minimum temperature, are included in the Supporting Information.

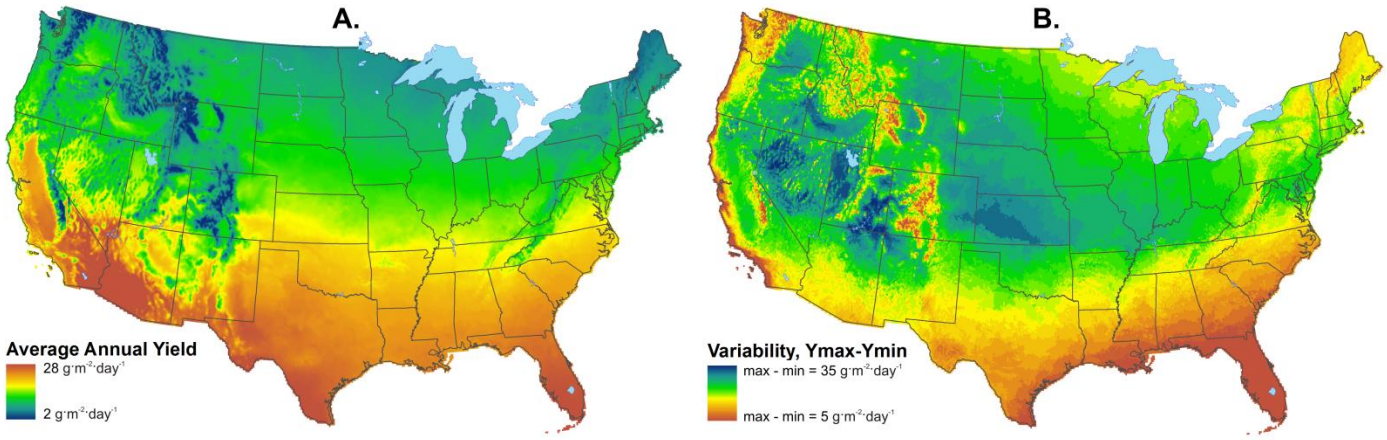

Figure 2.2 - Simulation results: A) Average annual yield, and B) Variation in yield, expressed as the maximum daily yield observed over the year minus the minimum yield observed over the year.

The growth formula (Equation 1) was then used to estimate areal yield for each of the cell locations for every day of the year. The average annual algae yield determined by the simulation is shown in Figure 2a. The results are within the range of values reported by other studies for specific sites. As expected, locations in the lower latitudes, where warmer temperatures and greater solar radiation prevail, tend to produce a higher average annual yield. While southern locations tend to outperform northern in general, however, there is a significant amount of variation in algae yield at any given latitude. This variation is due to the drastic differences in geography and climate across the breadth of the country. Latitude alone is an insufficient means for predicting algae production rates. In addition to geographic variation, seasonal variation in production is also noteworthy. Figure 2b illustrates this phenomenon, expressed as the difference between maximum and minimum algae yields over the course of the simulated 365 days. While the arid regions of the southwestern United States exhibit a relatively high variation in output, Texas and the southeast have average yields that are nearly as high,

but with more consistent production throughout the year. The state of Florida has particularly stable output, as do portions of the western coastline where the thermal mass of the ocean helps regulate the temperature.

The amount of algal biomass that can be cultivated and the rate of algae growth, as defined by the GIS growth model, have both been established and therefore the required pond size can be deduced. Here it is assumed that the size of the pond is simply the number of liters that can be produced divided by the average areal yield (when expressed as $L \cdot ha^{-1} \cdot year^{-1}$). So for example a site that could produce 10 million liters per year with an average productivity of 25,000 $L \cdot ha^{-1} \cdot year^{-1}$ would require a 400 hectare pond. According to the analysis by Lundquist et al. (2010), the annualized cost of the wastewater treatment facility incorporating a 100 hectare HRP is approximately $51,000 per hectare for both capital recovery and operational costs once carbon dioxide delivery costs have been removed. This value, which also includes oil extraction costs from a presumed shared facility, is used in the GIS analysis. It is likely that economies of scale could reduce this cost for larger facilities but this is not addressed. It is assumed that the costs of the entire treatment facility scale in proportion to the pond size.

2.4.3 Integrative GIS Overlay Analysis

Incorporating the values shown in Table 2 enables the transport costs and growth rate GIS layers to be summed in equal units, weighted according to the economic burdens. It is important to note that while evaluating the results in economic terms, ultimately expressed as dollars per liter, this is not a thorough economic analysis. The

results are a high-level comparison of economic feasibility across the expanse of the country. Factors such as costs of land and labor, for example, vary within the United States but are treated as constant in this analysis. But by expressing the results in terms of dollars the necessity to attribute arbitrary weighting schemes for combining the multiple data layers is avoided. An illustration of this GIS layering methodology is included in the Supporting Information.

Table 2.2 - Economic assumptions incorporated into GIS overlay analysis. Inflation adjustments from the US Bureau of Labor Statistics.

	Formula	Reference	Conversion Rate
Treatment Facility Cost	$C_P = \frac{\$50{,}900}{\text{ha of HRP} \cdot yr}$	Adapted from [14]	none
Wastewater Sewage Line[a]	$C_{T,WW} = \frac{\$2{,}800\sqrt{Q}}{km \cdot yr}$	Adapted from [39]	7.25
Carbon Dioxide Pipeline	$C_{T,CO2} = \frac{\$13.70}{ha \cdot km \cdot yr}$	Adapted from [14]	none
Wastewater Treatment Credit	$CR_{TRTMT} = \frac{\$1.23}{kg\ BOD}$	[14],[40]	none

2.5 Results and Discussion

Figure 3 shows the graphical results of the economic overlay analysis. Locations within the urban areas originally appear to be the most viable because the distance for wastewater transport is taken to be zero within the boundaries of the polygons. These regions are assumed not to be candidates for large-scale algae cultivation because by definition they have a high population density and therefore a lack of undeveloped land for facility siting. For this reason these areas are whitened out and excluded from the quantitative analysis.

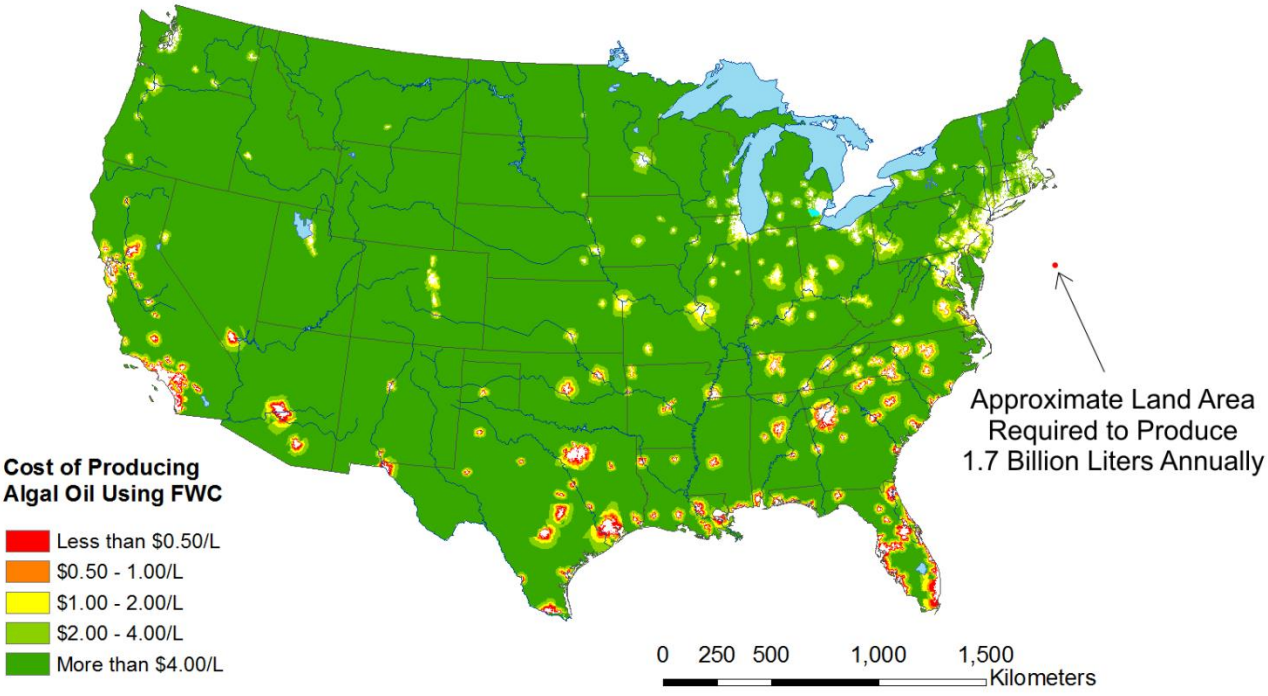

Figure 2.3 - Results of economic overlay analysis. The pond area shown to the right of the map is approximately 83,000 hectares, or the pond area required to produce 1.7 billion liters of algal bio-oil annually using FWC, the quantity that could be economically produced.

The results indicate, predictably, that regions near the urban areas are more favorable than regions that require construction of longer sewer lines. Power utility locations had a less noticeable influence on the results. A band 10km wide was created around each of the urban areas as a means to evaluate average results within that surrounding region. The Spatial Analyst toolbox provided by ArcGIS® was used to perform this analysis. Chisti (2007) indicates that the required cost of producing algal bio-oil to be competitive with crude oil is

$$C_{algaloil} = 6.9 \cdot 10^{-3} \cdot C_{petroleum}\,, \qquad (2)$$

where $C_{algal\ oil}$ is the cost to produce algal oil, expressed in dollars per liter, prior to taxes, marketing, and conversion to biofuel and $C_{petroleum}$ is the price of crude oil in dollars per

barrel[1]. With a cost of fossil crude oil of $80 per barrel, then, the cost to produce algal bio-oil would need to be less than $0.55 per liter to be considered viable. Using this cutoff to identify regions that would be competitive with fossil-derived petroleum suggests that approximately 1.7 billion liters of bio-oil could be produced. Using the more conservative pond temperature assumptions provided in the Supporting Information cuts these projections to less than half of the initial estimate. The true value is somewhere within this range. The average annual yield results used to project the upper limit, however, are more consistent with values observed in other literature for individual sites and therefore present a more likely scenario.

Given that this is a macro-level analysis, the model is heavily driven by a number of parameter assumptions. A baseline and range of values for these key variables, shown in Table 3, was explored in a Monte Carlo analysis using RiskSim©, with triangular probability distributions for each. A sensitivity analysis was also performed to better understand the individual effects of the variables. A boxplot of the 10,000 trial Monte Carlo analysis is shown alongside the results of the sensitivity analysis in Figure 4. The results are most sensitive to the economic variables of infrastructure cost and wastewater treatment (BOD removal) credit. If infrastructure costs were to be reduced by 25% the total production potential would increase to 2.9 billion liters annually. Increasing the wastewater treatment credit by 25% increases the production potential to 2.0 billion liters annually. The cost of crude oil had less of an impact because the shift

in the value used to identify economically viable regions was small relative to the shifts in cost and credit that arise from the other two economic variables.

Table 2.3 - Range of values used in the sensitivity and Monte Carlo analyses. The references for the TKN per capita loading refer to the low and high scenarios, respectively, while the other references refer to the baseline value.

Sensitivity Analysis Parameter	Units	Low	Baseline	High	Reference
CO2 Utilization Factor	Dimensionless	20%	30%	40%	[6]
Lipid Content	Dimensionless	20%	25%	30%	[14]
Infrastructure Costs	$\$\cdot ha^{-1}\cdot yr^{-1}$ for HRP	38,200	50,900	63,600	[14]
TKN per capita	$Kg\text{-}TKN\cdot person^{-1}\cdot yr^{-1}$	4.85	7.11	9.37	[28],[29]
Fossil Oil Costs	$\$\cdot barrel^{-1}$	60	80	100	
BOD Removal Credit	$\$\cdot kg\text{-}BOD^{-1}$	.98	1.23	1.48	[14],[40]

Of the six sensitivity variables explored, two manipulate the effective abundance of the two major resource constraints considered: nutrients from wastewater and carbon dioxide from flue gas. Adjusting the average TKN loading rate affects the potential yield of algal biomass per capita, and adjusting the CO_2 utilization factor affects the yield per tonne of carbon dioxide in flue gas emissions. The results are much more sensitive to changes in the nutrient availability than to carbon dioxide availability, as represented by the slopes of the lines shown in Figure 4. For example, increasing the TKN loading rate boosted the production potential proportionally, while increasing the utilization of carbon dioxide had a negligible effect. This observation reinforces the notion that nutrient availability is a significantly more active constraint than flue gas availability.

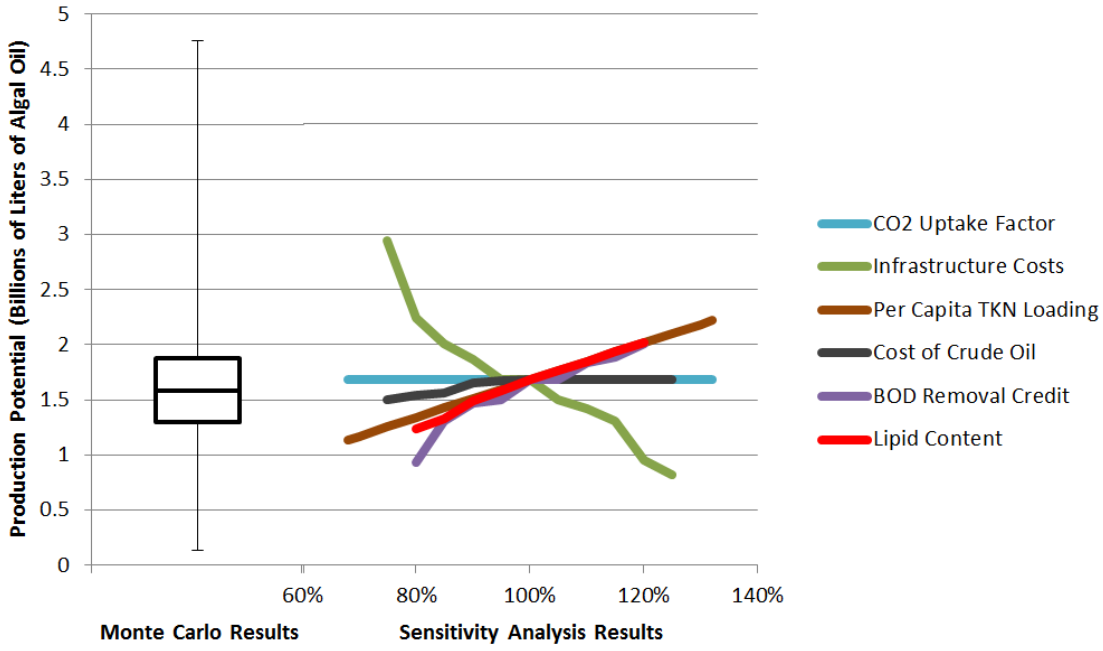

Figure 2.4 - Results of the Monte Carlo and sensitivity analyses, created by implementing the range of values shown in Table 3. The lines of the sensitivity analysis cross each other at 100%, which represents the result featuring baseline values. The boxplot on the left shows the distribution of the 10,000 results outputted by the Monte Carlo simulation. The central box spans from the first quartile through the third quartile, with the horizontal line indicating the mean value. The whiskers extend from the box to the sample minimum and maximum.

This analysis assumes there is no internal nutrient recycling loop occurring in the treatment scheme. Given that the facilities are heavily dependent up on the revenues from wastewater treatment to bring the cost of bio-oil to a competitive value, implementing high levels of nutrient recycling would require increased pond infrastructure to accommodate the boosted production yet would not receive increased revenue because the wastewater throughput would not change, thereby elevating the average cost per liter of algal bio-oil. It could still be possible, however, to recycle nutrients during portions of the year with peak algal growth rates without increasing the pond size or affecting the quality of treatment effluent[14]. Results of the sensitivity analysis demonstrate that increasing the effective availability of nutrients will bring a

proportional increase in production potential. For example, recycling 1/4 of the nutrients would bolster production potential by as much as a third; recycling 1/3 of the nutrients would increase production by as much as 50%. Optimizing the facility's operation to maximize nutrient recycling without detrimentally impacting treatment efficiency is an area that deserves further research.

The distribution of cost contributions for the production of a liter of algal oil using FWC is reported in Table 4. The predominant cost is the treatment facility, which varies greatly depending on the location. In cold climates like Duluth, MN, for example, the treatment facility contributes nearly $6 per liter while in Phoenix, AZ, it contributes less than $2 per liter. In the best location most, if not all, of this burden is offset by the $2.65 per liter credit assigned for the treatment service. Wastewater and flue gas transport had less impact on the final cost, contributing on average $0.13 and $0.03 per liter, respectively. For 73 of the 254 urban areas considered the net cost was negative, meaning that no revenue from the production of algae is required for the facility to make a profit. This result is consistent with other claims that using algae for wastewater treatment can be economically preferable to conventional approaches.

Table 2.4 - Distribution of costs and credits associated with the production of a liter of algal bio-oil using FWC for the 254 urban areas evaluated.

	Infrastructure, HRP	WW Transport	CO2 Transport	Treatment Credit	Total $/liter
Average	$ 3.27	$ 0.13	$ 0.03	$ (2.65)	$ 0.78
Minimum	$ 1.98	$ 0.02	$ 0.01	$ (2.65)	$ (0.61)
Maximum	$ 5.89	$ 0.20	$ 0.18	$ (2.65)	$ 3.45
St. Dev.	$ 0.89	$ 0.05	$ 0.02	$ -	$ 0.89

The Venn diagram in Figure 5 demonstrates that while the supply of carbon dioxide from flue gas is relatively vast, the supply of nutrients in wastewater limits the production potential to the order of billions of liters per year. This amount is further reduced by nearly 60% due to the inappropriate climate where most of the country's population resides.

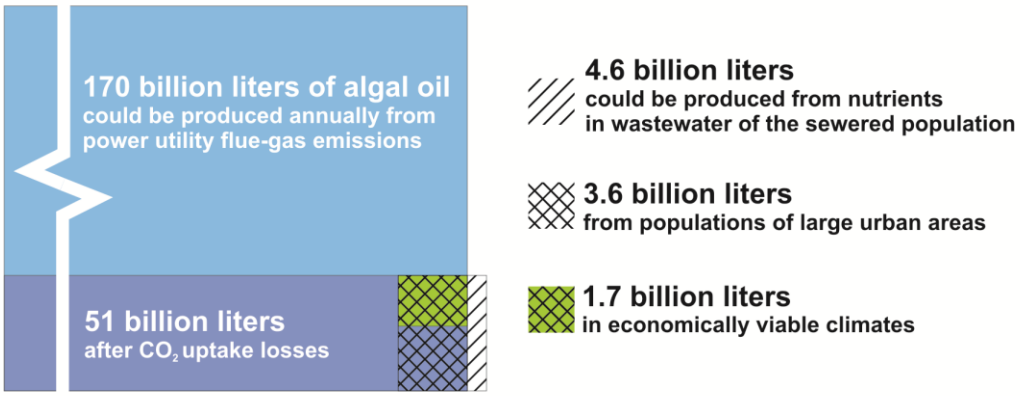

Figure 2.5 - Relative abundance of inputs for FWC, and where losses in national production potential occur.

2.6 Conclusion

Cultivating algae for bio-oil using FWC is an economically and environmentally worthwhile pursuit that is feasible with current technologies, presenting an opportunity to immediately escalate the country's biofuel production while providing the important service of removing nutrients from wastewater. But while this approach could have a relatively big impact relative to our current levels of renewable fuel production, limitations in the quantity of nutrients present in municipal wastewater prevent FWC from significantly reducing dependency on fossil-derived fuels. The amount of nutrients in wastewater limits yields to 20.5 liters of bio-oil per capita annually, and climatic

constraints further reduce this potential by nearly 60%. Flue gas supply constraints play a negligible role, though the proximity to flue gas emissions must not be overlooked nor should the technical and regulatory challenges associated with its transport. Nutrient recycle and use of animal feedlot wastestreams could increase this upper limit, but whether or not this could succeed economically has not been determined.

Because transporting wastewater is more expensive than doing so for the equivalent requirement of carbon dioxide, the most viable locations tend to be located nearest urban areas, and the economies of scale for constructing sewer trunks make those urban areas with high populations most favorable. Climatic conditions such as temperature and solar radiation, however, establish the rate at which algae can grow and therefore the size of cultivation facilities required, the predominant economic hurdle. For this reason an accurate GIS model to interpret climate variations in terms of theoretical algae yield is crucial. The analysis included in this study provides initial results.

Wastewater treatment is a needed service, so it makes sense to produce algal bio-oil as part of the process if it can be done in an economically competitive fashion. If eliminating dependence on fossil fuels is a priority of the country FWC should be employed in the near-term future, if not for the volume of immediate bio-oil production then for its potential to advance technologies that will enable algal bio-oil production that is not economically dependent on the revenue from wastewater treatment.

2.7 Chapter 2 References

(1) Chisti Y. Biodiesel from microalgae. Biotechnol Adv **2007**;25(3):294-306.

(2) Lardon L, Helias A, Sialve B, Steyer JP, Bernard O. Life-Cycle Assessment of Biodiesel Production from Microalgae. Environ Sci Technol **2009**;43(17):6475-81.

(3) Clarens AF, Resurreccion EP, White MA, and Colosi LM. Environmental Life Cycle Comparison of Algae to Other Bioenergy Feedstocks. Environ Sci Technol **2010**;44(5):1813-19.

(4) Liu X, Clarens AF, Colosi LM. Algae biodiesel has potential despite inconclusive results to date. Bioresource Technol **2012**;104: 803–6.

(5) Kadam KL. Power plant flue gas as a source of CO2 for microalgae cultivation: economic impact of different process options. Energ Convers Manage **1997**;38(1):505-10.

(6) Benemann JR. Utilization of Carbon Dioxide from Fossil Fuel-Burning Power Plants with Biological Systems. Energ Convers Manage **1993**;34(9-11):999-1004.

(7) Zeiler KG, Heacox DA, Toon ST, Kadam KL, and Brown LM. The Use of Microalgae for Assimilation and Utilization of Carbon Dioxide from Fossil Fuel-Fired Power Plant Flue Gas. Energ Convers Manage **1995**;36(6-9):707-12.

(8) Green FB, Bernstone LS, Lundquist TJ, Oswald WJ. Advanced Integrated Wastewater Pond Systems for Nitrogen Removal. Water Sci Technol **1996**;33(7):207-17.

(9) Oswald WJ, Gotaas HB, Ludwig HF, Lynch V. Algae Symbiosis in Oxidation Ponds: III. Photosynthetic Oxygenation. Sewage Ind Wastes **1953**;25(6):692–705.

(10) Woertz I, Feffer A, Lundquist T, Nelson Y. Algae Grown on Dairy and Municipal Wastewater for Simultaneous Nutrient Removal and Lipid Production for Biofuel Feedstock. J Environ Eng-ASCE **2009**;135: 1115.

(11) Clarens AF, Nassau H, Resurreccion EP, White MA, Colosi LM. Environmental Impacts of Algae-Derived Biodiesel and Bioelectricity for Transportation. Environ Sci Technol **2011**;45(17):7554-60.

(12) Oswald WK. Advanced integrated wastewater pond systems. Proceedings of the ASCE Convention **1990**: 73–80.

(13) Noüe J, Laliberté G, Proulx D. Algae and waste water. J App Phycol **1992**;4(3):247–54.

(14) Lundquist TJ, Woertz IC, Quinn NWT, Benemann JR. A Realistic Technology and Engineering Assessment of Algae Biofuel Production. Energy Biosciences Institute, University of California, Berkeley; **2010**.

(15) Wigmosta MS, Coleman MA, Skaggs RJ, Huesemann MH, Lane LJ. National microalgae biofuel production potential and resource demand. Water Resour Res **2011**;47(W00H04):13pp.

(16) Sheehan J, Dunahay T, Benemann J, Roessler P. A Look Back at the U.S. Department of Energy's Aquatic Species Program. Biodiesel from Algae. U.S. Department of Energy, Office of Fuels Development; **1998**.

(17) Stephenson AL, Kazamia E, Dennis JS, Howe CJ, Scott SA, Smith AG. Life-Cycle Assessment of Potential Algal Biodiesel Production in the United Kingdom: A Comparison of Raceways and Air-Lift Tubular Bioreactors. Energ Fuel **2010**;24(7):4062-77.

(18) Grobbelaar JU. Factors governing algal growth in photobioreactors: the 'open' versus 'closed' debate. J Appl Phycol **2008**;21(5):489-92.

(19) Matsumoto H, Shioji N, Hamasaki A, Ikuta Y, Fukuda Y, Sato M, Endo N, Tsukamoto T. Carbon dioxide fixation by microalgae photosynthesis using actual flue gas discharged from a boiler. Appl Biochem Biotech **1995**;51(1):681-92.

(20) Vunjak-Novakovic G, Kim Y, Wu X, Berzin I, Merchuk JC. Air-Lift Bioreactors for Algal Growth on Flue Gas: Mathematical Modeling and Pilot-Plant Studies. Ind Eng Chem Res **2005**;44(16):6154-63.

(21) Lee JS, Kim DK, Lee JP, Park SC, Koh JH, Cho H-S, Kim SW. Effects of SO2 and NO on Growth of Chlorella sp. KR-1. Bioresource Technol **2002**;82(1):1-4.

(22) Yoo C, Jun SY, Lee JY, Ahn CY, Oh HM. Selection of microalgae for lipid production under high levels carbon dioxide. Bioresource Technol **2010**;101(1):S71-4.

(23) Weissman JC, Goebel RP. Design and Analysis of Microalgal Open Pond Systems for the Purpose of Producing Fuels. Golden, CO: Solar Energy Research Institute; **1987**.

(24) Nielsen PH, Jørgensen KR. Municipal wastewater treatment. LCA food database, **2002**. Available at: http://www.lcafood.dk/processes/wastetreatment/wastewatertreatment.htm [Accessed: 05.05.11].

(25) Maurer M, Schwegler P, Larsen T. Nutrients in urine: energetic aspects of removal and recovery. Water Sci Technol **2003**;48(1):37-46.

(26) Grobbelaar JU. Mineral Nutrition. in Richmond A (ed) Handbook of Microalgal Culture Biotechnology and Applied Phycology, Oxford, UK: Blackwell; **2004**.

(27) Downing JB, Bracco E, Green FB, Ku AY, Lundquist TJ, Zubieta IX, Oswald WJ. Low cost reclamation using the Advanced Integrated Wastewater Pond Systems® Technology and reverse osmosis. Water Sci Technol **2002**;45(1):117-25.

(28) Crites RW, Tchobanoglous G. Small and Decentralized Wastewater Management Systems. McGraw-Hill; **1998**.

(29) Scheehle EA, Doorn MRJ. Improvements to the US Wastewater Methane and Nitrous Oxide Emissions Estimates. US EPA; **2001**.

(30) Oil: Crude and Petroleum Products - Energy Explained, Your Guide To Understanding Energy. Available at: http://www.eia.doe.gov/energyexplained/index.cfm [Accessed: 22.07.10].

(31) Clean Watersheds Needs Survey 2008. Report to Congress, U.S. Environmental Protection Agency; **2008**.

(32) EIA - Emissions of Greenhouse Gases in the U.S. **2008**-Carbon Dioxide Emissions. Available at: http://www.eia.doe.gov/oiaf/1605/ggrpt/carbon.html [Accessed: 03.08.10].

(33) United States Census 2000, United States Census Bureau. Available at: http://www.census.gov/main/www/cen2000.html [Accessed: 03.08.10].

(34) Gurney KR, Mendoza D, Zhou Y, Fischer M, Miller C, Geethakumar S, de la Rue S. The Vulcan Project: High resolution fossil fuel combustion CO2 emissions fluxes for the United States. Environ Sci Technol **2009**; 43(14):5535-41.

(35) Tamiya H, Hase E, Shibata K, Mituya A, Iwamura T, Nihei T, Sasa T. Kinetics of Growth of Chlorella, with Special Reference to its Dependence on Quantity of Available Light and on Temperature. In Burlew JS (ed) Algal Culture, from Laboratory to Pilot Plant. 5th ed. Carnegie Institution of Washington Publication 600; **1953**.

(36) Atkins WRG, Poole HH. Photoelectric measurements of the luminous efficiency of daylight. P Roy Soc Lond B Bio **1936**; 121(820):1-17.

(37) NREL: Dynamic Maps, GIS Data, and Analysis Tools. Available at: http://www.nrel.gov/gis/ [Accessed: 13.07.10].

(38) PRISM Climate Group, Oregon State University. Available at: http://www.prism.oregonstate.edu/ [Accessed: 13.07.10].

(39) Deininger RA, Su SY. Modelling Regional Waste Water Treatment Systems. Water Res **1973**; 7(4): 633-46.

(40) The 2002 Financial Survey: A National Survey of Municipal Wastewater Management Financing and Trends. Association of Metropolitan Sewerage Agencies; **2002**.

CHAPTER 3. GROWING ALGAE FOR BIODIESEL ON DIRECT SUNLIGHT OR SUGARS: A COMPARATIVE LIFE CYCLE ASSESSMENT

3.1 Abstract

Growing heterotrophic algae in fermenters with sugar as the energy and carbon source rather than sunlight and carbon dioxide is an approach being commercialized today. However, the full environmental impacts of this fuel pathway have not been explored. The objective of this analysis was to compare the life-cycle impacts of algal biodiesel produced heterotrophically to a phototrophic pathway featuring algae grown in ponds. A third, hybrid approach utilizing algae capable of both phototrophy and heterotrophy was also explored. Sugar beet and sugarcane were examined as feedstocks for the heterotrophic process.

The results indicate that a reduction in the global warming potential (GWP) and an improvement in the fossil energy ratio (FER) for algal biodiesel could be possible for the heterotrophic and hybrid pathways relative to the phototrophic, but only if fermentation can be performed efficiently and with sugarcane as the feedstock. Sugar crops used as feedstocks for heterotrophic cultivation require more land and present concerns about land constraints that are not an issue for the phototrophic pathway. No

pathway presented a clear advantage for the water stress impact metric. Reductions in the impact of heterotrophic algal biodiesel could be achieved by using cellulosic sugars or waste feedstocks for fermentation.

3.2 Introduction

The United States intends to increase domestic biofuel production in an effort to reduce dependence on imported petroleum and mitigate the impacts of global warming[1]. Since carbon dioxide from the atmosphere is sequestered via photosynthesis during feedstock production, biofuels have the potential to reduce the life-cycle emissions of greenhouse gases (GHGs) and the overall global warming potential (GWP) relative to conventional fossil fuels. However, life-cycle analyses (LCAs) of first-generation biofuels such as corn ethanol and soy biodiesel indicate that these benefits can be greatly reduced by the impacts associated with the production of these energy crops and their conversion into liquid fuels[2–5]. Furthermore, the land required to produce these crops could displace agricultural operations, presenting the possibility of land use change (LUC) and indirect land use change (iLUC)[6–9].

Phototrophic algae have been proposed as an alternative bioenergy feedstock because of its high growth rate and aerial productivity[10]. By growing algae in open ponds, biomass can be produced on marginal, non-arable lands that are not currently used for agriculture[11]. The proposed biofuels target of 36 billion gallons annually by 2022 set by the US Energy Independence and Security Act means that land constraints will become more important as production volumes increase[1]. Furthermore, cultivation

in ponds on marginal land means that the potentially deleterious effects of LUC and iLUC can be minimized.

Achieving large-scale production of phototrophic algae has proven difficult, however, primarily due to the capital and operational costs of open ponds[12,13]. Additionally, the relatively low biomass concentration (which typically does not exceed ~0.5 $g \cdot L^{-1}$) requires significant energy inputs to circulate the large volumes of water and to concentrate the harvested biomass[14]. These challenges have prompted exploration of an alternative approach to growing algae: heterotrophic cultivation. Unlike phototrophic algae, the metabolism of heterotrophic algae facilitates fast growth in unlit fermenters whereby energy is derived from an organic carbon source rather than sunlight[15]. Mixotrophic species of algae, which can use either sunlight or organic carbon for energy depending on their environment, have also been investigated as part of a hybrid pathway[16–18].

This study features a comparative life-cycle assessment (LCA) evaluating algal biofuel production pathways featuring photo-, mixo-, and heterotrophic metabolisms. To our knowledge, this is the first such analysis of its kind outside of private sector studies which have not been made public. While several recent LCAs have evaluated algal biofuel[19–22], compared biofuels from phototrophic algae to other biofuels[23], examined various cultivation strategies for algal biofuels[24,25], and focused on downstream conversion technologies[26,27], none have evaluated heterotrophic or hybrid cultivation strategies. This gap in the literature is noteworthy given that several of the leading

private firms in the algae industry, as well as numerous academic groups, are currently pursuing these approaches.

3.3 Methodology

3.3.1 Modeling Framework

Modeling was conducted using SimaPro LCA Software, Microsoft Excel spreadsheets, ArcMap spatial analysis software, and MATLAB. Phototrophic pathway process assumptions and operational parameters were based on Argonne National Laboratory's Greenhouse Gases, Regulated Emissions, and Energy Use in Transportation (GREET) model, a well-established analytical tool for fuel LCA modeling[28]. This framework was expanded to model additional pathways and to consider the environmental impact metrics of land use and water stress through a geographic information systems (GIS) approach.

The algal biofuel industry is still nascent and thus a variety of technologies are under development for nearly all major aspects of the production process (i.e., biomass cultivation, dewatering, biomass conversion, and nutrient recycling). The GREET model was selected for the baseline phototrophic pathway because it makes well-justified process technology selections and provides thorough supplementary resources that make the underlying computations transparent and replicable. The model's process assumptions include use of lipid-extracted algae (LEA, which is the biomass remaining after the lipid has been removed) as a feedstock for anaerobic digestion. An advantage

of this approach is that electricity and heat are produced and used onsite to displace energy imports rather than utilizing the LEA as a co-product (e.g., animal feed).

Another important assumption of the GREET model is that CO_2 is provided from a power utility's flue gas. The energy required to transport the flue gas is considered, but otherwise the CO_2 is treated as atmospheric because that would have been its fate had it not been pumped to the algae pond. An implication of such an assumption is that a carbon sequestration credit cannot be applied for both the power utility *and* the biofuel. Here, the sequestration credit is assigned to the algae. This analysis incorporates the same impact factor and distance assumptions as the GREET model for modeling the transportation of the digestate to the field and handling of the extracted oil through refinement and distribution. This model also adheres to the same co-product allocation used by GREET for calculating the energy balance and carbon emissions. The impacts associated with lipid production are shared between the algal oil and any energy sent beyond the system boundary, such as surplus electricity generated on site. The distribution was based on energy content of the oil and that of the exported electricity and was only applicable for the highest efficiency scenario explored for the heterotrophic and hybrid pathways. An allocation was also used for the lipid conversion step based on the energy in the fuel and the glycerin co-product[28,29].

The phototrophic pathway model used in this analysis deviates from the GREET model in several ways. Most notably, the GIS analysis described later explores the effect of spatially variable climate parameters on algae yield and evaporative water loss rather

than using fixed values. This analysis also incorporates a biomass stoichiometry outlined by Lardon et al. (2009)[26] and when applicable uses updated values provided in a harmonization study that was published more recently than the original GREET LCA[30].

A summary of the process flow model is shown in Figure 3.1 and a list of key parameters used to generate the material and energy inventories for the three pathways is provided in Table 3.1.

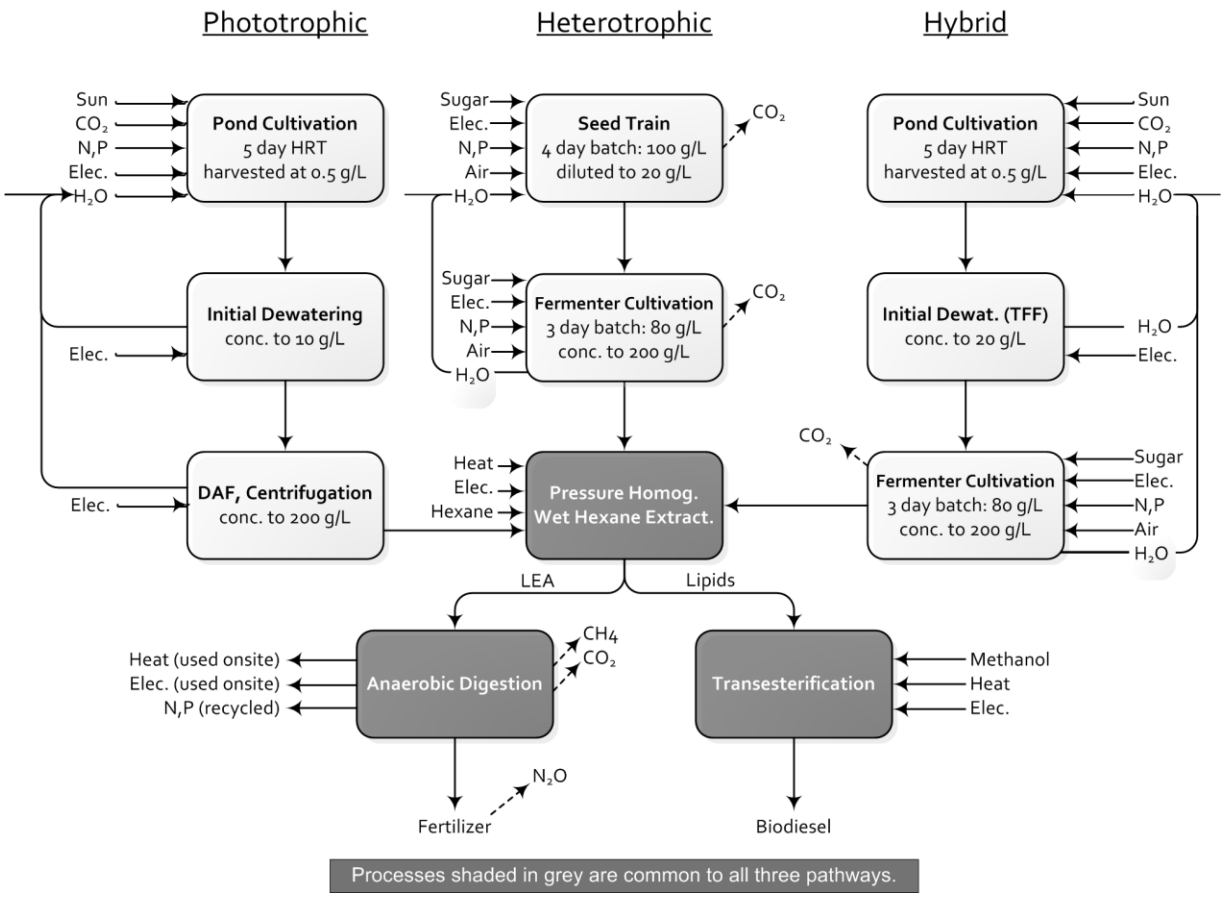

Figure 3.1 - Simplified process flow diagram summarizing the key inputs and outputs associated with the phototrophic, heterotrophic, and hybrid algal biodiesel production pathways.

3.3.2 Phototrophic Pathway

For the phototrophic pathway, algae biomass is assumed to be produced in open raceway ponds and circulated with a horizontal paddlewheel with operational assumptions conforming to those outlined by GREET[28]. While it is possible to cultivate algae in photobioreactors, recent analyses suggest that with current technologies this is impractical from both an environmental impact and economic perspective[25]. An average biomass yield of 25 $g \cdot m^{-2} \cdot day^{-1}$ for the baseline scenario allows for one fifth of the pond's volume to be withdrawn daily at a concentration of 0.5 $g \cdot L^{-1}$. Regional variations of this average yield are also explored in the assessment of the land use and water stress impacts. The dilute biomass is pumped to a settling pond where the addition of flocculants allows a concentration of the biomass to 10 $g \cdot L^{-1}$; removed water is recycled back to the pond. Subsequent dewatering using dissolved air flotation (DAF) and centrifugation further concentrates the biomass to 200 $g \cdot L^{-1}$.

This slurry is processed wet to extract to the oil because thermal drying would offset much of the energy content of the biodiesel product[26]. Algae cells are first lysed by pumping the slurry through a small orifice in a process called high-pressure homogenization and then contacted with hexane to extract the lipids. Following removal of the solids (i.e., LEA), the hexane is evaporated and recovered, resulting in crude algae oil. Removing the residual solvent from the solids yields the LEA. The crude oil is upgraded via transesterification with methanol to produce biodiesel while the LEA is sent to an anaerobic digester. The biogas produced from the digester is scrubbed to remove H_2S and then utilized in a combined heat and power (CHP) system to produce

heat and electricity to be used on site. The amount of energy recovered from the LEA is sufficient to meet all of the thermal energy demands for the phototrophic pathway and the majority of the electricity requirements. We assume here that approximately three quarters of the nitrogen and half of the phosphorus are recovered from the digester supernatant and recycled to the cultivation pond to reduce fertilizer inputs as outlined by the GREET process model[28].

Table 3.1 - Parameters used in biofuel process pathway modeling.

			Pathways Used			
Step	**Value**	**Units**	**Photo.**	**Hetero.**	**Hybrid**	**Ref.**
Open Pond Cultivation						
Paddle-Mixing Energy Inputs	2000	$W \cdot ha^{-1}$	✓		✓	12,28,30
CO_2 Uptake Efficiency	0.85	n/a			✓	28
Evaporative Water Loss (Make-Up Inputs)	GIS$^{\lambda}$	$m^3 \cdot kg\text{-}algae^{-1}$	✓		✓	31,32
Biomass Productivity	25$^{\alpha}$, GIS	$g \cdot m^{-2} \cdot day^{-1}$	✓		✓	12, 32–34
Phototrophic Biomass Lipid Content	0.25$^{\delta}$	n/a	✓		✓	12,28,30
Operational Period, per Year	330	days	✓	✓	✓	30
Pumping, to Site	$1.23 \cdot 10^{-4}$	$kWh \cdot L^{-1}$				30
Fermenter Cultivation						
Yield on Sugar	0.25$^{\zeta}$	$kg\text{-}lipid \cdot kg\text{-}glucose^{-1}$		✓	✓	35
Aeration/Mixing Energy for 80 $g \cdot L^{-1}$	3$^{\beta}$, 2, 1	$kW \cdot m^{-3}$		✓	✓	18,36,37
Heterotrophic Biomass Lipid Content	0.5			✓		38
Hybrid Pathway Heterotrophic Biomass Lipid Content	0.55$^{\tau}$				✓	18
Harvesting/Dewatering						
Pumping, on Site	$2.5 \cdot 10^{-5}$	$kWh \cdot L^{-1}$	✓	✓	✓	30
Centrifugation Energy Inputs	$1.93 \cdot 10^{-2}$	$kWh \cdot kg\text{-}algae^{-1}$	✓	✓		30
DAF Energy Inputs	0.133	$kWh \cdot kg\text{-}algae^{-1}$	✓			28,39
Tangential Flow Filtration (TFF)	$5 \cdot 10^{-4}$ $^{\gamma}$	$kWh \cdot L^{-1}$			✓	
Secondary Centrifugation Energy	$8 \cdot 10^{-3}$	$kWh \cdot L^{-1}$		✓	✓	28,40,41
Cell Preparation						
Pressure Homogenization Energy	0.204	$kWh \cdot kg\text{-}algae^{-1}$	✓	✓	✓	28,13,24
Pressure Homogenization Mass Ret. Efficiency	0.9		✓	✓	✓	28
(Wet) Hexane Extraction						
Extraction Electricity Inputs	0.069	$kWh \cdot kg\text{-}oil^{-1}$	✓	✓	✓	30
Extraction Heat Inputs	3.09	$kWh \cdot kg\text{-}oil^{-1}$	✓	✓	✓	30
Hexane Inputs (amount lost)	5.2	$g\text{-}hexane \cdot kg\text{-}oil^{-1}$	✓	✓	✓	28

Transesterification						
Methanol Requirement	0.1001	kg-methanol·kg-biodiesel^{-1}	✓	✓	✓	29,42,43
Transesterification Heat Inputs	2.07	MJ·kg-biodiesel^{-1}	✓	✓	✓	29,42,43
Transesterification Electricity Inputs	0.107	MJ·kg-biodiesel^{-1}	✓	✓	✓	29,42,43
Anaerobic Digestion						
Digestion Heat Inputs	0.22	kWh·kg-TS^{-1}	✓	✓	✓	30
Digestion Electrical Inputs	0.085	kWh·kg-TS^{-1}	✓	✓	✓	30
CHP Electrical Efficiency	0.33		✓	✓	✓	28
CHP Total Efficiency	0.76		✓	✓	✓	28
Biogas Yield	0.45	L-biogas·g-TS^{-1}	✓	✓	✓	28
Biogas Cleanup Electrical Inputs	0.25	kWh·m^{-3} biogas	✓	✓	✓	28,44
Fertilizer Co-Product						
Fraction of N in Digestate	0.20		✓	✓	✓	28
Fraction of P in Digestate	0.50		✓	✓	✓	28
Nitrous Oxide Emissions	0.01	kg-N_2O-N·kg-N^{-1} in fert.	✓	✓	✓	28,45
Sugar Sources						
Sugar Beet Crop Yield, Sucrose Content	GIS	tonnes·ha^{-1}, %		✓	✓	46
Sugarcane Crop Yield, Sucrose Content	GIS	tonnes·ha^{-1}, %		✓	✓	46
Sugar Beet, Sugarcane Irrigation Requirements	GIS	L-H_2O·tonne^{-1}		✓	✓	47,48
Surplus Bagasse Electricity	135$^{\rho}$	kWh·tonne-cane^{-1}		✓	✓	49

$^{\lambda}$The term *GIS* indicates that a variety of values were incorporated into the model using geographic information systems analyses conducted using the data sources referenced.

$^{\alpha}$A value of 25 g·m^{-2}·day^{-1} was used as a baseline, but the GIS analysis was used for determining land occupation and water stress results.

$^{\delta}$For the hybrid pathway, algae are harvested from the pond with a lipid content of 25% prior to being cultivated in the fermenter where the lipid content reaches 55%.

$^{\zeta}$The reference's authors state that 0.22 kg-lipid·kg-glucose^{-1} is a practical conversion limit with a maximum theoretical conversion limit of 0.33 kg-lipid·kg-glucose^{-1}. The value of 0.25 kg-lipid·kg-glucose^{-1} was selected as an optimistic approximation.

$^{\beta}$An average value of ~3 kW·m^{-3} for the entire duration of the fermentation batch was modeled based on derivations from the references listed. More efficient technology scenarios of 2 and 1 kW·m^{-3} were also explored.

$^{\tau}$In the authors' optimized scenario a maximum lipid content of 58% was achieved for this pathway. In a production setting the biomass would likely be harvested prior to achieving the maximum lipid content; the value of 55% was chosen as an approximation.

$^{\gamma}$This value is for the volume of water processed, based on communications with an industry manufacturer for a 40X concentration factor from 0.5 g·L^{-1} to 20 g·L^{-1}.

$^{\rho}$The authors cite this value as an achievable surplus of co-generated electricity (remaining after process requirements at the sugar plant) for the year 2020. In this model most or all of this electricity is used on-site for fermenter aeration/mixing and processing requirements.

3.3.3 Heterotrophic Pathway

Heterotrophic biomass is cultivated in a cylindrical fermenter modeled with a height to width ratio of 2:1. The algal biomass is grown from an initial concentration of 20 $g \cdot L^{-1}$ to 80 $g \cdot L^{-1}$ over a three day batch, approximations based on results from Xiong et al. (2010)[18]. The two most significant inputs for this stage are the aeration & mixing electrical energy inputs required for operating the fermenter and the upstream impacts associated with producing the sugar source that is fed to the algae. Modeling the fermenter energy requirements for aeration and mixing proved to be a challenge; there are limited examples in literature and within this small sample there are significant discrepancies in the maximum biomass concentrations observed and the time required to achieve these concentrations. Uncertainty is exacerbated by the fact that the private sector does not publicize details about its technology's performance. The 80 $g \cdot L^{-1}$ concentration achieved by Xiong et al. is relatively high compared to results reported in other academic papers [15,17,50–52], but is likely still lower than concentrations achieved by private sector firms with the financial resources to pursue optimized operations and to employ genetic engineering. Centrifugation is used to further concentrate the biomass to 200 $g \cdot L^{-1}$ prior to cell rupture and lipid extraction, which is modeled using the same process assumptions described above for the phototrophic pathway. The heterotrophic algal biomass is assumed to have 50% lipid content rather than the 25% lipids modeled for the phototrophic pathway. Studies have shown lipid content ranging from 15% to 55%[17,51–53], but 50% is typical. The high lipid content of heterotrophic algae means less total biomass must be processed to produce the same amount of fuel and less nitrogen

and phosphorus inputs are required, but also less energy can be recovered via anaerobic digestion due to reduced LEA yields.

Fermenter aeration & mixing energy was calculated based on the oxygen uptake rate reported by Bottomley and Baalen (1978) for a heterotrophic alga *Nostoc* and energy calculations were conducted as prescribed by the Environmental Protection Agency (EPA) Design Manual for Fine Pore Aeration Systems (1989)[36,37]. These energy inputs could most likely be reduced below our estimates by optimizing fermenter design and operation (e.g., impeller speed and blower size) as well as through the use of genetically engineered species with higher lipid content, increased glucose conversion efficiency, and lower oxygen requirements. Therefore the baseline fermenter aeration and mixing energy, determined to be ~3 $kw \cdot m^{-3}$ based on the outlined operating assumptions, was explored alongside two improved technology scenarios of 2 and 1 $kW \cdot m^{-3}$. Approximately 40% of this power is mechanical mixing and the remaining is for diffused air injection. A seed train has been modeled to provide the initial biomass for the production fermenter. This seed train is a fermenter vessel that is one-fifth the volume of the production fermenter, and it is assumed that a concentration of 100 $g \cdot L^{-1}$ is achieved after four days of cultivation. The biomass slurry is then transferred to the production fermenter along with additional sterile media to provide the diluted initial concentration of 20 $g \cdot L^{-1}$. The impacts associated with providing the inoculum for the seed train are neglected, as is the case with the phototrophic and hybrid pathways.

Sugarcane and sugar beet were considered in this analysis, as these are the two primary sources of sugar produced within the United States[46]. An inventory for the agricultural operations and sugar processing was adapted from work by Macedo et al. (2008), which analyzed sugarcane production in Brazil and projected a scenario for the future that is feasible with existing technologies[49]. Crop yields, sucrose content fractions, and irrigation requirements are of course different in the United States than in Brazil (and in fact have significant variations within the United States), so domestic data were used for these aspects of the study. A significant amount of energy from the sugarcane crop resides in the bagasse, the fibrous material remaining after the juice has been extracted[54]. This analysis incorporates the assumption that the bagasse is combusted and used in a high-pressure cogeneration steam cycle system to produce electricity onsite, similar to how sugarcane is used at ethanol refineries in Brazil. The model assumes that a surplus electricity export of 135 kW·hr per tonne of sugarcane is produced (after on-site energy is utilized at the sugar plant), corresponding to the technology forecast for Brazil in the year 2020[49]. This electricity export would be equivalent to 23% electrical efficiency if 28% of the sugarcane crop is bagasse with an energy content of 7.62 $MJ \cdot kg^{-1}$ (at 50% moisture), which are similar to values reported for a sugar plant in Florida[55]. The cogenerated electricity reduces the amount of electricity required to be imported from the grid. In the case of the 1 $kW \cdot m^{-3}$ aeration/mixing energy scenario there is a surplus of electricity that is exported and assumed to displace grid electricity.

3.3.4 *Hybrid Pathway*

The hybrid pathway is similar to the heterotrophic pathway but an open pond system is used in place of the seed train to provide the initial biomass. Biomass is grown to 0.5 g·L-1 in the pond and 20% of the pond volume is harvested each day, as in the phototrophic case. The harvested culture is concentrated by tangential flow filtration (TFF) to 20 g·L-1 and then pumped into a production fermenter. The two main rationales for exploring this pathway are that producing a fraction of the biomass photosynthetically reduces sugar demands and there is evidence to suggest the efficiency of heterotrophic growth can be improved by using a light-grown seed culture[18]. Xiong et al. (2010) showed that *Chlorella protothecoides* grown phototrophically and then heterotrophically exhibited a higher sugar conversion efficiency and a higher lipid content than cells grown only heterotrophically (cf. 58%[18] vs. 50%[38]). They hypothesized that phototrophically grown cells retain the capacity to uptake CO_2 released by heterotrophic metabolism after incubation with glucose, thereby more efficiently converting feedstock carbon into biomass. In a related work, Heredia-Arroyo et al. (2010) also demonstrated higher lipid content for mixotrophic biomass compared to heterotrophic biomass[17].

Therefore a lipid content of 55% is assumed rather than the value of 50% assumed for the heterotrophic system. Each pathway features the same processes mentioned previously for cell rupture, lipid extraction, oil upgrading, and energy recovery via anaerobic digestion. The composition of the biomass is different for each of the pathways, however, based on assumptions of the macromolecule composition (i.e. lipid,

carbohydrate, and protein fraction) provided by Lardon et al. (2009)[26] and consequently the elemental mass flows (i.e. carbon, nitrogen, phosphorus) are unique to each process. The Supporting Information provides further detail about these assumptions.

3.4 Spatial Analysis

As with any bioenergy system, the environmental impacts vary greatly depending on the region. The locations where phototrophic algae grow most quickly, for example, also typically experience more evaporation than rainfall. If the make-up water is removed from a depleted resource, the stress to the aquifer can be substantial[28,56]. Similarly, the amount of occupied land and water use associated with cultivating algae on sugars depends largely on the type of crop used (sugarcane or sugar beet) to produce the sugar. The water stress depends on the crop's yield, the amount of irrigation water required, and, as with the phototrophic pathway, the condition of the aquifer from which the water is withdrawn[56,57]. Therefore a GIS approach was used to evaluate the effect of these regional considerations toward the variability of the results.

Annual pan evaporation data from the National Oceanic and Atmospheric Administration (NOAA) for several hundred specific sites[31] was used in conjunction with a dataset of national average annual precipitation[58] and overlaid with a GIS layer summarizing the average growth rate for algae grown in phototrophic ponds across the nation[59]. The average phototrophic growth rate data layer was built upon national historical solar insolation and temperature profiles and a growth model that predicts algae yield based on these criteria. The evaporation data was published by NOAA in

1982; it is possible that national climate trends have shifted slightly in the last three decades, but the dataset was chosen due to a lack of an alternate national data source. Statewide average crop-specific irrigation water use data[47] was used with county-level crop yield estimates from the National Agricultural Statistics Service (NASS) [46] and previous research results outlining water stress indices for specific aquifers[56] to derive the occupied land and water stress of the mixotrophic and heterotrophic pathways.

Figure 3.2 illustrates the approach used to determine the water stress. On the lower tier of graphic *A* each point represents a location where evaporation rates have been measured; the difference between evaporation and precipitation at that location is indicated by the height of the bar extending from that point. Net losses (more evaporation than precipitation) are shown in red and net gains are in blue with the losses protruding downward and the gains upward. The top tier of graphic *A* indicates the average annual phototrophic algae yield, with red being the greatest yield and blue the least. The growth rate affects the water use because locations with high yields require smaller ponds and hence less area exposed to evaporative losses. The points that are emphasized with a black circle have average annual phototrophic biomass yields exceeding 20 $g \cdot m^{-2} \cdot day^{-1}$ and are therefore considered realistic sites for open pond cultivation; the other, less productive, sites are excluded from the analysis. In both graphics the grayscale shading indicates the water stress index (WSI) of the groundwater source at that location, with darker shades indicating the most stressed aquifers. The WSI values, which are derived from the ratio of water withdrawn from the aquifer to the total amount of water available, were obtained from Pfister et al.

(2009)[56]. To simplify the analysis it is assumed that the water withdrawn for power generation comes from the same aquifer used for algae and/or sugar cultivation for all three pathways. In graphic *B,* the counties shaded with red produce sugar from sugar beet and counties shaded with blue from sugarcane. The pie charts indicate the fraction of blue, green, and grey water required to produce the crop. Blue water refers to water that is withdrawn from a surface or groundwater source, as opposed to green water which is received from precipitation. The size of the pie indicates the volume of sugar produced in that state as reported by the NASS[46]. The scale of production in each of the regions is significant because the results are reported by the volume-weighted average.

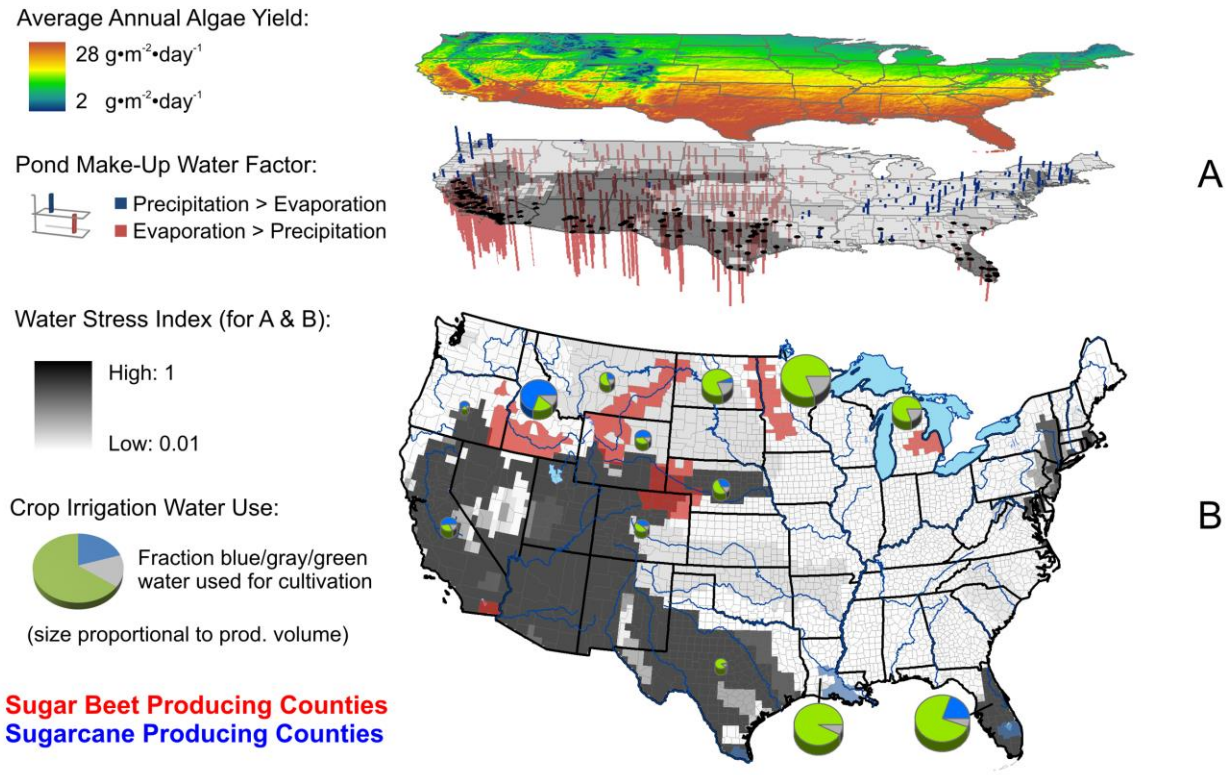

Figure 3.2 - Summary of the GIS analysis used to determine the water stress impact of the phototrophic pathway (A) and heterotrophic pathway (B). Water stress for the hybrid pathway is derived from co-located results of the other two pathways.

Recall that a benefit of phototrophic algae is that it can be grown with higher aerial productivity than terrestrial crops and on marginal lands that could not be used for agriculture. The arable land used to grow sugar for cultivation of algae in fermenters, conversely, is not exempt from the land constraint concerns that surround other biofuels. The effects of land use change must therefore also be discussed in the analysis. The premise of including effects of LUC and iLUC is that as food crops are diverted for use in biofuels, the global food market will respond by adding new agricultural capacity elsewhere to satisfy global demand[60]. As land is cleared to serve its new purpose substantial amounts of carbon emissions are released as organic carbon stocks, both above ground and below, are converted to GHGs by microbial decay and burning[61,62]. The amount of carbon emitted depends heavily on the type of land converted and the long-term accumulation or continued release of soil organic carbon depends on the vegetation type that is planted[63].Plevin et al. (2010) evaluated the effects of iLUC with special attention to uncertainty[64]. Their model was only applied to US corn ethanol, however, and therefore cannot be directly incorporated into this study.

Two agencies within the United States have published land use carbon emission factor values for sugarcane ethanol. The EPA implemented the model developed by the Food and Agricultural Policy and Research Institute in the Center for Agricultural and Rural Development (FAPRI-CARD) at Iowa State University[65]. The California Air Resource Board (CARB) implemented the Global Trade Analysis Project (GTAP) model developed by the Center for Global Trade Analysis at Purdue University[66]. The results obtained by these two models highlights the uncertainty associated with such calculations, as the

emissions reported by the CARB are nearly an order of magnitude greater than those reported by the EPA[67–69]. The discrepancy between the models is primarily due to differences in assumptions on volume of increased ethanol production, elasticity of input parameters, and the land conversion emission values[67]. Results from these models were adapted for this analysis to demonstrate the range of possible emissions from LUC and iLUC. The energy content of algal biodiesel is higher than that of ethanol while the yield of fuel per unit of sugar is lower, so adjustments to the emissions factors were required. Comparable studies for production of ethanol from sugar beets have not been conducted, so this analysis assumes that the carbon emissions from LUC and iLUC will be the same regardless of whether the sugar is sourced from sugarcane or sugar beet. This is an oversimplification, but regardless of the sugar crop used to source the sugar the effect on global demand is similar and therefore the implications on indirect land use are likely also similar.

3.5 Results & Discussion

3.5.1 Fossil Energy Ratio

The fossil energy ratio (FER) was calculated for biodiesel produced from each pathway and the results are shown in Figure 3a. It is apparent that biodiesel from each pathway, with the exception of the heterotrophic and hybrid pathways with the highest fermenter operational energy expenditure (3 $kW \cdot m^{-3}$), achieve a FER greater than unity and represent an improvement relative to fossil diesel. For example, the baseline phototrophic case produces fuel with a FER that is about 2-fold higher than fossil diesel.

The sharp decline in FER with an increase in fermenter operational energy input suggest this is one of the key determinants of the impact of biodiesel arising from the heterotrophic and hybrid pathways. Notably, the data presented in Figure 3a assumes sugarcane is the carbon feedstock. In contrast, when using sugar beet, a FER greater than one is not achieved in any of the technology scenarios (results provided in the Supporting Information).

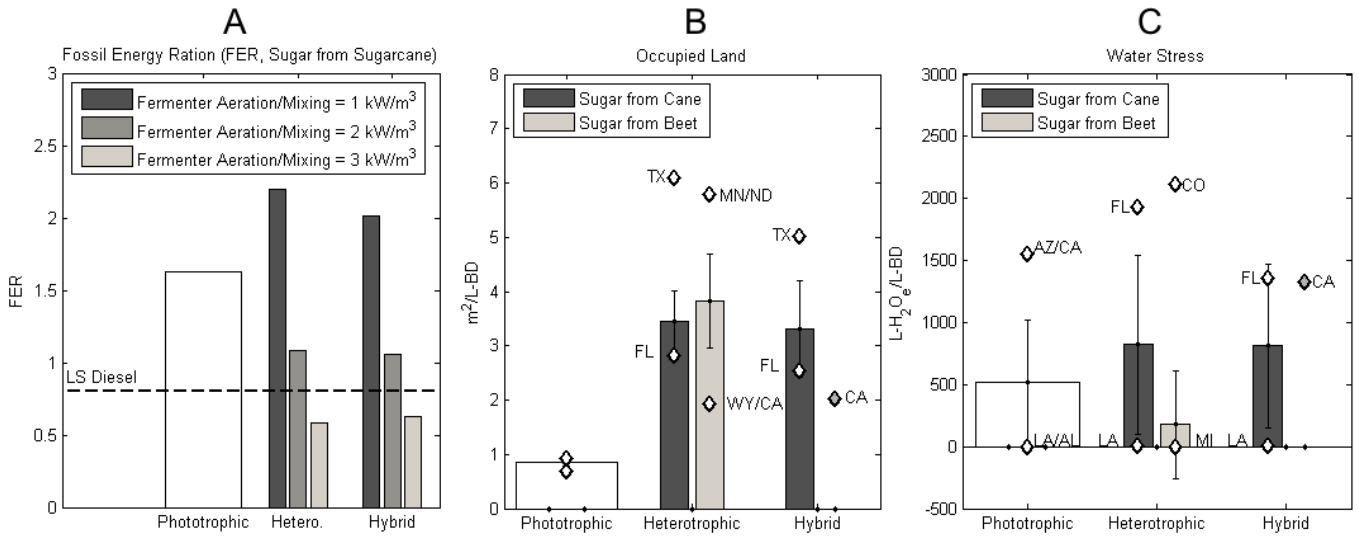

Figure 3.3 - Results of the life-cycle assessment for the fossil energy ratio (FER), occupied land, and water stress impact metrics. The dashed line on chart A indicates the baseline for conventional diesel fuel. The diamonds on charts B and C indicate high/low values based on the range of locations considered in the GIS analysis.

3.5.2 Occupied Land

The phototrophic pathway requires less land than the other pathways, as shown in Figure 3b. This result is not surprising because one of the appealing features of phototrophic algae is its fast growth rate relative to terrestrial bioenergy crops like sugar beet and sugarcane. In the United States, sugar beet and sugarcane have comparable sugar production per hectare, so the land footprint is similar. The diamond

points indicate the full range of values observed in the GIS analysis, with the labels indicating the state where the maximum or minimum value was observed. The occupied land associated with upstream fertilizer and electricity production accounted for less than 3% of the land footprint for the phototrophic pathway, with the rest of the impacts coming from the cultivation ponds. Land for growing the sugar crop dominated the footprint for the heterotrophic pathway, with the upstream impacts of the rest of the inputs contributing less than a percent of the total result.

3.5.3 *Water Stress*

Water stress results were highly geographically dependent, as shown in Figure 3c, with no clear difference among the three pathways. Sites with high precipitation relative to evaporation and access to aquifers that are not stressed will have a low water stress impact regardless of which pathway or sugar crop is used. Heterotrophic algae cultivated on sugar from sugar beet had the lowest average water stress, but, as with each of the scenarios, a range of results was observed depending primarily on the regional stress indices. Recall that blue water refers to withdrawn water while green water is that which is received from precipitation. Sugar beet or sugarcane cultivation sites that have sufficient precipitation require little or no blue water extraction for irrigation and hence inflict less water stress. This correlation is not always true, however. For example, sugar beet farms in Idaho require more blue water than farms in Colorado, but the aquifers in Idaho are under less stress and therefore the water stress impact of sugar from Colorado sugar beet is greater. For phototrophic cultivation, focus has typically been on the southwestern portion of the United States such as Arizona and

New Mexico, but these arid locations have high evaporative losses and the water resources are often stressed. For reduced water stress, open pond cultivation should shift toward southeastern locations like Louisiana and Alabama where the water stress is much lower despite the slightly lower average algal biomass yields.

3.5.4 Global Warming Potential

This analysis indicates that biodiesel produced from algae can reduce GHGs by more than 50% compared to conventional diesel, thereby meeting the definition of an advanced biofuel as stipulated by the National Renewable Fuels Standard program. For example, when grown phototrophically, we predicted a 56% reduction in GHGs for algal biodiesel relative to fossil diesel. The utility of a heterotrophic algal production platform, either in isolation or as a hybrid system utilizing ponds to generate seed material, was analyzed to determine whether further reductions in life-cycle impacts could be achieved relative to the phototrophic scenario. Figure 4 illustrates the results for the GWP metric. Reductions in GWP were predicated on fermenter efficiency and the sugar source; under the most optimistic case for the heterotrophic and hybrid pathways (i.e., high efficiency fermentation, sugarcane as the sugar source, and ILUC ignored), GWP was reduced 88% and 74% relative to conventional diesel or the phototrophic pathway, respectively. If sugar beet is used, none of the heterotrophic or hybrid pathways offer a GWP reduction relative to conventional diesel (Figure 4b).

The ability to recover energy from bagasse makes sugarcane a more attractive option from the perspective of GWP and FER. In the most efficient fermentation

scenario (1 $kW \cdot m^{-3}$), there is a surplus of electricity from bagasse combustion, so all of the electricity input for the fermenter is offset and a portion of the electricity produced is returned to the grid. For the other scenarios, however, the electricity input requirements are reduced but not fully met. Sugar beets, conversely, do not have energy-rich residuals that can be utilized for energy production on site and consequently have a higher GWP. The GWP results featuring sugar from sugar beet are shown in Figure 4b, showing that in no scenario can GWP improve beyond that of fossil diesel. The Supporting Information contains a more detailed plot illustrating the impacts and credits toward the GWP results highlighting the significance of energy recovery from both anaerobic digestion of the LEA and cogenerated electricity from sugarcane bagasse.

3.5.5 Indirect Land Use Change

The potential of the most efficient heterotrophic or hybrid scenario to reduce GWP relative to the phototrophic model must be considered in light of the effects of LUC and iLUC. For example, if the values reported by CARB are used all GWP improvements are negated and the resulting release of GHGs is comparable to that of fossil petroleum-derived diesel. The black squares in Figure 4 show the results with LUC and iLUC included if the adapted values from the EPA are used and the white squares include adapted values from CARB.

The effects of LUC and iLUC are complex and therefore difficult to quantify. The concerns regarding land use as well as the uncertainties associated with the

methodologies for quantifying its impact are pursued in greater depth in academic literature elsewhere [60–62,64] and are beyond the scope of this work. The purpose of including the potential impacts from LUC and iLUC in this analysis is not to state the impacts definitively but rather to bring the topic into the discussion and provide an approximate scale of these impacts in terms of GWP. Notably, the hybrid pathway has less of a contribution to GWP from LUC and iLUC than the heterotrophic pathway because less sugar is required to produce the same functional unit of fuel due to the cultivation of a portion of the biomass in open ponds.

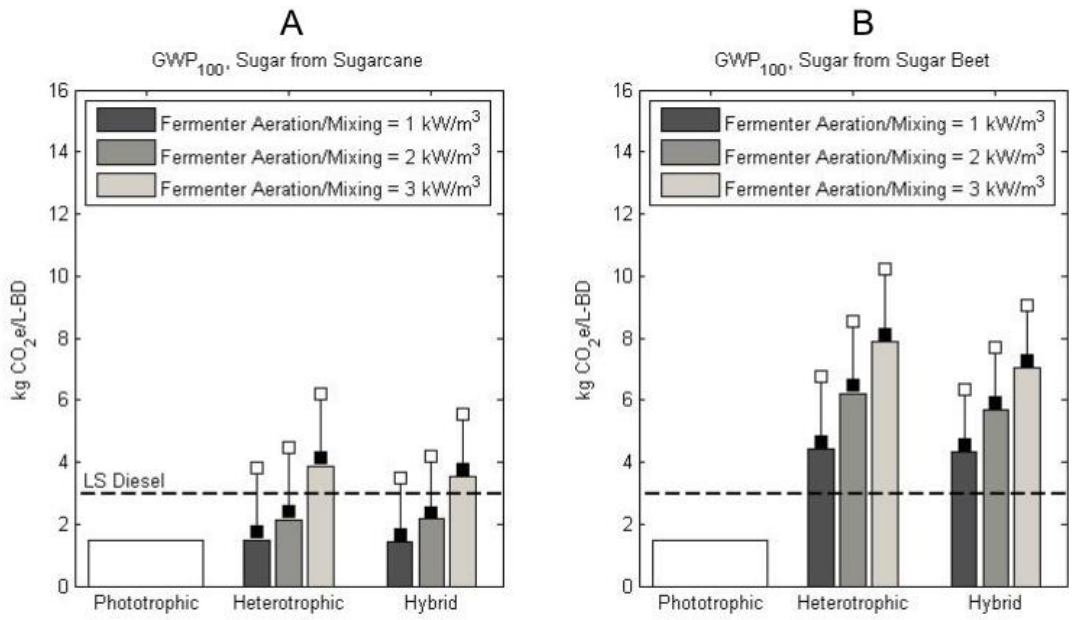

Figure 3.4 - The global warming potential (GWP) metric considering both sugar from sugarcane (A) and sugar from sugar beet (B). The black squares show the results with ILUC included if the EPA value is used and the white squares include ILUC impacts if the CARB value is used. Phototrophic cultivation does not utilize sugar and is assumed to not compete with agriculture and therefore there are no ILUC impacts.

3.5.6 Outlook

The heterotrophic and hybrid pathways have the potential to produce an algal biodiesel with reduced GWP and an improved FER relative to the phototrophic pathway

and conventional diesel, but if these technologies are to be scaled to large production volumes the consumption of sugar could result in land use changes that cannot be overlooked. The use of waste feedstocks or cellulosic bioenergy crops as the carbon source for heterotrophic cultivation could reduce these concerns, but the availability of these feedstocks is limited today (e.g., glycerol) and the technology required to process them (e.g., cellulosic sugars) have yet to be reliably demonstrated at scale. This is an area of research that deserves further exploration.

The high consumption rate of petroleum for transportation fuels suggests that purpose-grown bioenergy sources will be required if noticeable reductions in petroleum use are to be achieved. While the heterotrophic pathway is attractive since it utilizes well-established fermentation technologies, the land and resource constraints associated with producing the carbon source must be critically evaluated. The relatively small land footprint of the phototrophic pathway, conversely, facilitates scaling to large production volumes without being constrained by the availability of sugars or other carbon sources.

3.6 Chapter 3 References

(1) Act, A. Energy Independence and Security Act of 2007. *Security* **2007**, *Public Law*, 1–311.

(2) Farrell, A. E.; Plevin, R. J.; Turner, B. T.; Jones, A. D.; O'Hare, M.; Kammen, D. M. Ethanol can contribute to energy and environmental goals. *Science* **2006**, *311*, 506–508.

(3) Wang, M.; Wu, M.; Huo, H. Life-cycle energy and greenhouse gas emission impacts of different corn ethanol plant types. *Environmental Research Letters* **2007**, *2*, 024001.

(4) Pimentel, D.; Marklein, A.; Toth, M. A.; Karpoff, M. N.; Paul, G. S.; McCormack, R.; Kyriazis, J.; Krueger, T. Food Versus Biofuels: Environmental and Economic Costs. *Human Ecology* **2009**, *37*, 1–12.

(5) Wang, M.; Han, J.; Dunn, J. B.; Cai, H.; Elgowainy, A. Well-to-wheels energy use and greenhouse gas emissions of ethanol from corn, sugarcane and cellulosic biomass for US use. *Environmental Research Letters* **2012**, *7*, 045905.

(6) Pimentel, D.; Patzek, T. W. Ethanol Production Using Corn, Switchgrass, and Wood; Biodiesel Production Using Soybean and Sunflower. *Natural Resources Research* **2005**, *14*, 65–76.

(7) Taheripour, F.; Tyner, W. E.; Wang, M. Q. *GTAP Cellulosic Biofuels Analysis of Land Use Changes*; Argonne, IL, 2011.

(8) Kwon, H.-Y.; Mueller, S.; Dunn, J. B.; Wander, M. M. Modeling state-level soil carbon emission factors under various scenarios for direct land use change associated with United States biofuel feedstock production. *Biomass and Bioenergy* **2013**, *55*, 299–310.

(9) Dunn, J. B.; Mueller, S.; Kwon, H. Y.; Wang, M. Q. Land-use change and greenhouse gas emissions from corn and cellulosic ethanol. *Biotechnology for Biofuels* **2013**, *6*.

(10) Sheehan, J.; Dunahay, T.; Benemann, J.; Roessler, P. Look Back at the U.S. Department of Energy's Aquatic Species Program: Biodiesel from Algae; Close-Out Report. **1998**.

(11) Chisti, Y. Biodiesel from microalgae beats bioethanol. *Trends in biotechnology* **2008**, *26*, 126–131.

(12) Lundquist, T. J.; Woertz, I. C.; Quinn, N. W. T.; Benemann, J. R. A Realistic Technology and Engineering Assessment of Algae Biofuel Production. *Assessment* **2010**, *October*, 1.

(13) Davis, R.; Aden, A.; Pienkos, P. T. Techno-economic analysis of autotrophic microalgae for fuel production. *Applied Energy* **2011**, *88*, 3524–3531.

(14) Pienkos, P. T.; Darzins, A. The promise and challenges of microalgal-derived biofuels. *Biofuels Bioproducts and Biorefining* **2009**, *3*, 431–440.

(15) Miao, X.; Wu, Q. Biodiesel production from heterotrophic microalgal oil. *Bioresource Technology* **2006**, *97*, 841–846.

(16) Brennan, L.; Owende, P. Biofuels from microalgae—A review of technologies for production, processing, and extractions of biofuels and co-products. *Renewable and Sustainable Energy Reviews* **2010**, *14*, 557–577.

(17) Heredia-Arroyo, T.; Wei, W.; Hu, B. Oil accumulation via heterotrophic/mixotrophic Chlorella protothecoides. *Applied Biochemistry And Biotechnology* **2010**, *162*, 1978–95.

(18) Xiong, W.; Gao, C.; Yan, D.; Wu, C.; Wu, Q. Double CO(2) fixation in photosynthesis-fermentation model enhances algal lipid synthesis for biodiesel production. *Bioresource Technology* **2010**, *101*, 2287–2293.

(19) Sander, K.; Murthy, G. S. Life cycle analysis of algae biodiesel. *The International Journal of Life Cycle Assessment* **2010**, *15*, 704–714.

(20) Campbell, P. K.; Beer, T.; Batten, D. Life cycle assessment of biodiesel production from microalgae in ponds. *Bioresource Technology* **2011**, *102*, 50–56.

(21) Collet, P.; Hélias, A.; Lardon, L.; Ras, M.; Goy, R.-A.; Steyer, J.-P. Life-cycle assessment of microalgae culture coupled to biogas production. *Bioresource technology* **2011**, *102*, 207–14.

(22) Batan, L.; Quinn, J.; Willson, B.; Bradley, T. Net energy and greenhouse gas emission evaluation of biodiesel derived from microalgae. *Environmental science technology* **2010**, *44*, 7975–7980.

(23) Clarens, A. F.; Resurreccion, E. P.; White, M. A.; Colosi, L. M. Environmental life cycle comparison of algae to other bioenergy feedstocks. *Environmental science & technology* **2010**, *44*, 1813–9.

(24) Stephenson, A. L.; Kazamia, E.; Dennis, J. S.; Howe, C. J.; Scott, S. A.; Smith, A. G. Life-Cycle Assessment of Potential Algal Biodiesel Production in the United Kingdom: A Comparison of Raceways and Air-Lift Tubular Bioreactors. *Energy & Fuels* **2010**, *24*, 4062–4077.

(25) Resurreccion, E. P.; Colosi, L. M.; White, M. A.; Clarens, A. F. Comparison of algae cultivation methods for bioenergy production using a combined life cycle assessment and life cycle costing approach. *Bioresource Technology* **2012**, *126*, 298–306.

(26) Lardon, L.; Hélias, A.; Sialve, B.; Steyer, J.-P.; Bernard, O. Life-Cycle Assessment of Biodiesel Production from Microalgae. *Environmental Science & Technology* **2009**, *43*, 6475–6481.

(27) Frank, E. D.; Elgowainy, A.; Han, J.; Wang, Z. Life cycle comparison of hydrothermal liquefaction and lipid extraction pathways to renewable diesel from algae. *Mitigation and Adaptation Strategies for Global Change* **2012**.

(28) Frank, E. D.; Han, J.; Palou-Rivera, I.; Elgowainy, A.; Wang, M. Q. *Life-Cycle Analysis of Algal Lipid Fuels with the GREET Model*; 2011.

(29) Haas, M. J.; McAloon, A. J.; Yee, W. C.; Foglia, T. A. A process model to estimate biodiesel production costs. *Bioresource technology* **2006**, *97*, 671–8.

(30) Davis, R.; Fishman, D.; Frank, E. D.; Wigmosta, M. S.; Aden, A.; Coleman, A. M.; Pienkos, P. T.; Skaggs, R. J.; Venteris, E. R.; Wang, M. Q. *Renewable Diesel from Algal Lipids: An Integrated Baseline for Cost, Emissions, and Resource Potential from a Harmonized Model*; Argonne, IL, 2012; p. 85.

(31) Farnsworth, R. K.; Thompson, E. S. *Mean Monthly, Seasonal, and Annual Pan Evaporation for the United States*; Washington, D.C., 1982.

(32) PRISM Climate Group - 1981-2010 U.S. Climatology Normals http://www.prism.oregonstate.edu/ (accessed May 13, 2010).

(33) Dynamic Maps, GIS Data, and Analysis Tools www.nrel.gov/gis (accessed Jan 13, 2010).

(34) Tamiya, H.; Hase, E.; Shibata, K.; Mituya, A.; Iwamura, T.; Nihei, T.; Sasa, T. Kinetics of Growth of Chlorella, with Special Reference to its Dependence on Quantity of Available Light and on Temperature. In *Algal Culture From Laboratory to Pilot Plant, John S. Burlew Ed.*; Carnegie Institution of Washington, 1953; p. 357.

(35) Ratledge, C.; Cohen, Z. Microbial and algal oils: Do they have a future for biodiesel or as commodity oils? *Lipid Technology* **2008**, *20*, 155–160.

(36) Environmental Protection Agency *Design Manual for Fine Pore Aeration Systems*; 1989.

(37) BOTTOMLEY, P. J.; VAN BAALEN, C. Characteristics of Heterotrophic Growth in the Blue-Green Alga Nostoc sp. Strain Mac. *Journal of General Microbiology* **1978**, *107*, 309–318.

(38) Xiong, W.; Li, X.; Xiang, J.; Wu, Q. High-density fermentation of microalga Chlorella protothecoides in bioreactor for microbio-diesel production. *Applied microbiology and biotechnology* **2008**, *78*, 29–36.

(39) Harris, R. W.; Cullinane, M. J., Jr.; Sun, P. T. *Process Design and Cost Estimating Algorithms for the Computer Assisted Procedure for Design and Evaluation of Wastewater Treatment Systems (CAPDET).*; ARMY ENGINEER WATERWAYS EXPERIMENT STATION VICKSBURG MS, 1982; p. 1706.

(40) Mohn, F. Experiences and strategies in the recovery of biomass from mass cultures of microalgae. *Algae Biomass* **1980**, 547–71.

(41) Grima, E. M.; Fernandez, F. A.; Medina, A. R. Downstream Processing of Cell-mass and Products. *Handbook of Microalgal Culture: Biotechnology and Applied Phycology* **2004**.

(42) Huo, H.; Wang, M.; Bloyd, C.; Putsche, V. Life-cycle assessment of energy use and greenhouse gas emissions of soybean-derived biodiesel and renewable fuels. *Environmental science technology* **2009**, *43*, 750–756.

(43) Sheehan, J.; Camobreco, V.; Duffield, J.; Graboski, M.; Shapouri, H. Life cycle inventory of biodiesel and petroleum diesel for use in an urban bus. Final report. **1998**.

(44) Petersson, A.; Wellinger, A. *Biogas upgrading technologies – developments and innovations*; 2009.

(45) N2O EMISSIONS FROM MANAGED SOILS , AND CO2 EMISSIONS FROM LIME AND UREA APPLICATION. In *2006 IPCC Guidelines for National Greenhouse Gas Inventories Volume IV*; Eggleston, H. S.; Buendia, L.; Miwa, K.; Ngara, T.; Tanabe, K., Eds.; The National Greenhouse Gas Inventories Programme, Intergovernmental Panel on Climate Change, 2006; pp. 11.1–11.54.

(46) Usda National Agricultural Statistics Service http://www.nass.usda.gov/.

(47) Mekonnen, M. M.; Hoekstra, A. Y. The green, blue and grey water footprint of crops and derived crop products. *Hydrology and Earth System Sciences* **2011**, *15*, 1577–1600.

(48) Gerbens-Leenes, W.; Hoekstra, A. Y.; Van Der Meer, T. H. The water footprint of bioenergy. *Proceedings of the National Academy of Sciences of the United States of America* **2009**, *106*, 10219–10223.

(49) MACEDO, I.; SEABRA, J.; SILVA, J. Green house gases emissions in the production and use of ethanol from sugarcane in Brazil: The 2005/2006 averages and a prediction for 2020. *Biomass and Bioenergy* **2008**, *32*, 582–595.

(50) Chen, F. High cell density culture of microalgae in heterotrophic growth. *Trends in Biotechnology* **1996**, *14*, 421–426.

(51) Li, X.; Xu, H.; Wu, Q. Large-scale biodiesel production from microalga Chlorella protothecoides through heterotrophic cultivation in bioreactors. *Biotechnology and bioengineering* **2007**, *98*, 764–71.

(52) Gao, C.; Zhai, Y.; Ding, Y.; Wu, Q. Application of sweet sorghum for biodiesel production by heterotrophic microalga Chlorella protothecoides. *Applied Energy* **2010**, *87*, 756–761.

(53) Xu, H.; Miao, X.; Wu, Q. High quality biodiesel production from a microalga Chlorella protothecoides by heterotrophic growth in fermenters. *Journal of Biotechnology* **2006**, *126*, 499–507.

(54) Pandey, A.; Soccol, C. R.; Nigam, P.; Soccol, V. T. Biotechnological potential of agro-industrial residues . I : sugarcane bagasse. *Bioresource Technology* **2000**, *74*, 81–87.

(55) Baker, R.; Lahre, T. F. Background document: bagasse combustion in sugar mills. **1977**.

(56) Pfister, S.; Koehler, A.; Hellweg, S. Assessing the environmental impacts of freshwater consumption in LCA. *Environmental science technology* **2009**, *43*, 4098–4104.

(57) Gerbens-Leenes, W.; Hoekstra, A. Y. The water footprint of sweeteners and bio-ethanol. *Environment international* **2012**, *40*, 202–11.

(58) Precipitation: Annual Climatology (1981-2010) **2012**.

(59) Orfield, N.; Keoleian, G.; Love, N. A GIS based national assessment of algal biofuel production potential through flue gas and wastewater co-utilization. *Biomass and Bioenergy* **2013**.

(60) Mathews, J. A.; Tan, H. Biofuels and indirect land use change effects : the debate continues. *Biofuels Bioproducts and Biorefining* **2009**, *3*, 305–317.

(61) Fargione, J.; Hill, J.; Tilman, D.; Polasky, S.; Hawthorne, P. Land clearing and the biofuel carbon debt. *Science (New York, N.Y.)* **2008**, *319*, 1235–8.

(62) Searchinger, T.; Heimlich, R.; Houghton, R. A.; Dong, F.; Elobeid, A.; Fabiosa, J.; Tokgoz, S.; Hayes, D.; Yu, T.-H. Use of U.S. croplands for biofuels increases greenhouse gases through emissions from land-use change. *Science* **2008**, *319*, 1238–1240.

(63) Taheripour, F.; Tyner, W. E. Induced land use emissions due to first and second generation biofuels and uncertainty in land use emission factors. *Economics Research International* **2013**.

(64) Plevin, R. J.; O'Hare, M.; Jones, A. D.; Torn, M. S.; Gibbs, H. K. Greenhouse gas emissions from biofuels' indirect land use change are uncertain but may be much greater than previously estimated. *Environmental science & technology* **2010**, *44*, 8015–21.

(65) *Food and Agricultural Policy Research Institute (FAPRI) International Ethanol Model*. Center for Agricultural and Rural Development, Iowa State University

(66) *GTAP (Global Trade Analysis Project) Model*. Purdue University.

(67) Khatiwada, D.; Seabra, J.; Silveira, S.; Walter, A. Accounting greenhouse gas emissions in the lifecycle of Brazilian sugarcane bioethanol: Methodological references in European and American regulations. *Energy Policy* **2012**, *47*, 384–397.

(68) *Updated Renewable Fuels Standard (RFS2), Final Rule Making (FRM)—Life Cycle Assessment, public docket (RFS2-FRM-LCA-DocketMaterials).*; 2010.

(69) *Proposed Regulation to Implement the Low Carbon Fuel Standard Volume I Staff Report: Initial Statement of Reasons*; 2009.

CHAPTER 4. LIFE CYCLE DESIGN OF AN ALGAL BIOREFINERY FEATURING HYDROTHERMAL LIQUEFACTION: EFFECT OF REACTION CONDITIONS AND AN ALTERNATIVE PATHWAY INCLUDING MICROBIAL REGROWTH

4.1 Abstract

Algae are an appealing source of bioenergy due to their high yields relative to terrestrial energy crops. The high cost of production, however, has prohibited commercialization despite significant investment by the private sector. Hydrothermal liquefaction (HTL) is a technology that converts a higher fraction of the algae into biocrude oil than alternative technologies, thereby reducing the amount of expensive pond infrastructure and energy required to cultivate the feedstock. Recent experimental work has provided insight into the HTL reaction pathways involved in the conversion of algal biomass to biocrude oil. We incorporate these results into an analysis that models the performance of an algal biorefinery featuring HTL across a range of reaction conditions to explore the optimal scenario for the life cycle and economic objectives considered. Additionally, we explore a novel regrowth pathway that boosts oil yields by

cultivating *E. coli* on the aqueous phase products from HTL and recycling the additional biomass back through the reactor.

We found that the life cycle results varied significantly depending on the HTL reaction conditions, with the net energy ratio (NER) ranging from 1.5 to 2.8 and the global warming potential (GWP) ranging from 0.85 to 1.4 kg $CO_2e \cdot L^{-1}$. For both of these metrics the optimal HTL condition occurred at 250°C with a reaction time of either 57 minutes for minimizing the GWP or 49 minutes for maximizing the NER. At these conditions a large amount of organic carbon is available in the aqueous phase, enabling substantial amounts of on-site electrical and thermal energy recovery. The optimal economic and occupied land results, conversely, corresponded to HTL conditions where oil yields were highest, at 400°C and 5 minutes. The cost of biocrude at these conditions was $\$1.64 \cdot L^{-1}$. For the regrowth pathway featuring *E. coli*, the optimal cost could be further reduced at these same conditions to $\$1.59 \cdot L^{-1}$. Disabling gasification in favor of boosting oil yields has a detrimental effect on other metrics, however, increasing the GWP to 1.66 kg $CO_2e \cdot L^{-1}$ and decreasing the NER to 1.38.

4.2 Introduction

Algal biomass is a promising source of bioenergy that could potentially produce billions of liters of biofuel annually in the United States[1,2]. An appealing characteristic of algae is that they occupy significantly less land than terrestrial biofuel crops due to their high growth rate and that the use of engineered ponds enables algae to be cultivated on marginal land that could not otherwise be used for agriculture[3–7]. Despite substantial

investment from government and within the private sector, however, a scalable and economically viable means for producing algal biofuel has not emerged. The primary economical hurdle is the high cost to build and operate the ponds[8–11], and a major technical hurdle is a means to convert the algal biomass into a usable transport fuel[12,13]. This article focuses on methods to advance a technology, hydrothermal liquefaction (HTL), that could address both of these obstacles by providing a means to convert wet algal biomass to biocrude oil while reducing the amount of pond infrastructure required to produce a given quantity of algal biofuel.

A life cycle assessment (LCA) by Lardon et al. (2009) illustrated that the solvent-based oil extraction technologies used for other energy crops such as soybean cannot be relied upon for algae; the amount of energy required to dry the biomass to levels typical of terrestrial crops would exceed the energy content in the algal oil[14]. Several studies have demonstrated the viability of "wet" solvent extraction strategies to separate the lipid fraction of the algal biomass as an oil that can be upgraded via transesterification to a biodiesel product[14,15]. This approach still has not been implemented at commercial scale, however, and efficient recovery of the solvent (typically hexane) has proven to be a challenge[12]. Another limitation of solvent extraction is that the yield of oil per unit of biomass is limited to the fraction of the biomass that is lipid. Currently the most economical strategy for cultivating phototrophic algae is an open, paddle-wheel mixed pond, and the species grown in these ponds typically have just 10-25% lipid content[16].

By contrast, HTL converts a portion of the carbohydrate and protein fractions of the algal biomass into oil in addition to the lipid fraction[17]. This process works by converting a wet (~15-20% solids) algal slurry under high temperature and pressure (e.g., 350 °C, 16.5 MPa) into a variety of products including a biocrude oil. HTL mimics the way fossil crude oil was formed in nature, by geologic heat and compression of plant tissue, but does so in minutes rather than millions of years. In addition to the oil that is formed, HTL produces solids, gas, and soluble products remaining in the water, or the "aqueous phase".

Use of the non-product portions of the algal biomass (e.g., the lipid extracted algae (LEA) remaining after oil extraction or the aqueous phase products from HTL) is significant and has the potential to improve the economics and life cycle impacts of the biorefinery. Frank et al. (2012) performed an LCA that demonstrated the benefits of solvent-based lipid extraction compared to HTL due to the relatively high amount of non-product portion of the algae available for energy recovery via gasification[18]. To date the work by Frank et al. has been the only LCA performed of an algal biofuel product featuring HTL, and the authors acknowledged the limitations of their analysis due to limited experimental results.

Recent research exploring in detail the range of products from HTL across a range of conditions has enabled a more thorough analysis rooted in experimental results[19]. The objective of this study is to incorporate the reaction network model developed by Valdez et al. (2013) into an LCA that evaluates the life cycle impacts of an algal biocrude

oil from HTL across a range of reaction conditions[20]. The study will examine the effect of HTL reaction conditions ranging from 250-400°C and 5-90 minutes. Given the importance of reducing costs to enable commercialization of algal biofuels, this analysis will evaluate an economic metric in addition to the life cycle metrics of net energy ratio (NER, total energy produced divided by the total life cycle energy inputs), global warming potential (GWP), and occupied land.

In addition to being the first study to analyze the sensitivity of LCA performance to the HTL reaction conditions, this study will examine the viability of a novel pathway for boosting oil yields proposed by Nelson et al. (2013)[21]. While several studies have theorized schemes for on-site energy recovery from the non-product portion of the algal biomass either by anaerobic digestion or hydrothermal gasification[18,22,23], none has explored the possibility of utilizing the aqueous phase products from HTL to grow a secondary source of biomass for HTL processing. Nelson et al. (2013) demonstrated that *E. coli* can be grown on the aqueous phase products from HTL[21] and Valdez et al. (2013) demonstrated recovery of crude bio-oil from *E. coli* biomass via HTL with yields similar to those of algae (i.e. 29% yield for *E. coli* compared to 38% for *Nannochloropsis sp.* for the same conditions)[24]. Therefore the proposed regrowth pathway could incorporate cultivation of microbial biomass such as *E. coli* to recycle carbon and thereby yield more oil per unit of initial algal biomass. Growth of microbial biomass on the aqueous phase could also serve as a pre-processing step enabling nutrient recycle back to the algae pond, as other HTL research has shown that direct recycle of aqueous phase to algae

growth operations can be problematic due to suspected toxicity[25] and/or nutrient availability[17,26,27].

The Energy Independence and Security Act of 2007 (EISA) has targeted the production of 36 billion ethanol-equivalent gallons of biofuel annually by 2022. Of those targets, 21 billion gallons are to be non-corn starch derived "advanced biofuels"[28]. To qualify as an advanced biofuel the final product must have 50% less life cycle greenhouse gas emissions relative to conventional fossil gasoline. This analysis will therefore examine the life cycle performance of the biocrude oil produced by HTL in the context of these policy objectives.

4.3 Methodology

A challenge of conducting biofuel LCAs is that results and data from multiple sources must be aggregated into a single model with the premise that the results derived from the independent scenarios remain valid in the integrated system. In some key areas (i.e., energy recovery schemes and nutrient recycle) these assumptions must remain in question until they have been examined experimentally. This study features an interdisciplinary collaboration between experimentalists and environmental systems analysts in an attempt to derive results that are realistic. Not all aspects of the model have been verified in the laboratory, however, as processes such as algae cultivation and harvesting remain the specialty of others and have technical challenges that are independent of oil extraction and conversion.

4.3.1 Experimental Data Sources Used

This research builds upon work performed by Valdez et al. (2013) characterizing the products from HTL[19] and a recent study featuring a model that predicts the biocrude yield from *Nannochloropsis sp.* across the two dimensional design space of HTL performed between 250-400°C and from 5-90 minutes[20]. The model also calculates the yields of other HTL product fractions, such as gas, solids, and aqueous phase products. Accurate information about the aqueous phase is particularly important to this analysis as its constituents will be used either for energy recovery via gasification for the standard pathway or growth of secondary *E. coli* biomass for the regrowth pathway. Details about the two pathways considered in this analysis, the standard pathway and regrowth pathway, will be explained later in the report. Data from Valdez et al. allows for determination of the amount of carbon remaining in the aqueous phase and specifies the fraction that is organic vs. inorganic.

In addition to the dataset characterizing HTL, this analysis also incorporates results from Nelson et al. (2013) for modeling the secondary growth of microbial biomass. Nelson characterized *E.coli* growth on the aqueous phase products from an HTL reactor, specifically the fraction of organic carbon removed as a function of the level of dilution[21]. A separate study demonstrates the feasibility of converting the *E. coli* to biocrude via HTL. The microbial biomass exhibited biocrude yield of approximately 29% compared to a yield of 38% from *Nannochloropsis* from HTL at the same conditions[24]. There is no model that can predict a detailed product distribution from HTL of *E. coli* over the full design space of 250-400°C and 5-90 minutes so this study will assume the

oil yield and product distribution are the same for *E. coli* as the algal biomass. The elemental composition of the *E. coli* and algae will be used to determine the mass balance of elemental flows through the biorefinery.

4.3.2 Data Sources for Life Cycle Modeling

The upstream processes of algae cultivation and dewatering were based on the operational assumptions outlined by Frank et al. (2011) in the Greenhouse Gases, Regulated Emissions, and Energy Use in Transportation (GREET) model published by Argonne National Laboratory and a subsequent report including collaboration from the National Renewable Energy Laboratory and the Pacific Northwest National Laboratory[22,29]. This harmonized study by Davis et al. (2012) assimilates data from multiple research institutions. Though it does incorporate some assumptions that have not been validated empirically, it provides a foundation that has been cross-examined by the collaborators. To align with the aforementioned harmonized study the algal biomass is assumed to be grown in an open pond with circulation provided by a paddle-wheel mixer, and flue gas is assumed to be the CO_2 source.

Algae yield is modeled as 13.2 $g \cdot m^{-2} \cdot day^{-1}$, which is also in alignment with the report by Davis et al. (2012) when seasonal variation in productivity is considered. The pond is harvested at a concentration of 0.5 $g \cdot L^{-1}$ and then concentrated to 10 $g \cdot L^{-1}$ by flocculation and settling. Dissolved air flotation and centrifugation accomplish secondary dewatering to ultimately achieve a final concentration of 150 $g \cdot L^{-1}$. This concentration deviates from that assumed by Davis et al. (2012), 200 $g \cdot L^{-1}$, but it aligns

with the experimental conditions used by Valdez et al. (2013). The authors found, however, that the yields of the HTL product fractions were not significantly affected by the concentration of the incoming algae slurry over this small range[19]. Another deviation of this model from that of Davis et al. (2012) is the use of *Nannochloropsis* sp. which is the biomass source used by Valdez et al. (2013) in the generation of their predictive model. The biomass is therefore assumed to contain 14% lipid, 59% protein, and 20% carbohydrates[19] to be consistent with the experimental work.

Another important assumption for the standard pathway is that energy can be recovered from the organic carbon within the aqueous phase solution by catalytic hydrothermal gasification (CHG). In this process, the nutrients are, in principle, able to be nearly entirely recycled while the organic carbon is converted to biogas[18]. Combustion of the biogas in a combined heat and power (CHP) generator that allows for onsite production of thermal and electrical energy. This energy recovery scheme will be used for the standard pathway, but an alternative regrowth pathway featuring secondary biomass cultivation for boosted oil yields is also explored. The regrowth pathway is discussed later in this study.

The biocrude recovered from HTL is assumed to be upgraded by hydrotreating. The crude oil is heated and processed with hydrogen for the removal of O and N as H_2O and NH_3, respectively[18,30]. The hydrogen demand is modeled on the formula outlined by Li and Savage (2013)[31].

4.3.3 Modeling Framework

Figure 1 illustrates the structure of the core model and the differences between the standard pathway and the regrowth pathway. Mass balances around each of the process units (represented by rectangles in Figure 4.1) serve to track nutrient flows and calculate energy and water demand. The core model was assembled in Microsoft Excel© but featured intermediate datasets that were derived in MATLAB©.

Determining how the algal biomass was altered after undergoing the HTL process was crucial to the model. To determine the yields of the product fractions from the HTL reactor, the predictive model derived by Valdez et al. (2013) was developed by solving a system of first-order differential equations to fit replicate sets of experimental data[20]. Valdez et al. used a constrained non-linear solver in MATLAB© to minimize the value of the squared difference between the experimental and predicted values. The resulting function was implemented to predict the distribution of the original algal biomass into the HTL products of light biocrude, heavy biocrude, solids, gas, and aqueous phase constituents. The elemental composition of the aqueous phase was calculated by difference for each combination of reaction conditions across the reaction temperature and duration design space.

Solid products, though always in low yields, are more abundant at low temperatures and short reaction times. These are considered as unconverted biomass and therefore assumed to have the same composition as the original biomass fed into the HTL reactor. Gas yields are also low, and the gas produced during HTL is assumed to be entirely CO_2, which is consistent with other studies for gasification of biomass, particularly at lower

temperatures[32]. At higher temperatures, especially above the critical temperature of 374°C, hydrocarbons such as methane, ethylene, and ethane are present. At the highest temperature considered, 400 °C, however, the gas phase is still primarily CO_2 [32]. The elemental composition of the biocrude constituents is well-characterized[33,34], meaning the elemental composition of the aqueous phase products can be calculated by mass balance. The Dulong formula was used to estimate the higher heating value (HHV) of the biocrude oil based on its elemental composition[33].

Only a portion of the carbon in the aqueous phase is available for gasification or secondary biomass growth and this fraction depends on the reaction conditions. For example more of the carbon is inorganic at the more severe reaction conditions, with a maximum inorganic fraction of 47% observed at the highest temperature and longest duration[19]. The study by Valdez et al. (2012) reported the fraction of carbon in the aqueous phase that is organic for 22 reaction conditions in the reaction design space. The MATLAB© curve fitting toolbox was then used to interpolate the results across the entire design space using a cubic spline. Details about this fitting technique can be found in the Supporting Information.

Nelson et al. (2013) proposed utilizing a secondary microbial biomass pathway to recover carbon and nutrients in the aqueous phase products from the HTL. Because the HTL reaction is able to convert carbohydrates and proteins into biocrude in addition to the lipids, the secondary biomass could then also be converted into additional biocrude through the same HTL process used for the algal biomass. This secondary biomass

growth is therefore a means to boost the oil yield for the same unit of initial algal biomass. Nelson et al. demonstrated the feasibility of growing both *E. coli* and *P. putida* on the aqueous phase, but this report will focus solely on *E. coli* as it exhibited greater organic carbon uptake efficiency.

After depressurization and separation from the biocrude, the aqueous phase solution is neutralized to a pH of 7 using hydrochloric acid (HCl) then diluted with a standard organic-buffered media for enterobacteria[35]. Upon addition of the HCl the inorganic carbon is off-gassed as CO_2. Media varying between 10 and 50 vol% were tested by Nelson et al. for various microbial growth characteristics, including the fraction of organic carbon removed by the cell culture. The maximum organic carbon removal (45%) occurred with *E.coli* growing in 10 vol% aqueous phase medium [21]. Growth in concentrations above 40 vol% aqueous phase was found to be too toxic for the *E. coli*, a higher tolerance threshold than has been exhibited by algae[17,26].

Despite the dilution, the process of cultivating the *E. coli* in a continuous, fed-batch culture results in a harvested concentration projected to be 40-60 $g \cdot L^{-1}$. Therefore it is assumed that the microbial biomass can be combined with the final centrifugation step used for dewatering the algae for concentration to 150 $g \cdot L^{-1}$ prior to conversion in the HTL reactor. Fed-batch cultures of *E. coli* have been demonstrated to grow to concentrations denser than those projected in this analysis, with measurements in excess of 100 $g \cdot L^{-1}$ reported[36].

The C:N:P ratio of the aqueous phase solution compared to that of the *E. coli* indicates that carbon will be the limiting nutrient, which was confirmed by Nelson et al. in their analysis. Of the fraction of organic carbon removed by the bacteria, a portion is respired as CO_2 during cell maintenance rather than being synthesized directly into biomass. Modeling for this study was based on the yield to substrate removal ratios for carbon-limited *E. coli* reported by Chen and Strevett (2002)[37].

This analysis assumes that there will be no energy recovery from CHG in the regrowth pathway. Recall that the *E. coli* consume at most 45% of the organic carbon, meaning the majority is still theoretically available for energy recovery via a technology such as CHG or anaerobic digestion. However, unlike the standard pathway, the aqueous phase products were diluted and cooled for cultivation of the microbial biomass. The amount of energy required reheat and concentrate the solution to the level required for CHG was determined to be in excess of the energy recovered. It was decided that CHG is not a viable option for the spent aqueous phase downstream of *E. coli* growth and the solution would instead be sent back to the pond for algae growth.

The elemental mass flows through each of the processes were calculated by mass balance. Recall that the aqueous phase composition was calculated by difference given the biocrude and biomass compositions and assumptions about the solid and gas products from HTL. An illustration of the mass flows for the elements C, N, and P is shown for the standard pathway in Figure 4.1a and for the *E. coli* regrowth pathway in

Figure 4.1b. The mass flows shown in Figure 4.1 represent baseline conditions of 350°C and 60 minutes.

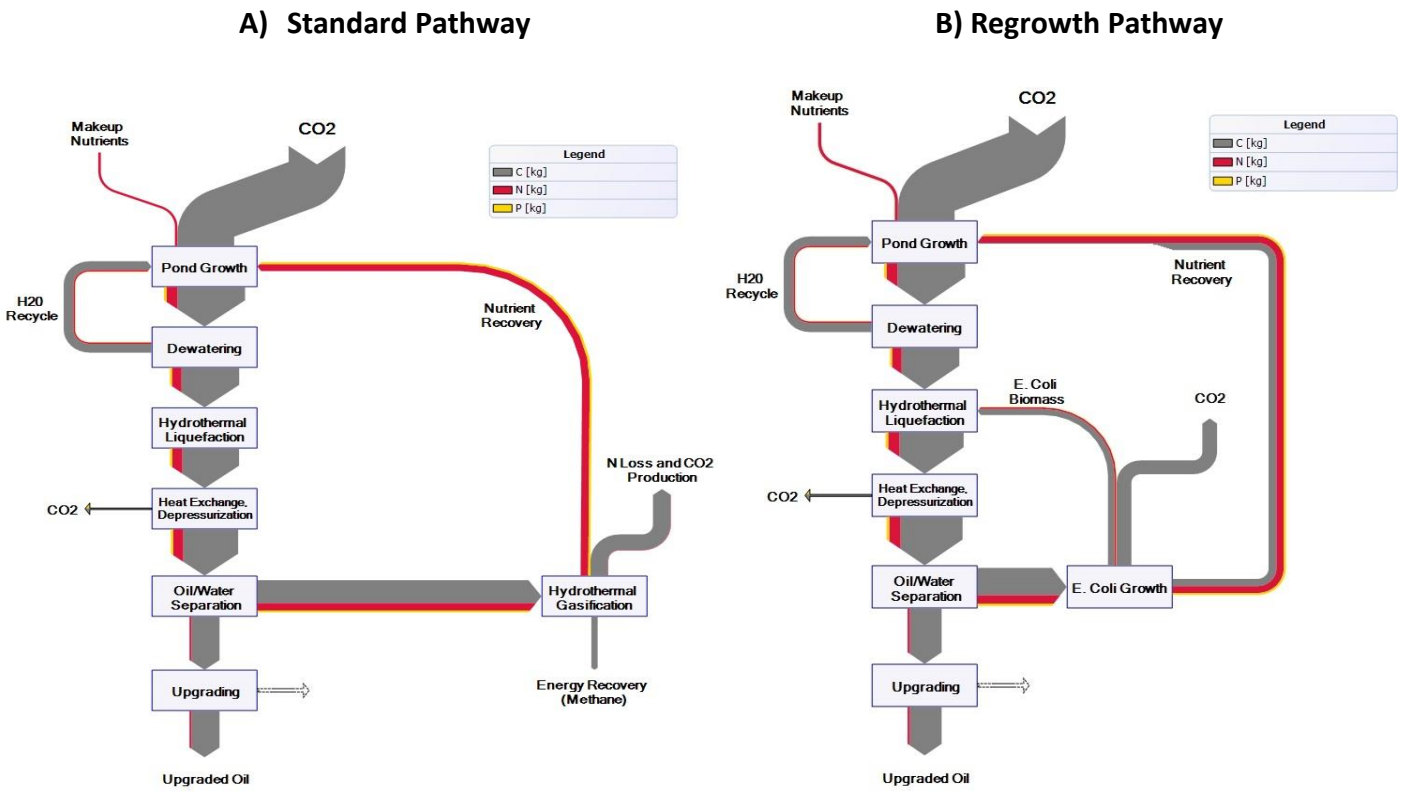

Figure 4.1 - A Sankey diagram illustrating the mass flows of carbon, nitrogen, and phosphorus for A) The standard pathway which assumes energy recovery from the aqueous phase products of HTL via catalytic hydrothermal gasification, and B) the regrowth pathway featuring cultivation of a secondary biomass, E. coli, on the nutrients available in the aqueous phase products which can be processed via HTL to boost the net oil yield.

HTL reactions at 350°C for 60 minutes are commonly used in the literature, so this study will compare the life cycle impacts at these baseline conditions to those across the full design space (250-400°C, 5-90 minutes). Uncertainty was estimated by implementing a Monte Carlo simulation using the RiskSim Excel© plugin tool. Details about the parameters and the range of values incorporated into the simulation can be found in the Supporting Information.

Cost assumptions were adapted from the techno-economic model implemented in the harmonized study published Davis et al. (2012)[29]. Each line item in the harmonized model was normalized by the operational parameters of their baseline facility and then classified into three groups: Costs that scale in proportion to the 1) pond size, 2) algal biomass throughput, and 3) total oil produced. Costs for the HTL and CHG reactors[38] were added to the line items of the harmonized model while the cell rupture, solvent extraction, and anaerobic digestion costs were removed. The table showing the financial modeling details can be found in the Supplemental Information section.

4.4 Results & Discussion

4.4.1 Effect of Hydrothermal Liquefaction Reaction Conditions

The NER for the standard pathway (without *E. coli* regrowth) is depicted in Figure 4.2a for the full range of HTL reaction conditions. These results illustrate the significance of the HTL reaction conditions on the life cycle energy balance, with NER results varying from as low as 1.5 (at 250°C, 5 minutes) to as high as 2.8 (at 250°C, 57 minutes, marked with a black square). The GWP results (included in the Supporting Information) track closely to the NER, with the minimum value of 0.85 kg $CO_2e \cdot L^{-1}$ occurring at 250°C and 49 minutes. The highest oil yield from HTL is 42%, occurring at 400°C and 5 minutes, but at the higher temperatures a greater portion of the biomass is also converted to CO_2. Furthermore, an increased oil yield results in less of the initial algal biomass ending up in the aqueous phase solution where it could be converted into useful energy via CHG when using the standard pathway. Displacing electrical energy in particular is beneficial

in terms of the GWP and NER impact metrics, as electricity has a relatively high life cycle energy burden.

A biorefinery featuring HTL reaction conditions with relatively high temperatures and long reaction times results in an aqueous phase containing a higher fraction of carbon in the inorganic form rather than organic. Inorganic carbon is not available for energy recovery via CHG which is why the NER drops significantly as temperatures and reaction times are increased.

Figure 4.2b illustrates the effect of the HTL reaction conditions on the economics of the biorefinery. Given that the pond costs dominate the economic model, the lowest-cost scenarios occur where the oil yield is highest and therefore the least amount of pond is required per liter of biocrude produced. The lowest cost therefore occurs at reaction conditions of 400°C and 5 minutes (marked with a black square), where a liter of biocrude would cost $\$1.64 \cdot L^{-1}$. This cost represents a 9% reduction compared to the cost of $\$1.79 \cdot L^{-1}$ at standard conditions (350 °C, 60 min). Conditions with low temperatures and short reaction times, conversely, produce a biocrude with significantly higher costs because a relatively large portion of the initial biomass remains as solids and therefore the oil yields are low. The land occupation metric tracks closely with the economic results because both are driven primarily by the size of the pond required for cultivation.

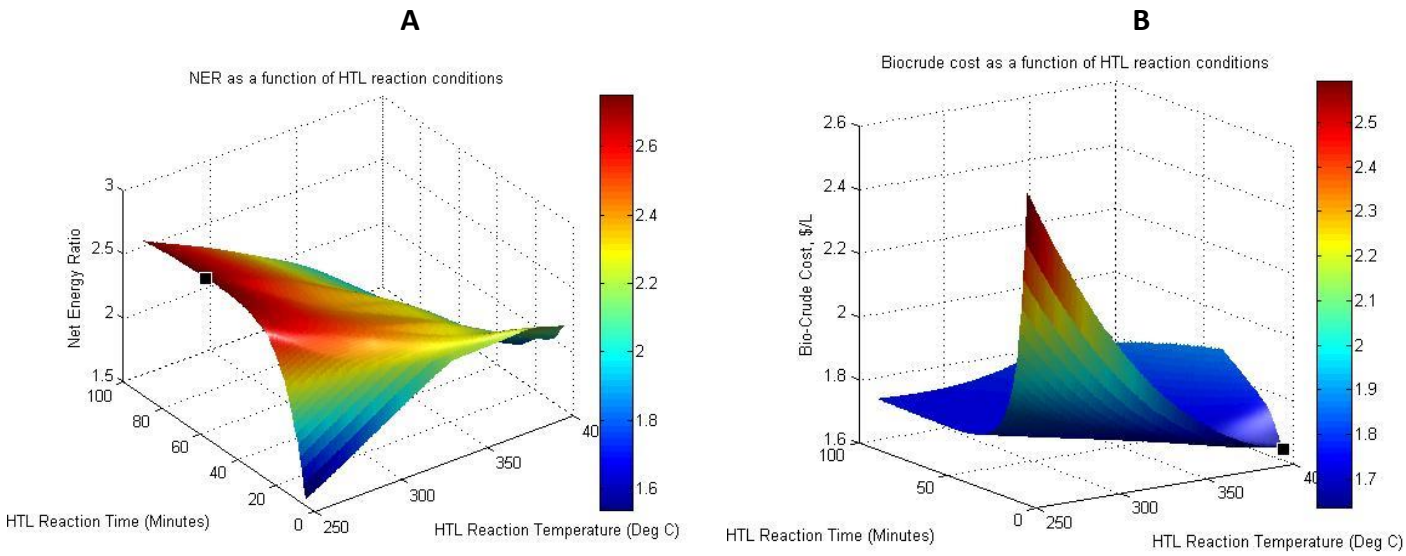

Figure 4.2 - The effect of hydrothermal liquefaction reaction conditions on the life cycle net energy ratio (NER, A) and cost of producing bio-crude oil (B). In both figures the optimal reaction condition for that metric is indicated with a black square.

Figure 4.3 compares the four metrics over three sets of reaction conditions: standard conditions (350°C, 60 minutes), optimal conditions for the NER metric (250°C, 57 minutes), and optimal conditions for economics (400°C, 5 minutes). A design trade-off is present, then, because the second set of conditions has the lowest energy input requirement but 7% more cost compared to the third set of conditions.

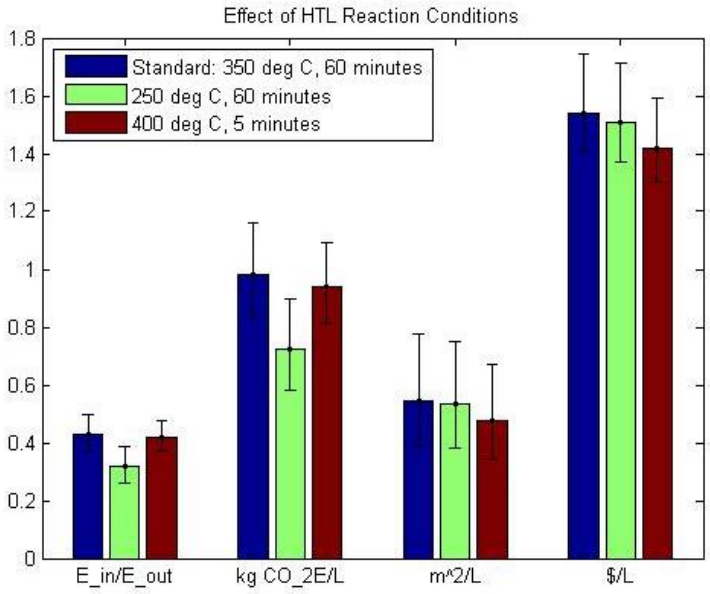

Figure 4.3 - Comparison of all four metrics for the standard pathway at three sets of reaction conditions: Standard conditions, the optimal conditions for minimizing the global warming potential, and the optimal conditions for minimizing production costs.

4.4.2 E. coli Regrowth Pathway Results

The previous results illustrate the tradeoff between high oil yields (which minimizes the cost and land footprint) and high energy recovery via CHG of the aqueous phase (which minimizes the NER and GWP). A pathway featuring *E. coli* growth on the aqueous phase rather than energy recovery essentially amplifies this tradeoff. That is, using the aqueous phase to produce additional biomass boosts the total oil yield per unit of biomass but does so at the expense of energy recovery via CHG.

The greatest boost to the oil yield, 21%, occurs at conditions of 250°C and 60 minutes where the aqueous phase product fraction is large and the fraction of inorganic carbon present in the aqueous phase is low. Adding *E. coli* regrowth in these conditions would increase the total oil yield from 39% to 46% of the initial algal biomass. The greatest total oil yield for the regrowth pathway, however, occurs at 400°C and 5

minutes, where an 11% boost brings the initial yield of 42% up to 47% of the initial algal biomass.

Given that on-site energy recovery is not considered for the regrowth pathway, then, the conditions for maximum total oil yield also correspond to the best performance for the four metrics considered in this analysis. The GWP results track closely with the NER results and the land occupation results track closely with the economic results, as was the case with the standard pathway. In both Figure 4.4a and Figure 4.4b a line connects the optimal conditions for the regrowth pathway (marked with a circle) to the optimal conditions for the standard pathway (marked with a square) for clarity.

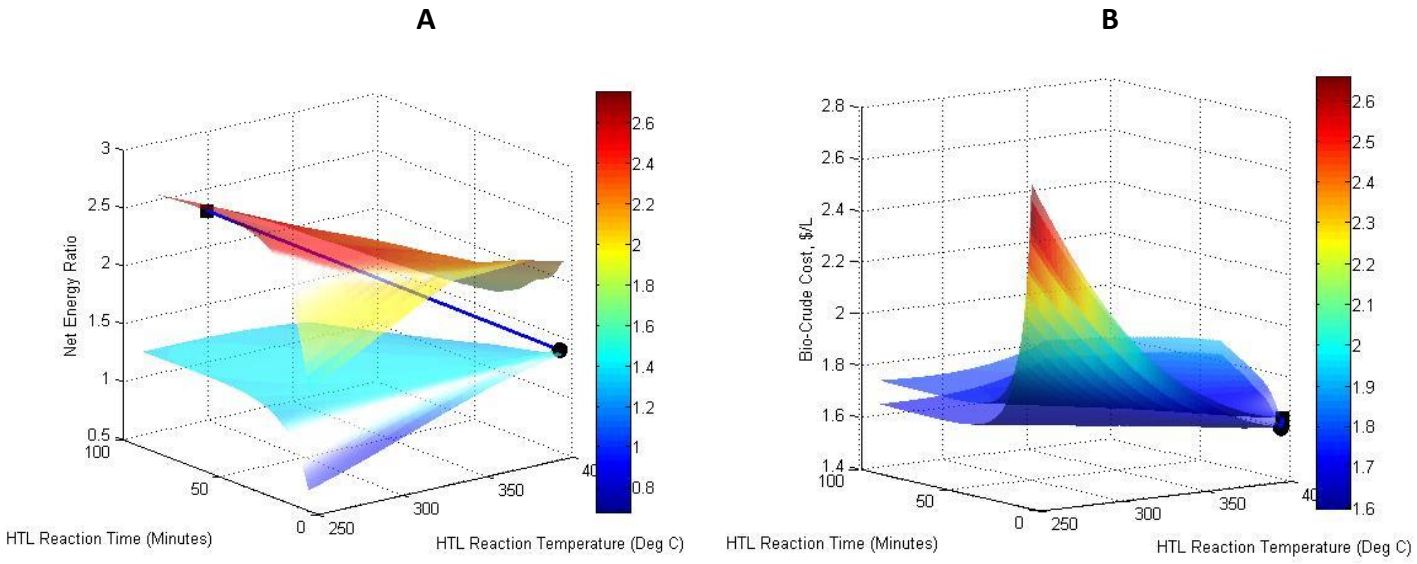

Figure 4.4 - A comparison of results for the standard pathway (the surface marked with a square at the optimal conditions) to the regrowth pathway (marked with a circle) across the full range of reaction conditions considered in the analysis. The net energy ratio (NER) is shown in plot A and the cost for producing the biocrude oil is shown in plot B. A line connects the optimal points on both surfaces for clarity.

Figure 4.5 compares two sets of reaction conditions for each of the two pathways. The first set of reaction conditions is the standard scenario (350°C and 60 minutes) and the second is the optimal for the regrowth pathway (400°C and 5 minutes). These results show that the lowest-cost scenario for the standard pathway can be further reduced from $\$1.64 \cdot L^{-1}$ to $\$1.59 \cdot L^{-1}$ by incorporating *E. coli* regrowth. Doing so, however, reduces the NER by 37% and increases the GWP 58% to 1.68 kg $CO_2e \cdot L^{-1}$, again, due to the elimination of energy recovery via CHG.

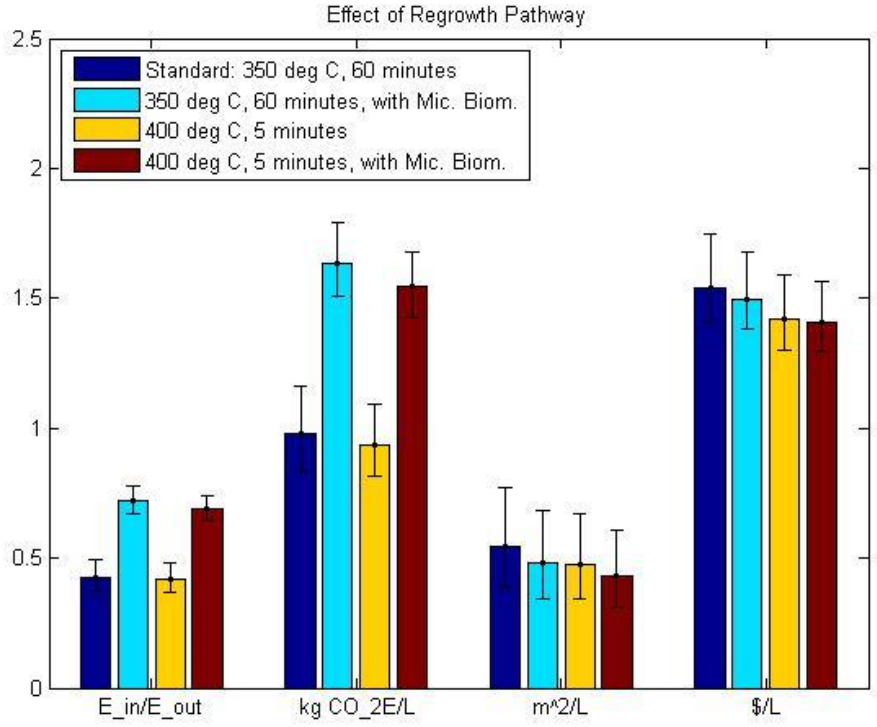

Figure 4.5 - Comparison of all four metrics representing two scenarios for each of the pathways considered: 1) Standard reaction conditions for the standard pathway, 2) Standard conditions for the regrowth pathway, 3) optimal economic conditions for the standard pathway, and 4) optimal economic conditions for the regrowth pathway.

The greenhouse gas reduction threshold to qualify as an advanced biofuel for the EISA production targets require a 50% reduction in GHGs relative to conventional fossil fuels[28]. Adjusting for the energy intensity of the biocrude, the equivalent emissions from

fossil fuel is 3.0 kg $CO_2e \cdot L^{-1}$, so the 58% increase caused by bypassing CHG to instead facilitate *E. coli* regrowth could jeopardize the fuel's qualification as an advanced biofuel.

Table 4.1 summarizes the optimal conditions for each of the metrics considered in this analysis.

Table 4.1 - A summary of the optimal conditions for each of the metrics considered in this analysis and for both of the pathways examined.

	Standard Pathway		Regrowth Pathway	
	Opt. Conditions	Value	Opt. Conditions	Value
NER ($E_{out} \cdot E_{in}^{-1}$)	250°C, 57m	2.8	400°C, 7m	1.4
GWP (kg $CO_{2e} \cdot L^{-1}$)	250°C, 49m	0.85	400°C, 6m	1.7
Land Footprint ($m^2 \cdot L^{-1}$)	400°C, 5m	0.72	400°C, 5m	0.66
Economics ($\$ \cdot L^{-1}$)	400°C, 5m	1.64	400°C, 5m	1.59

4.5 Conclusions

Previous studies have focused on HTL of algal biomass at a single reaction condition, but varying the reaction temperature and duration can have a profound influence on life cycle impacts of the final product in addition to its economic viability. To minimize the cost of producing an algal biocrude using HTL, conditions that maximize oil yield should be sought. To maximize the NER or minimize the GWP, conversely, conditions that produce high proportions of aqueous phase solution that is rich in organic carbon are ideal.

Recovery of aqueous phase products from HTL is clearly instrumental to the overall life cycle performance and economics of the biorefinery, so the material should be used

prudently. If CHG of the aqueous solution is feasible it would be an attractive means to significantly offset the amount of electrical and thermal energy required to be imported onsite to run the biorefinery. This is an area that deserves further experimental validation.

Preliminary experimental research indicates that a pathway featuring regrowth of biomass such as *E. coli* on the aqueous phase products from HTL enables boosting the yield of oil per unit of algal biomass by 10-20% without significant additional infrastructure investment. Doing so requires forgoing energy recovery via CHG and therefore reduces the NER by 37% and increases the carbon footprint of the fuel to 1.68 kg $CO_2e \cdot L^{-1}$.

This study analyzed only the use of *E. coli* for boosting oil yields via a regrowth pathway, but other species could provide the same service and should therefore be examined. Examples of species that have been examined in other research include *Pseudomonas putida* and *Saccharomyces cerevisiae*. Ideal traits for these organisms are a high conversion efficiency of organic carbon into biomass, high oil yield of these organisms when processed via HTL, and a high toxicity threshold for regrowth on aqueous phase products[20,21]. This analysis did not consider energy recovery from the spent aqueous phase, or the solution remaining after *E. coli* growth which still contains valuable nutrients and organic carbon. If an organism were able to be grown on the aqueous phase without dilution it is possible that the carbon concentration would be sufficient to recover energy via CHG as was modeled for the standard pathway.

Alternatively it is possible that recycling the spent aqueous phase directly to the pond could induce mixotrophic algae growth providing another means for boosted yields, if the species were capable of such metabolisms. In this model over half of the organic carbon present in the aqueous phase is unused, leaving a valuable substrate for more biomass growth in addition to the nitrogen and phosphorus that is recycled. This is another area that should be researched further.

Oil from microalgae is currently too expensive to compete with fossil fuels, so technological advancements will be necessary to make the product commercially viable. The combined cost reductions that can be achieved by selecting HTL conditions for the highest oil yield and by recovering oil from a secondary biomass such as *E. coli* could exceed 11%. These reductions are insufficient to lower the cost to the point where oil from algae can compete with fossil fuel, but it provides a step in that direction.

4.6 Chapter 4 References

(1) Wigmosta, M. S.; Coleman, A. M.; Skaggs, R. J.; Huesemann, M. H.; Lane, L. J. National microalgae biofuel production potential and resource demand. *Water Resources Research* **2011**, *47*, 1–13.

(2) Pate, R.; Klise, G.; Wu, B. Resource demand implications for US algae biofuels production scale-up. *Applied Energy* **2011**, *88*, 3377–3388.

(3) Singh, A.; Nigam, P. S.; Murphy, J. D. Renewable fuels from algae: an answer to debatable land based fuels. *Bioresource Technology* **2011**, *102*, 10–16.

(4) Clarens, A. F.; Resurreccion, E. P.; White, M. A.; Colosi, L. M. Environmental life cycle comparison of algae to other bioenergy feedstocks. *Environmental science & technology* **2010**, *44*, 1813–9.

(5) Dismukes, G. C.; Carrieri, D.; Bennette, N.; Ananyev, G. M.; Posewitz, M. C. Aquatic phototrophs: efficient alternatives to land-based crops for biofuels. *Current opinion in biotechnology* **2008**, *19*, 235–40.

(6) Demirbas, A.; Fatih Demirbas, M. Importance of algae oil as a source of biodiesel. *Energy Conversion and Management* **2011**, *52*, 163–170.

(7) Chisti, Y. Biodiesel from microalgae beats bioethanol. *Trends in biotechnology* **2008**, *26*, 126–131.

(8) Benemann, J. R.; Oswald, W. J. Systems and economic analysis of microalgae ponds for conversion of CO{sub 2} to biomass. Final report. **1996**.

(9) Davis, R.; Aden, A.; Pienkos, P. T. Techno-economic analysis of autotrophic microalgae for fuel production. *Applied Energy* **2011**, *88*, 3524–3531.

(10) Gallagher, B. J. The economics of producing biodiesel from algae. *Renewable Energy* **2011**, *36*, 158–162.

(11) Sun, A.; Davis, R.; Starbuck, M.; Ben-Amotz, A.; Pate, R.; Pienkos, P. T. Comparative cost analysis of algal oil production for biofuels. *Energy* **2011**, *36*, 5169–5179.

(12) Mercer, P.; Armenta, R. E. Developments in oil extraction from microalgae. *European Journal of Lipid Science and Technology* **2011**, *113*, 539–547.

(13) Pienkos, P. T.; Darzins, A. The promise and challenges of microalgal-derived biofuels. *Biofuels Bioproducts and Biorefining* **2009**, *3*, 431–440.

(14) Lardon, L.; Hélias, A.; Sialve, B.; Steyer, J.-P.; Bernard, O. Life-Cycle Assessment of Biodiesel Production from Microalgae. *Environmental Science & Technology* **2009**, *43*, 6475–6481.

(15) Halim, R.; Gladman, B.; Danquah, M. K.; Webley, P. A. Oil extraction from microalgae for biodiesel production. *Bioresource Technology* **2011**, *102*, 178–85.

(16) Becker, E. W. *Microalgae: biotechnology and microbiology*; Baddiley, J.; Carey, N. H.; Higgins, I. J.; Potter, W. G., Eds.; Cambridge University Press, 1994; Vol. 10, p. 293.

(17) Biller, P.; Ross, A. B. Potential yields and properties of oil from the hydrothermal liquefaction of microalgae with different biochemical content. *Bioresource technology* **2011**, *102*, 215–25.

(18) Frank, E. D.; Elgowainy, A.; Han, J.; Wang, Z. Life cycle comparison of hydrothermal liquefaction and lipid extraction pathways to renewable diesel from algae. *Mitigation and Adaptation Strategies for Global Change* **2012**.

(19) Valdez, P. J.; Nelson, M. C.; Wang, H. Y.; Lin, X. N.; Savage, P. E. Hydrothermal liquefaction of Nannochloropsis sp.: Systematic study of process variables and analysis of the product fractions. *Biomass and Bioenergy* **2012**, *46*, 317–331.

(20) Valdez, P.; Savage, P. A Reaction Network for the Hydrothermal Liquefaction of Nannochloropsis sp. *Manuscript Submitted, Algal Research* **2013**.

(21) Nelson, M.; Zhu, L.; Thiel, A.; Wu, Y.; Guan, M.; Minty, J.; Wang, H. Y.; Lin, X. N. Microbial utilization of aqueous co-products from hydrothermal liquefaction of microalgae Nannochloropsis oculata. *Bioresource technology* **2013**, *136*, 522–8.

(22) Frank, E. D.; Han, J.; Palou-Rivera, I.; Elgowainy, A.; Wang, M. Q. *Life-Cycle Analysis of Algal Lipid Fuels with the GREET Model*; 2011.

(23) Campbell, P. K.; Beer, T.; Batten, D. Life cycle assessment of biodiesel production from microalgae in ponds. *Bioresource Technology* **2011**, *102*, 50–56.

(24) Valdez, P.; Nelson, M.; Faeth, J.; Wang, H.; Lin, X.; Savage, P. Hydrothermal Liquefaction of Bacteria and Yeast. *Energy & Fuels (manuscript submitted)* **2013**.

(25) Pham, M.; Schideman, L.; Scott, J.; Rajagopalan, N.; Plewa, M. J. Chemical and biological characterization of wastewater generated from hydrothermal liquefaction of Spirulina. *Environmental science & technology* **2013**, *47*, 2131–8.

(26) Jena, U.; Vaidyanathan, N.; Chinnasamy, S.; Das, K. C. Evaluation of microalgae cultivation using recovered aqueous co-product from thermochemical liquefaction of algal biomass. *Bioresource technology* **2011**, *102*, 3380–7.

(27) Garcia Alba, L.; Torri, C.; Fabbri, D.; Kersten, S. R. a.; (Wim) Brilman, D. W. F. Microalgae growth on the aqueous phase from Hydrothermal Liquefaction of the same microalgae. *Chemical Engineering Journal* **2013**, *228*, 214–223.

(28) Energy Independence and Security Act of 2007. **2007**, *Public Law*, 1–311.

(29) Davis, R.; Fishman, D.; Frank, E. D.; Wigmosta, M. S.; Aden, A.; Coleman, A. M.; Pienkos, P. T.; Skaggs, R. J.; Venteris, E. R.; Wang, M. Q. *Renewable Diesel from Algal Lipids: An Integrated Baseline for Cost, Emissions, and Resource Potential from a Harmonized Model*; Argonne, IL, 2012; p. 85.

(30) G, B. E.; C, E. D. Catalytic Hydrotreating of Biomass-Derived Oils. In *Pyrolysis Oils from Biomass*; American Chemical Society, 1988; pp. 228–240.

(31) Li, Z.; Savage, P. E. Feedstocks for fuels and chemicals from algae: Treatment of crude bio-oil over HZSM-5. *Algal Research* **2013**, *2*, 154–163.

(32) Guan, Q.; Savage, P. E.; Wei, C. Gasification of alga Nannochloropsis sp. in supercritical water. *The Journal of Supercritical Fluids* **2012**, *61*, 139–145.

(33) Brown, T. M.; Duan, P.; Savage, P. E. Hydrothermal Liquefaction and Gasification of Nannochloropsis sp. *Energy & Fuels* **2010**, *24*, 3639–3646.

(34) Duan, P.; Savage, P. E. Upgrading of crude algal bio-oil in supercritical water. *Bioresource Technology* **2011**, *102*, 1899–906.

(35) Neidhardt, F. C.; Bloch, P. L.; Smith, D. F. Culture Medium for Enterobacteria. *Journal Of Bacteriology* **1974**, *119*, 736–747.

(36) Korz, D. J.; Rinas, U.; Hellmuth, K.; Sanders, E. A.; Deckwer, W. D. Simple fed-batch technique for high cell density cultivation of Escherichia coli. *Journal of Biotechnology* **1995**, *39*, 59–65.

(37) Chen, G.; Strevett, K. A. Impact of carbon and nitrogen conditions on E. coli surface thermodynamics. *Colloids and surfaces B Biointerfaces* **2002**, *28*, 135–146.

(38) Elliott, D.; Neuenschwander, G.; Hart, T. *Catalytic hydrothermal gasification of lignin-rich biorefinery residues and algae*; **2009**.

CHAPTER 5. CONCLUSIONS

The results of this dissertation indicate that while algal biofuels remain an alluring source of domestic biofuel, a technological breakthrough capable of propelling the industry into the production targets outlined by the EISA was not revealed. Using waste materials such as wastewater and flue gas as inputs for cultivating algae would reduce costs and the environmental footprint of the biofuel and is therefore an approach worth consideration. As Chapter 2 demonstrates, however, this strategy cannot be scaled to significant volumes due to the limited amount of nutrients in wastewater and an unsuitable climate where a large fraction of the population resides.

Given the limitations in scalability found for flue gas and wastewater co-utilization (FWC), Chapter 3 of the dissertation shifted toward an alternative strategy, heterotrophic cultivation of algae, that is devoid of waste material as an input resource. While such an approach is less technically and economically challenging than using phototrophic algae grown in ponds, it introduces environmental concerns that were previously irrelevant. Chief among these concerns is the footprint associated with producing the sugar that is fed to the algae during fermentation. The advantages of algae relative to a terrestrial bioenergy source are diminished when a terrestrial energy crop is used to provide the foundational energy source for growing the algae.

Building on these results, Chapter 4 reverts to the assumption of open pond cultivation with flue gas as the carbon source but removes the wastewater input constraint and focuses instead on opportunities related to biomass conversion. Improving the economics of the algal biorefinery is critical to achieving national production targets. A fuel with a low life cycle impact but high cost will not contribute to these objectives, after all, if it is never commercialized. The opportunity to produce more fuel per unit of biomass afforded by hydrothermal liquefaction (HTL) allows the biorefinery to reduce the amount of infrastructure required and therefore reduce the costs of production. Investigating the specific conditions that will enhance these attributes revealed the importance of such process decisions. Furthermore, an analysis of a novel pathway featuring growth of *E. coli* to extract as much oil as possible demonstrated the potential to further reduce costs.

5.1 Key Findings

5.1.1 Algal bio-oil production potential through flue gas and wastewater co-utilization

Chapter 2 featured an analysis of the national production potential of algal biofuel using FWC, the first such assessment in literature. The availability of the flue gas and wastewater inputs for algae growth provide an upper limit for how much algae can be cultivated, but even locations where these inputs are abundant may not be appropriate for FWC, as not all locations have suitable climates for algae cultivation. A MATLAB® growth model was used in to calculate an average annual algae yield for any location across the United States based on historical solar radiation and temperature records. A

GIS economic overlay model was then used to integrate the locations and quantities of the input resources with the output from the algae growth model. The results of this overlay analysis highlighted the importance of siting the facilities near large cities to minimize the cost of transporting wastewater; power utility locations had a less noticeable influence on the results. The model also showed that while the supply of carbon dioxide from flue gas is relatively vast, the supply of nutrients in wastewater limits the production potential to the order of billions of liters per year. This amount is further reduced by nearly 60% due to the inappropriate climate where most of the country's population is located.

The predominant cost of producing algal biofuel using FWC is the pond and treatment facility, which varies greatly depending on the location. Costs for this infrastructure range from nearly $6 per liter in cool climates to less than $2 per liter in locations such as Arizona. In the best location most, if not all, of this burden is offset by the $2.65 per liter credit assigned for the treatment service. Wastewater and flue gas transport had less impact on the final cost, contributing on average $0.13 and $0.03 per liter, respectively.

In summary, FWC was found to be economical and sustainable largely because of the treatment service credited to the biofuel for removing nutrients from wastewater, but the limited availability of nutrients in wastewater prevent scaling production to more than 1.7 billion liters per year, or 0.45 billion gallons. The broad metrics outlined in Section 1.4 (sustainable, scalable, and salable) are reintroduced here to summarize the

results, as shown in Figure 5.1. Subtracting the cost from $2 for the "salable" metric allows for a target of 1.0 when the cost is $1·L^{-1} then reduces the score for amounts greater than that amount. A full score for the "scalable" metric corresponds to a production potential of at least 10 billion gallons annually.

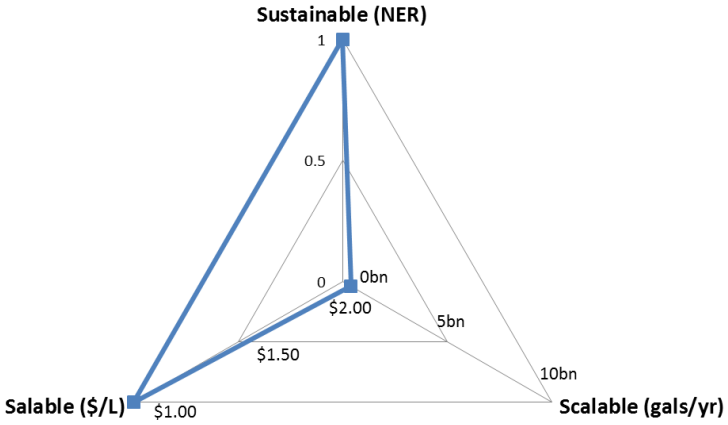

Figure 5.1 - Performance of flue gas and wastewater co-utilization (FWC) in terms of the overarching metrics considered in this dissertation.

5.1.2 Growing algae for biofuel on direct sunlight vs. sugars

Chapter 3 featured an analysis that compared an algal biofuel derived from phototrophic algae grown in open ponds to heterotrophic algae grown on sugars in unlit fermenters. The life cycle model assimilated data from literature for the baseline phototrophic pathway and to create the first-ever LCA of a heterotrophic algal biofuel. Given that this was a simulated system, extra attention was given to the sensitivity of results to key operational parameters such as the fermenter aeration/mixing energy input, the type of crop used for producing the sugar, and the fermentation batch length required to achieve the target cell concentration. As with Chapter 2, a GIS-based model was used to capture the spatial variability of results. The model therefore leveraged

historical climate, evaporation, water stress indices, and agricultural irrigation and yield data. Domestically produced sugar from both sugarcane and sugar beet were considered. A third, hybrid pathway was also investigated to explore potential benefits of mixotrophic algae that can be grown initially in sunlight then subsequently in a fermenter.

The results of the analysis showed that heterotrophic and hybrid pathways have the potential to produce an algal biodiesel with reduced GWP and an improved FER relative to the phototrophic pathway and conventional diesel, but only if efficient fermentation technology, sugarcane is used as the sugar crop, and the sugarcane bagasse is used to recover energy on-site to reduce fossil energy inputs. The water stress results were found to be widely geographically variable for all three pathways, with the sensitivity of results most dependent on the conditions of the aquifer from which the water was withdrawn. The amount of occupied land required for the heterotrophic and hybrid pathways, however, was definitively larger than the phototrophic pathway. Using terrestrial crops for biofuel also requires revisiting the "food vs. fuel" debate. Recall that a primary motivation for algal biofuel was that it could be grown on marginal lands that do not compete with agriculture; this remains valid for phototrophic but not heterotrophic nor hybrid algal biofuel. Furthermore, the potential carbon emissions caused by land use change must also be considered for the heterotrophic and hybrid pathways because diverting sugar for the purpose of producing biofuel could shift sugar production elsewhere to meet global demand.

Figure 5.2 summarizes the results in terms of the broad metrics of sustainability, scalability, and salability. Production scale was outside the scope of Chapter 3, but simple calculations indicate that given the current cost of sugar (~$\$0.30 \cdot kg^{-1}$) it is possible that hetotrophic algal biofuel could be produced for as cheap as $\$1.20 \cdot L^{-1}$, and current volumes of sugar production within the United States enable producing up to 2 billion gallons per year if all sugar production is diverted for this purpose. With conventional fermenter performance, however, the NER is less than 1.0. The more complex issues regarding land use change and food vs. fuel are not captured in the sustainability metric of NER used here, but these issues must not be overlooked.

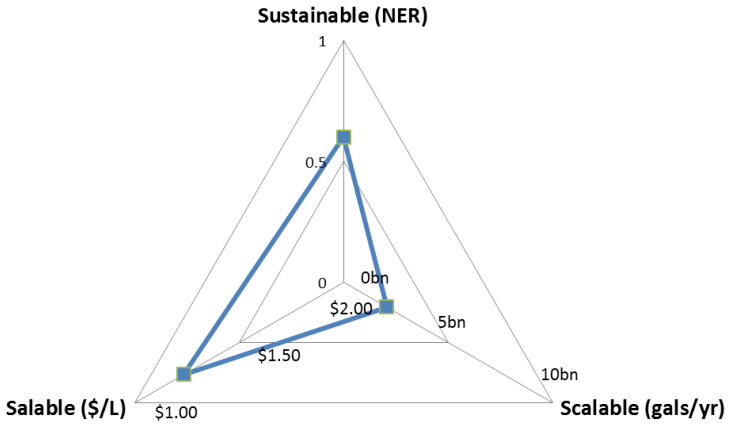

Figure 5.2 - Performance of the heterotrophic and hybrid pathways in terms of the overarching metrics considered in this dissertation.

5.1.3 The effect of hydrothermal liquefaction (HTL) reaction conditions and an alternative pathway featuring microbial regrowth on the life cycle and economic performance of an algal biorefinery

Chapter 4 featured the first life cycle assessment of phototrophic algal biofuel to focus specifically on the role of reaction conditions in the conversion of algal biomass into biocrude oil via HTL. The model includes recent experimental findings from collaborators in the Department of Chemical Engineering studying the yields of the various HTL products across a range of conditions and regrowth of *E. coli* biomass on the aqueous phase portion. The baseline model assumes that onsite electricity and heat can be recovered from the aqueous phase products via catalytic hydrothermal gasification (CHG) while the regrowth pathway replaces CHG with *E. coli* growth. The microbial biomass can be recycled back to the HTL reactor for boosted oil yields.

Results of the model highlighted the importance of the HTL reaction conditions on the life cycle and economics of the biorefinery, with results varying significantly across the design space considered (250-400°C, and 5-90 minutes). The GWP results track closely to the NER, with the minimum value of 0.74 kg $CO_2e \cdot L^{-1}$ occurring at 250°C and 60 minutes. The highest oil yield from HTL is 42% at conditions of 400°C and 5 minutes. An increased oil yield does not translate into a lower carbon footprint, however, for the standard pathway; high oil yields mean less of the algal biomass ends up in the aqueous phase solution where it could be converted into useful energy via CHG. Given that the pond costs dominate the economic model, however, the lowest-cost scenarios does correspond to where the oil yield is highest and therefore the least amount of pond is

required per liter of biocrude produced. Optimal conditions for the economic metric therefore occur at 400°C and 5 minutes where a liter of biocrude would cost $\$1.72 \cdot L^{-1}$. This cost represents a 9% reduction compared to the cost at standard conditions (350 °C, 60 min). The land occupation metric tracks closely with the economic results because both are driven primarily by the size of the pond required for cultivation.

The model also revealed that the greatest total oil yield for the regrowth pathway also occurs 400°C and 5 minutes. At these conditions the additional *E. coli* biomass boost the oil yield from 42% up to 47% of the initial algal biomass and in doing so further reduce the costs to $\$1.67 \cdot L^{-1}$. These cost savings come at the expense of the carbon footprint of the fuel, however, as the GWP increases 80% relative to the standard pathway (to 1.49 kg $CO_2e \cdot L^{-1}$) due to the elimination of energy recovery via CHG. Even so, this represents a 50% reduction in GWP relative to conventional fossil fuel and therefore still qualifies as an advanced biofuel.

Figure 5.3 summarizes the results in terms of the broader metrics mentioned earlier. An algal biorefinery with the *E. coli* regrowth pathway optimized for the lowest cost (reaction conditions of 400°C, 5 minute) has a NER greater than one and can be scaled to high production volumes because it is dependent on neither waste resources nor a sugar source. This configuration produces an upgraded oil with the cost of $\$1.67 \cdot L^{-1}$ and therefore exceeds the target, but still represents a marginal improvement that could meaningfully contribute toward the commercial viability of algal biofuel in conjunction with other technological advancements.

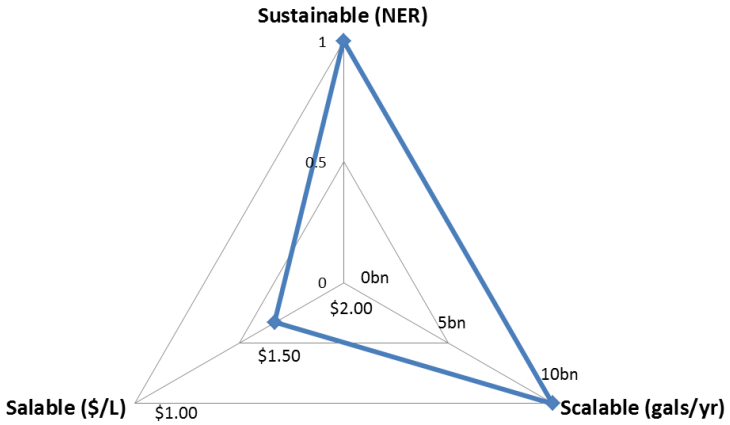

Figure 5.3 - Performance of an algal biorefinery featuring HTL and an *E. coli* regrowth pathway in terms of the overarching metrics considered in this dissertation.

5.2 Summary

In summary, each of the three technologies explored in this dissertation had unique advantages, but none were found to exhibit high performance for each of the three overarching metrics explored, as shown in Figure 5.4. The approach for producing algal biomass using wastewater as the nutrient source and power utility flue gas as the carbon dioxide source is appealing from an environmental and economic perspective. But although incorporating waste materials into the biorefinery does provide distinct advantages, dependence on these feedstocks also limits the scalability. For FWC, then, while the technology could economically produce a biofuel that meets the sustainability metrics outlined previously, the availability of nutrients within wastewater prevented scaling beyond 0.5 billion gallons annually.

Growing heterotrophic algae on domestically produced sugars presents an advantage over FWC in terms of scalability, as the total sugar production within the US could support up to 2 billion gallons annually. The current cost of sugar indicates that

while an algal biofuel could be produced more cheaply than an open pond system, it still could not compete with fossil fuels. Additionally, the environmental impacts of such an approach are questionable, particularly because of the reliance on a terrestrial food crop and the aeration/mixing energy required to run the aerobic fermentation process.

Growing phototrophic algae in open ponds and then converting the biomass into oil using HTL, conversely, meets the sustainability criteria and can be scaled to significant production volumes because it does not rely on sugar or waste feedstocks. The cost of such an approach is greater than the two previous technologies that were explored, however, primarily because of the pond infrastructure. Optimizing the HTL reaction conditions to obtain the greatest amount of oil per unit of biomass grown can reduce these costs, as could recovering the non-fuel fraction of the carbon by growing a secondary type of heterotrophic biomass such as *E. coli*.

Therefore the key to achieving an algal biofuel that is commercially viable and can also offer environmental benefits relative to fossil fuels is either to 1) identify waste feedstocks that will not become limiting at large production volumes, 2) develop less expensive pond and conversion infrastructure, or 3) extract more oil per unit of algal biomass thereby reducing the amount of infrastructure required. Designing an integrated biorefinery that features internal recycling loops to recover intermediate waste products will also be crucial to minimize the input requirements and therefore reduce the environmental and economic costs.

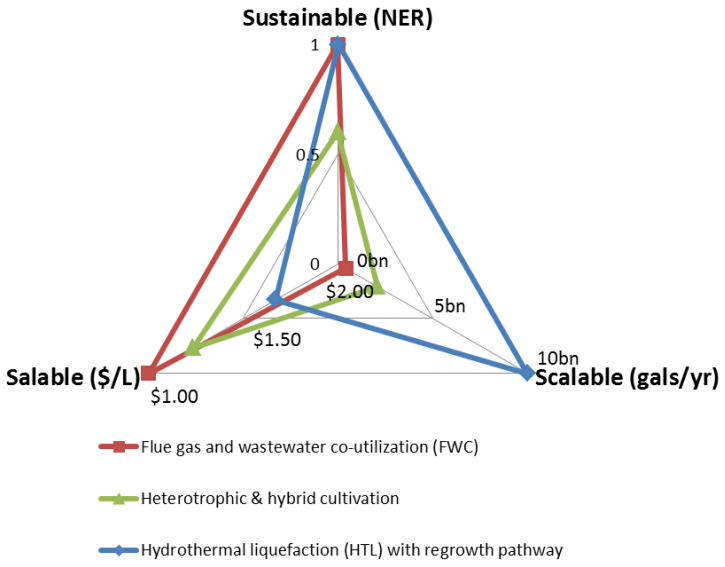

Figure 5.4 - A summary of the performance of the three technologies explored in this dissertation in terms of the overarching metrics of Sustainability, Scalability, and Salability.

5.3 Future Work

The RFS standards outlined by the US EPA stipulate that advanced biofuels must have life cycle carbon emissions that are at least 50% less than a baseline fossil fuel. The threshold is relaxed for corn ethanol (20% reduction) and stricter for ligno-cellulosic ethanol (60% reduction). These criteria present the only example of an LCA metric implemented within US public policy. As this dissertation has demonstrated, however, calculating the life cycle impacts of a biofuel is highly sensitive to process assumptions and can exhibit significant variation geographically. The GIS based methods implemented in Chapters 2 and 3 could be extended to evaluate regional variation in life cycle impacts and the national production potential of other, terrestrial bioenergy systems.

The models implemented as part of this dissertation could also be updated with values reported by the private sector to demonstrate qualification for the designation as an advanced biofuel. The private firms currently working toward commercialization have no motivation to publish academic literature because doing so would provide a competitive disadvantage. As a consequence, there is potentially a significant discrepancy between the values and process assumptions passed amongst academic LCAs and those that are actually being implemented by private companies. The models developed within this dissertation could be of particular value to companies leveraging genetic engineering and therefore have more control over the composition and growth behavior of their species.

The LCA models developed to analyze the performance of HTL across a range of reaction conditions for Chapter 4 could also be repeated as more data emerges. The results indicated the economic benefits of achieving maximum oil yields that occurred at high temperatures with a low process time. Recall that the lowest cost scenario occurred at the limit of the design space for both design variables (400°C was the highest temperature and 5 minutes was the shortest reaction duration considered). A better understanding of what is capable at higher temperatures or faster reactions could reveal improved performance. The LCA results for the regrowth pathway could also be updated to explore the performance of a biorefinery featuring growth of alternative types of microbial biomass on the aqueous phase products. If other organisms can demonstrate higher organic carbon uptake efficiencies than *E. coli* the benefits of the regrowth pathway could be amplified.

APPENDIX 1. SUPPORTING INFORMATION FOR CHAPTER 2

A1.1 Wastewater Treatment Energy Credit Calculations

In the Background section of the article the overall energy benefits of treating wastewater in conjunction with algal bio-oil production are explored. To determine the effect of using flue gas and wastewater co-utilization (FWC) on the overall net energy ratio (NER), values for energy 'credits' must be identified. Using the stoichiometry of algal biomass shown in Table 1, a lower heating value (LHV) for algal bio-oil of 30 $MJ \cdot kg^{-1}$ [1], and the values for energy of nitrogen and phosphorus removal provided by Maurer et al. (2003) these credits can be calculated as shown in the following equations [1,2]. The life cycle assessment performed by Lardon et al. (2009) assumes a lipid content of 18% [3], but to be consistent with the assumptions used later in the analysis a 25% lipid fraction will be used to deduce the energy credits. Lowering the lipid content from 25% to 18% would *increase* the total of these credits by 28% because more wastewater would be treated per unit bio-oil produced.

For Nitrogen Removal:

$$EC_{NR} = \left(\frac{45MJ}{kg\ N}\right)\left(\frac{1\ kg\ oil_{algal}}{30\ MJ}\right)\left(\frac{0.066\ kg\ N}{1\ kg\ algal\ biomass}\right)\left(\frac{1\ kg\ algal\ biomass}{0.25\ kg\ oil_{algal}}\right)$$

$$= \mathbf{0.40\ MJ\ per\ MJ\ of\ oil_{algal}}$$

For Phosphorus Removal:

$$EC_{PR} = \left(\frac{49MJ}{kg\ P}\right)\left(\frac{1\ kg\ oil_{algal}}{30\ MJ}\right)\left(\frac{0.013\ kg\ P}{1\ kg\ algal\ biomass}\right)\left(\frac{1\ kg\ algal\ biomass}{0.25\ kg\ oil_{algal}}\right)$$

$$= \mathbf{0.08\ MJ\ per\ MJ\ of\ oil_{algal}}$$

For Aeration:

The energy credit for providing aeration is based on the value of 0.20 kW·h required per cubic meter of wastewater treated, as reported by Nielsen and Jørgensen (2002)[4]:

$$E_{RO}$$

$$= \left(\frac{0.20\ kW \cdot h}{m^3\ WW}\right)\left(\frac{1\ MJ}{0.278\ kW \cdot h}\right)\left(\frac{11{,}600\ m^3\ WW}{m^3\ oil_{algal}}\right)\left(\frac{m^3\ oil_{algal}}{920\ kg\ oil_{algal}}\right)\left(\frac{kg\ oil_{algal}}{30\ MJ\ oil_{algal}}\right)$$

$$= \mathbf{0.30\ MJ\ per\ MJ\ of\ oil_{algal}}$$

The ratio of volumetric ratio of wastewater treated per volume of bio-oil produced is established by the following conversion:

$$\left(\frac{0.066\ kgN}{kg\ algae}\right)\left(\frac{L\ WW}{30\ mg\ N}\right)\left(\frac{1}{0.7}\right)\left(\frac{10^6\ mg}{kg}\right)\left(\frac{kg\ algae}{0.25\ kg\ oil_{algal}}\right)\left(\frac{0.92\ kg\ oil_{algal}}{L\ oil_{algal}}\right)$$

$$= \mathbf{11{,}600\ L - WW\ per\ L - oil_{algal}}$$

The conversion assumes a nutrient uptake efficiency of 70%, toward the upper limit of what is deemed possible (80%) by Lundquist et al. (2010), who assumed just 44% removal in their baseline analysis [5]. The nitrogen concentration in wastewater is assumed to be 30 mg·L^{-1} and the density of the bio-oil 0.92 kg·L^{-1}.

The energy credits for nitrogen removal, phosphorus removal, and aeration, can then be summed to determine a total energy credit, EC_{TOT}:

$$EC_{TOT} = EC_{NR} + EC_{PR} + EC_{RO} = 0.40MJ + 0.08MJ + 0.30MJ$$

$$= \mathbf{0.78\ MJ\ per\ MJ\ of\ oil_{algal}}$$

A1.2 Algal Biomass Composition

Data from Grobbelaar (2004) suggests a stoichiometry of approximately $C_{100}H_{183}O_{48}N_{11}P$, which results in the mass apportionment shown in Table A1.1[2].

Table A1.1 - Assumed composition of algal biomass [2].

Element	Quantity	Molecular Weight	Total	Percentage (by mass)
Carbon	100	12	1,200	51.4%
Hydrogen	183	1	183	7.8%
Oxygen	48	16	768	32.9%
Nitrogen	11	14	154	6.6%
Phosphorus	1	31	31	1.3%
			2,336	**100%**

A1.3 Nutrient Availability Conversions

Crites and Tchobanoglous (1998) report that the average per capita Total Kjeldahl Nitrogen (TKN, sum of ammonia and organic nitrogen) mass loading rate is 4.85 kg·person^{-1}·year^{-1} , while Scheehle (1997) reports a higher value of 9.37 kg·person^{-1}·year^{-1} [6,7]. The average of these values, 7.11 kg-TKN·person^{-1}·year^{-1} was used as the baseline. For simplicity, this analysis assumes 100% conversion of lipids to bio-oil. Maintaining the 70% nutrient uptake efficiency, the conversion rate between the population and algal bio-oil can be established as:

$$\left(\frac{7.1\ kg\ TKN}{person\ \cdot year}\right)\left(\frac{1kg\ algae}{0.066\ kg\ TKN}\right)\left(\frac{0.25\ kg\ oil_{algal}}{kg\ algae}\right)\left(\frac{L\ oil_{algal}}{0.92\ kg\ oil_{algal}}\right)(0.7)$$

$$= \frac{\mathbf{20.5\ L\ oil_{algal}}}{\boldsymbol{person \cdot year}}$$

Based on the biomass composition and simple stoichiometry, it follows that 1.88 kg of carbon dioxide is required per every kilogram of algal biomass grown. It is assumed that a substantial amount of carbon is collected in the primary sedimentation basin and processed in an anaerobic digester (along with the non-lipid algal biomass residuals). The carbon dioxide that is emitted from the combustion of the biogas is sufficient to meet the algal growth requirements for much of the year, though some carbon dioxide will need to be imported from an external source such as power utility flue gas [5]. Based on approximations by Lundquist et al. (2010), this analysis assumes that an annual average of 8% of the carbon in the algal biomass will need to be supplemented by flue gas imports [5]. Maintaining our assumption of 25% lipid content, therefore, and

assuming a carbon dioxide uptake efficiency of 30% due to nighttime losses and mismatch of production with algae growth cycles [8], the conversion rate can be established as:

$$\left(\frac{1000\ kg}{tonne}\right)\left(\frac{1kg\ algae}{0.08 \cdot 1.88kg\ CO_2}\right)\left(\frac{0.25\ kg\ oil_{algal}}{kg\ algae}\right)\left(\frac{L\ oil_{algal}}{0.92\ kg\ oil_{algal}}\right) \quad (0.3)$$

$$= \frac{\mathbf{540\ L\ oil_{algal}}}{\mathbf{tonne\ CO_2}}.$$

A1.4 Algae Growth Model Calculations

The growth model inputs were based on the data and formula from Tamiya et al. (1953) [9]. The areal algae yield, Y_a (measured in g·m^{-2}·day^{-1}) is reported to be

$$Y_a = \left(\frac{10}{2}\right) \cdot \left(5.3\frac{k_G}{\varepsilon}\right) \log\left(1 + \frac{\alpha\gamma L}{Hk_G}\right) \cdot C. \quad (1)$$

The parameters used in this formula along with their descriptions, units, and empirically derived values are included in Table 2.

Table A1.2 - Growth formula inputs. Source: Tamiya et al. (1953) [9].

Parameter	Description	Units	Value
L	Solar radiation	kilolux-hour·day^{-1} ·m^{-2}	Input, measured in field
K_G	Kinetic parameter	day^{-1}·m^{-2}	0.07*Temp -0.44
γ	Light intensity correction factor	dimensionless	0.64
ε	Extinction coefficient	ml^{-1}	0.41
α	Rectangular hyperbola shape parameter	day^{-1}·kilolux^{-1}	0.45
H	Duration of sunlight	hours·day^{-1}	12
C	Dry weight conversion	g·ml^{-1}	0.25

Current solar irradiance data sources are available in the flux density units of $kW \cdot m^{-2}$ rather than Kilolux (lux = $lumen \cdot m^{-2}$). Here it is assumed that the average sun and sky luminous efficiency is 108 lumens per watt [10].

The kinetic parameter, K_G , is related to temperature by the formula listed for the parameter in Table 2. Values of K_G for three temperatures experimentally determined by Tamiya et al. and are listed in Table 2. The linear least-squares regression line used to define the relationship is shown in Figure A1.1. Note that this linear relationship suggests that increased temperature always results in increased productivity. In practice this is not always the case, depending on the species. Chlorella pyrenoidosa, for example, exhibits a higher growth rate at 25° C than at 20 or 30° C [11]. In the referenced text, however, no such data points are available to establish such a trend for the model organism, Chlorella ellipsoidea. For a thermophilic Chlorella species (Tx 115), conversely a K_G value is reported to be 2.7 $day^{-1} \cdot m^{-2}$ at 39° C which fits with the linear trend, as indicated by the fourth point in Figure A1.1. The general relationship between temperature, solar radiation, and estimated daily algae yield is shown in Figure A1.2.

Table A1.3 - Relationship between kinetic parameter and temperature [9].

Temperature (° C)	K_G ($day^{-1} \cdot m^{-2}$)
7°	0.092
15°	0.52
25°	1.34

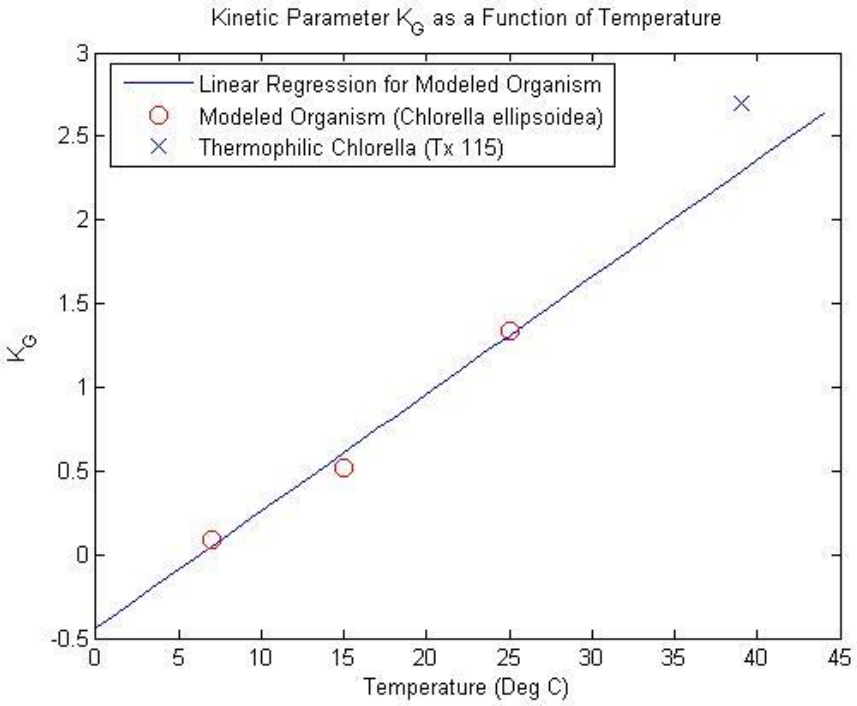

Figure A1.1- Relationship between algae growth kinetic factor and ambient temperature, $r^2 = 0.987$.

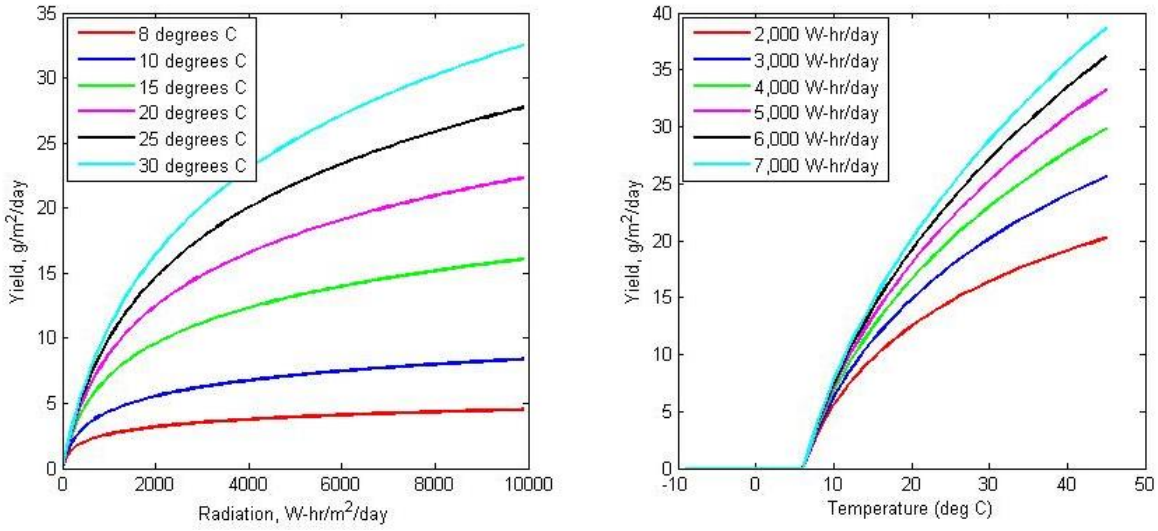

Figure A1.2 - Algae growth rate formula illustrated as a function of radiation for multiple temperatures, and as a function of temperature for multiple daily radiation quantities.

A convenient way to visualize how algae biomass yield responds to climatic variations is by using what is here referred to as a “seasonal growth plot”. These plots display solar radiation on the x-axis, temperature on the y-axis, and the resulting algae yield by color. Sample seasonal growth plots are shown for four cities with distinct climates in Figure A1.3. In these figures the climatic coordinates throughout the year are traced with a line; markers denote the start of a new month. An interesting phenomenon is that for nearly all locations a counter-clockwise motion is observed as the climatic coordinates are traced. An explanation for this occurrence is that the thermal mass of the earth requires a lag time between solar radiation and the resultant increase in temperature. That is, the warmest period of the year is generally later in the season than the sunniest because it takes time for the landscape and atmosphere to absorb the radiation and heat up. Notice that the more fluctuating, desert-like setting of Phoenix, AZ, allows for periods of exceptionally high productivity when high temperatures and high solar radiation coincide. Pensacola, FL, conversely has a lower average yield but more consistent production throughout the seasons. A more thorough site selection process should include consideration of these seasonal attributes and an optimization of the algae pond size based on the length of the growing season. For the purposes of this basic assessment only the average annual output will be considered. This is a reasonable starting point, especially because the most likely “ideal” locations will be in regions where cultivation is viable throughout the year.

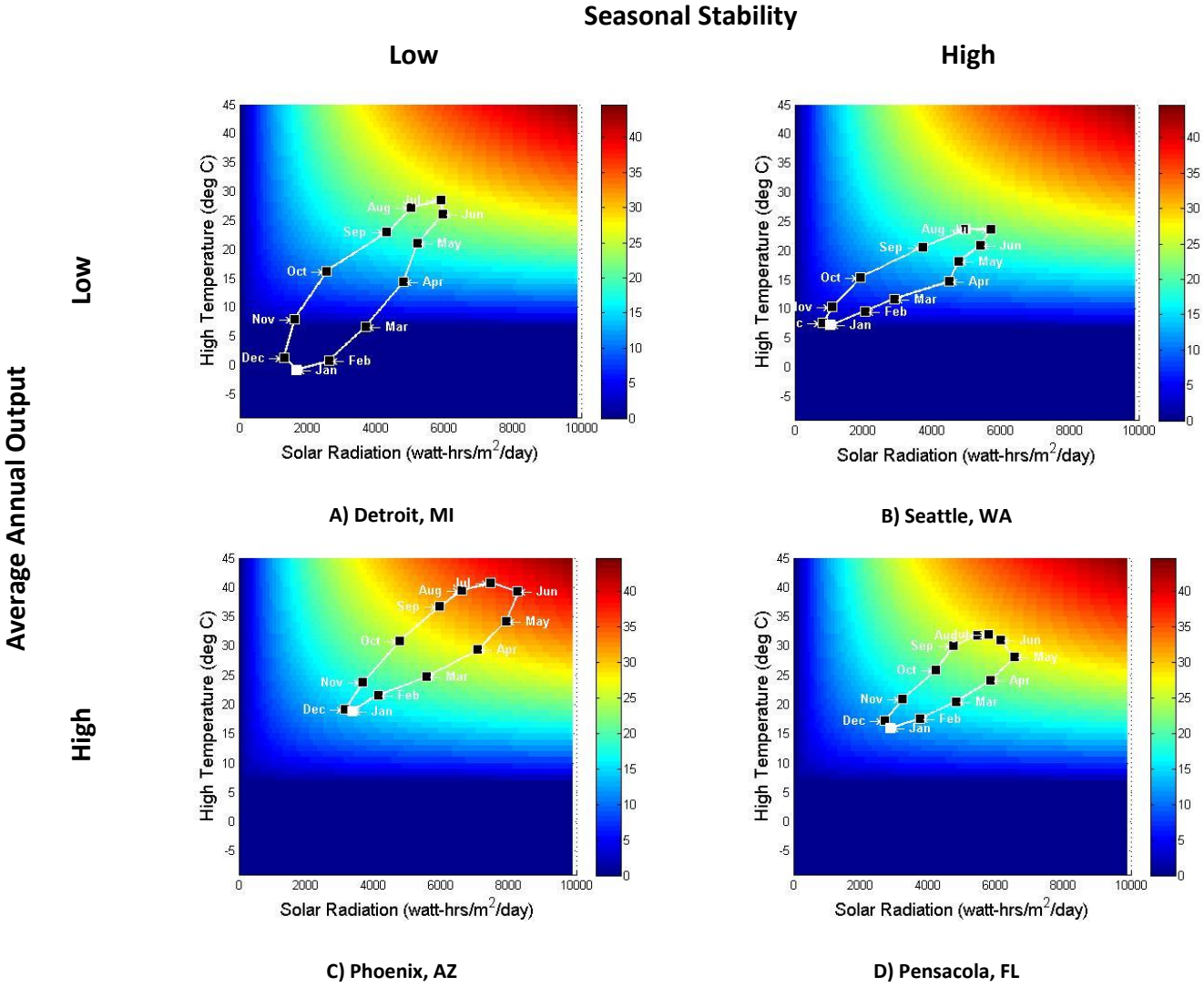

Figure A1.3 - Seasonal growth plots for four sample locations as produced by the simulation.

As expected, locations in the lower latitudes tend to produce a higher average annual yield. As Figure A1.4 demonstrates, however, while southern locations tend to outperform northern in general, there is a significant amount of variation in algae yield at any given latitude. This variation is due to the drastic differences in geography and climate across the breadth of the country. The elevated cooler regions of the Rocky Mountains reside adjacent to the Great Basin Desert, for example, yet produce

dramatically different results. Therefore it is apparent that latitude alone is an insufficient means for predicting algae production rates.

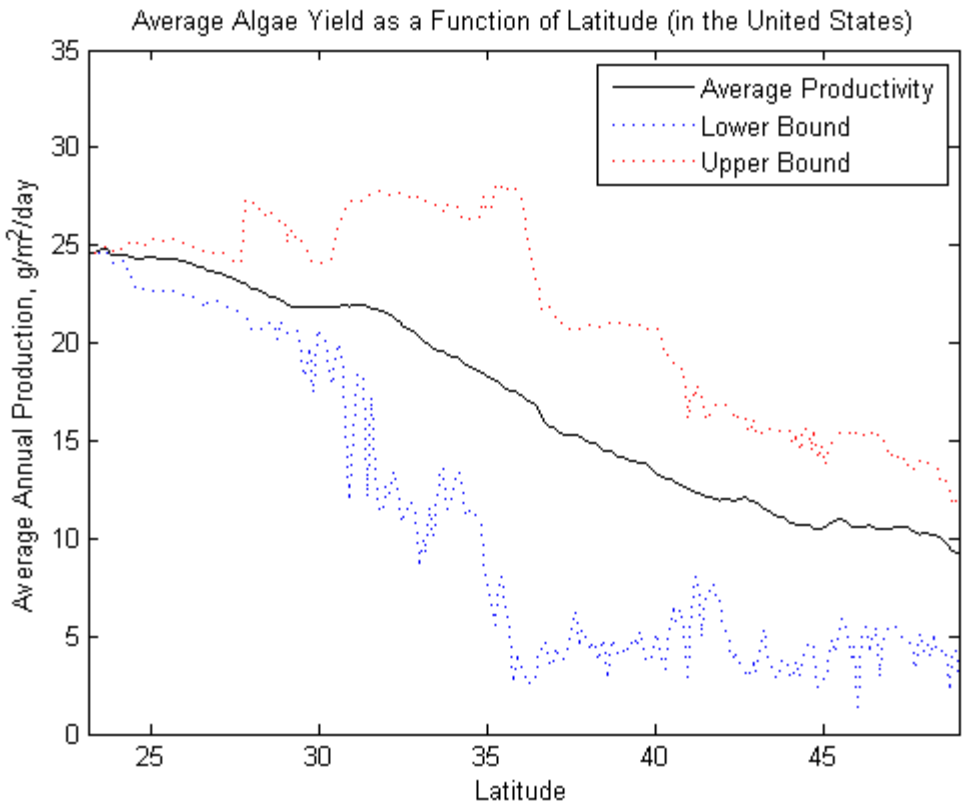

Figure A1.4 - Algae yield as a function of latitude (assuming a lipid content of 25%).

A1.5 GIS Overlay Analysis

The GIS analysis uses a dataset containing populations of "urban areas" from the 2000 United States Census [12]. Clusters of cities often containing surrounding suburbs are lumped into a single region, with boundaries of polygons designating the extent of the area with a sufficiently high population density. Only polygons with large populations, those containing more than 100,000 people, were considered. These 254 regions

include nearly 180 million people, or approximately 60% of the total population. A dataset including point locations of power utilities and their carbon dioxide emissions as reported under the EPA's Acid Rain legislation was obtained from Purdue University's Vulcan Project [13]. Only facilities that produce enough carbon dioxide to meet the equivalent bio-oil production from the population cutoff of 100,000 people were considered. This cutoff was implemented as a filter to remove small power utilities from the GIS algorithm. Doing so allowed the implementation of the assumption that any location uses the C resources from the nearest power utility and N resources from the nearest urban area. There were many small power utilities that portrayed some locations as being carbon-limited, even if a much larger utility was slightly farther away (thereby underestimating production potential). Creating the cutoff eliminated this issue.

A total of 948 power utilities were therefore included, producing a total of more than 2.4 billion metric tons of carbon dioxide per year, or approximately 40% of total anthropogenic carbon dioxide emissions in the United States.

The methodology employed here relies on the assumption that at any point in the United States, wastewater will be piped in from the edge of the nearest urban area polygon and carbon dioxide from the point of the nearest power utility. Because of this assumption, the zone assigned to each resource can be defined using Theissen polygons, which divide the terrain into regions such that any location within the polygon is closer to its associated point than to any other point. The urban area polygons therefore were

first converted to points prior to Theissen polygons. The total amount of bio-oil that can be produced based on these inputs can then be established by multiplying the conversion ratios from the previous section with the respective nutrient availability within each of the sets of zones. It will be the lesser of these two quantities that determines how much bio-oil can be produced at that point.

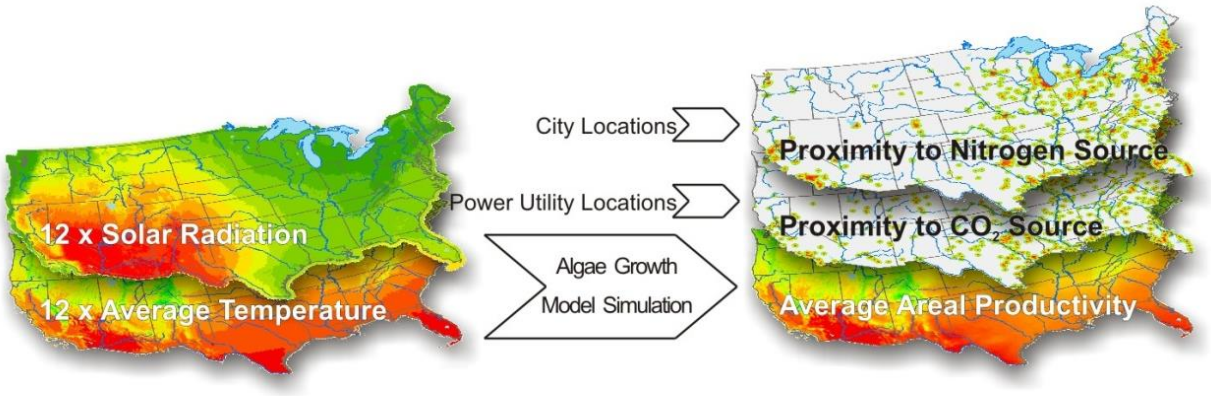

Figure A1.5 - Summary of the GIS overlay analysis process.

In summary, any point in the contiguous United States falls within a Theissen polygon indicating the nearest urban area and thus the bio-oil that can be produced based on the size of the population, and any point also falls within a separate Theissen polygon indicating the nearest power utility and thus the bio-oil that can be produced based on the carbon dioxide emissions. Neither of these two values alone determines the amount of bio-oil that can be produced at that location, however, but rather the minimum of the two. Figure A1.6 through Figure A1.11 outline the general process for arriving at this quantity, zoomed in on a region in Southern Louisiana for clarity.

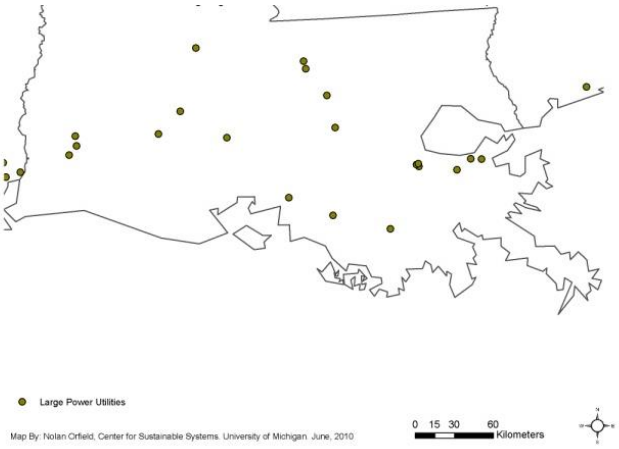

Figure A1.6 - Large power utility locations in southern Louisiana.

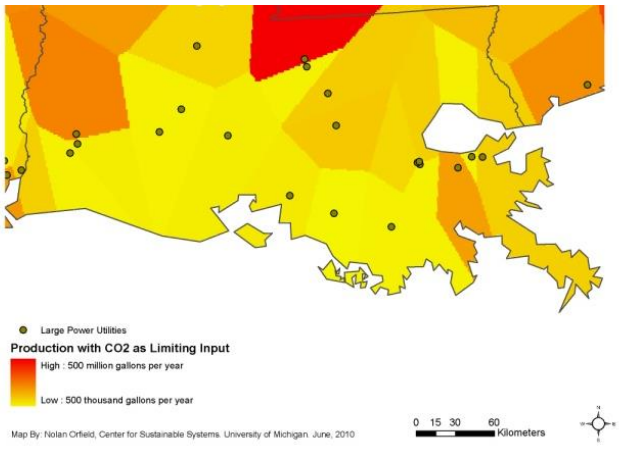

Figure A1.7 - Production of algal bio-oil in southern Louisiana assuming no nutrient limitations.

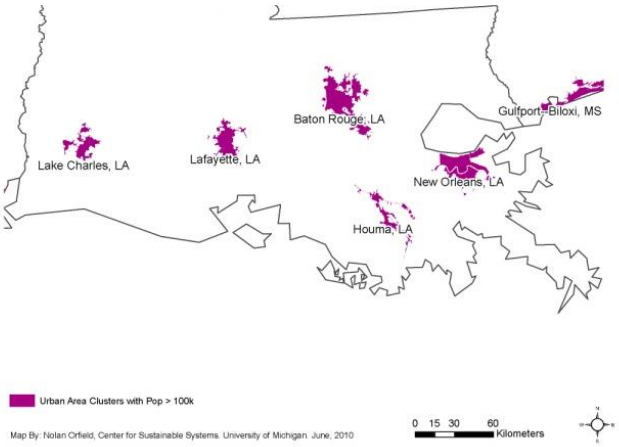

Figure A1.8 - Urban area clusters in southern Louisiana.

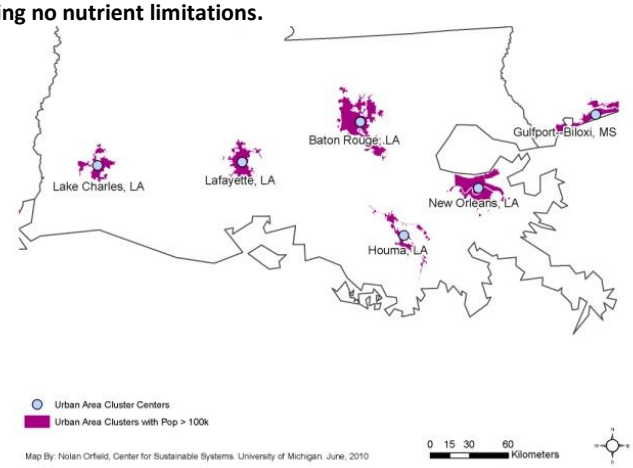

Figure A1.9 - Geographic center points of urban area clusters in southern Louisiana.

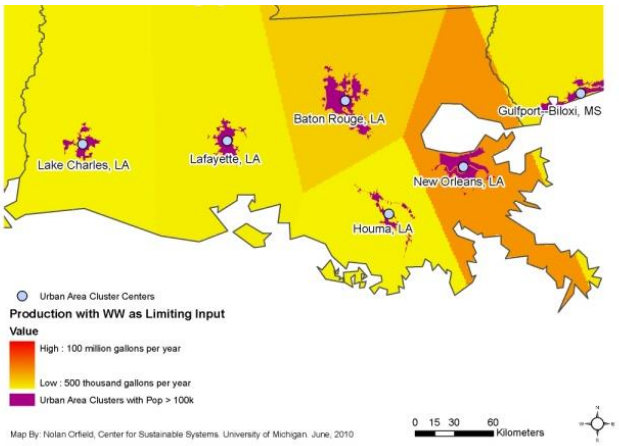

Figure A1.10 - Production of algal bio-oil in southern Louisiana assuming no carbon dioxide limitations.

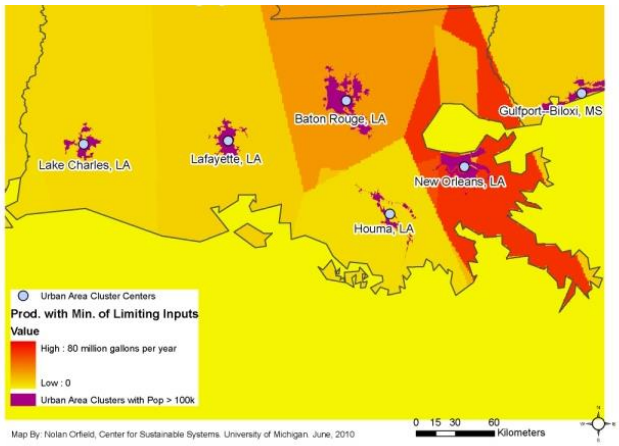

Figure A1.11 - Maximum production of algal bio-oil in southern Louisiana based on relative abundance of nutrient and carbon dioxide availability.

While the populations of urban areas and quantities of carbon dioxide emissions from power utilities are useful for determining how *much* bio-oil can be created, their locations are also significant. When assessing potential algae cultivation sites, consideration must be given to the proximity to both of the resources providing the nutrients inputs. Figure A1.12 and Figure A1.13 depict the distance from any point to the nearest power utility and urban area, respectively. Transporting these nutrients this distance has an associated cost, as represented by the economic assumptions presented in the article text.

In this model it is assumed that only the amount of nutrient required to produce the bio-oil will be transported. So, for example, in a location that is limited by wastewater availability rather than carbon dioxide, all of the wastewater will be piped to that location but only the required fraction of flue gas.

To locate the most ideal sites, however, neither nutrient availability data nor climatic parameters nor transport distances alone will reveal meaningful an answer. Rather, the multiple GIS datasets, or "layers", must be combined into a single results calculation. It is for this reason that the proximity and growth rate datasets were expressed in economic terms, enabling the layers to be summed in equivalent units.

To assign a wastewater treatment credit, a value was assigned based on the assumed BOD removal from 200 down to 14 mg/L and economic value of $1.23/kg to be consistent with Lundquist et al. (2010) [14,15], as shown below:

$$\left(\frac{11{,}600\ liters\ WW}{L\ oil_{algal}}\right)\left(\frac{200-14\ mg\ BOD\ removed}{L\ WW}\right)\left(\frac{kg\ BOD}{10^6\ mg\ BOD}\right)\left(\frac{\$1.23}{kg\ BOD\ removed}\right)$$

$$=\frac{\mathbf{\$2.65}}{\boldsymbol{L\ oil_{algal}}}$$

Figure A1.14 depicts the average annual algae yield, which is the output of the algae growth model presented earlier. This value establishes the pond size (and hence cost) required for producing the quantity of bio-oil shown in Figure A1.11. The result of summing each of the aforementioned costs and dividing by the quantity of biooil produced is shown in Figure A1.15 and again in Figure A1.16 but with the interior of the "urban area" polygons whitened out. Figure A1.17 illustrates the 10km wide buffer created around each of the urban areas for analyzing the cost distribution of the region. Layer values were extrapolated and compiled to yield final results using the ArcGIS © Zonal Statistics tool within the Spatial Analyst toolbox.

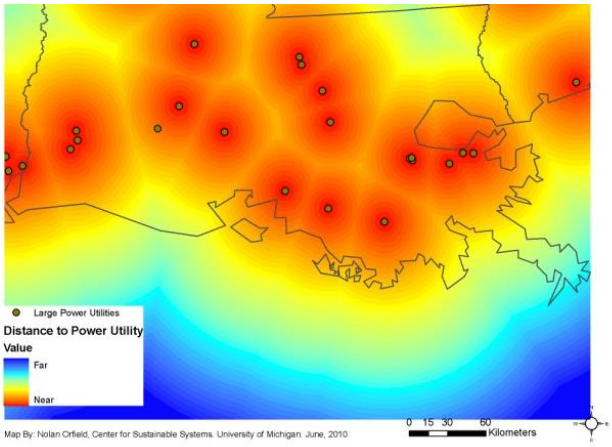

Figure A1.12 - Distance to nearest large power utility in southern Louisiana.

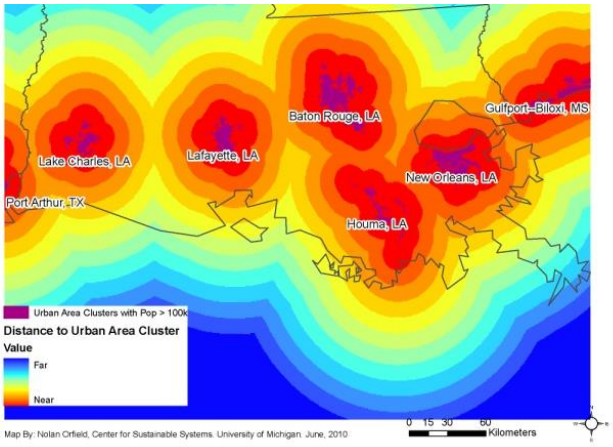

Figure A1.13 - Distance to nearest large urban area cluster in southern Louisiana.

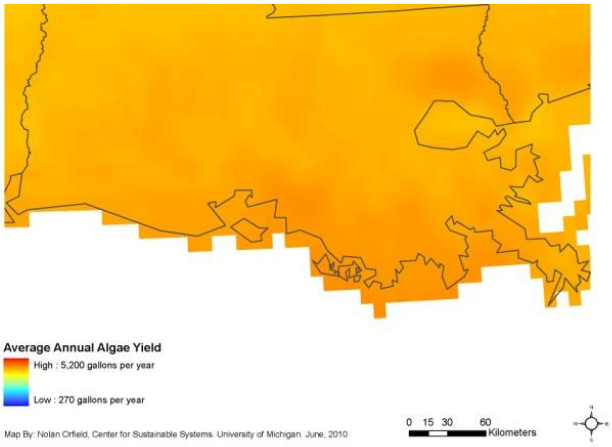

Figure A1.14 - Average areal algal bio-oil production in southern Louisiana.

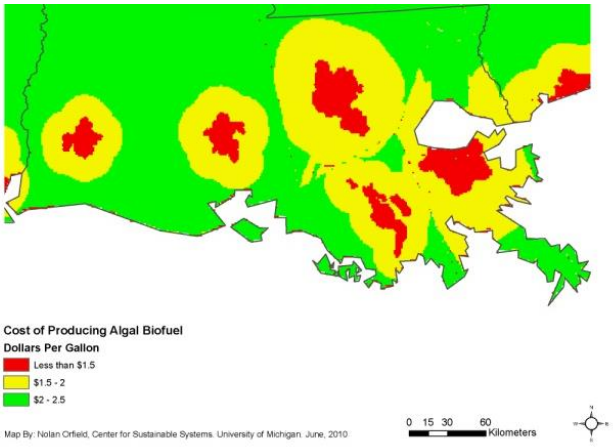

Figure A1.15 - Results of economic overlay analysis.

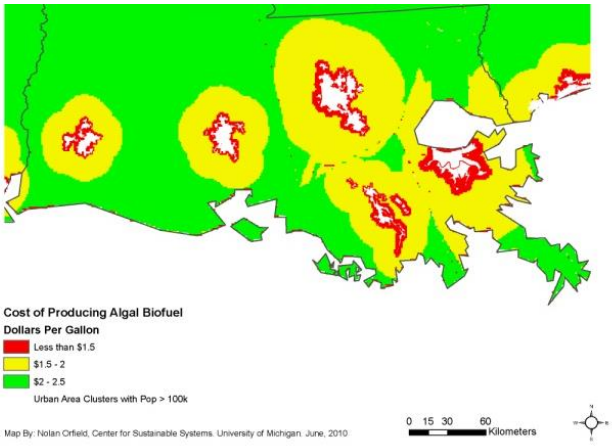

Figure A1.16 - Results of economic overlay analysis with area defined as the urban area cluster concealed in white.

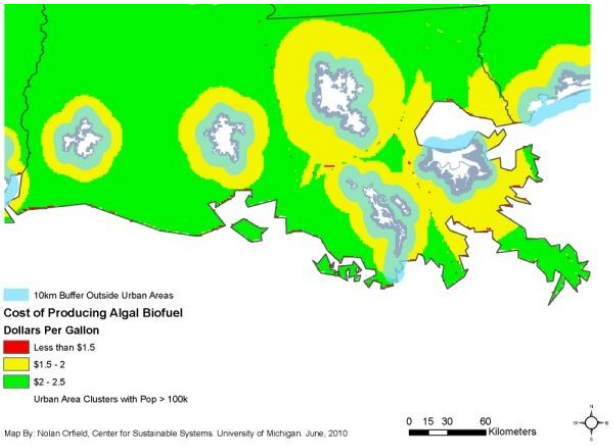

Figure A1.17 - Results of economic overlay analysis with 10km buffer surrounding the urban area shown in a semi-transparent blue.

An example of a typical cost distribution for a location where producing algal oil is economically viable is shown in Figure A1.18.

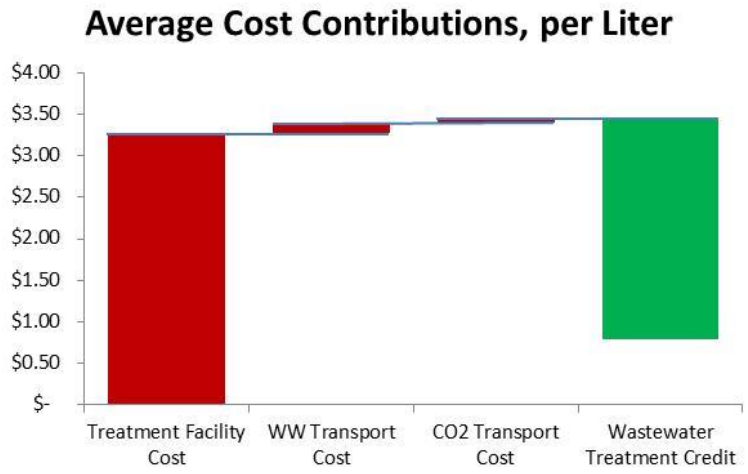

Figure A1.18 – Average costs and credits associated with the production of a liter of algal oil using FWC. The resulting average cost is $0.78/Liter.

A1.6 Sensitivity of Results to Pond Temperature Assumption

The article mentions that for the algae growth model simulation, average annual high temperatures for each location were used. This assumption was based on the premise that most of the algae growth will occur during the warmest portion of the day and that because of the shallow depth of the pond the water temperature can be assumed to match the ambient atmosphere. Such assumptions may overestimate the growth rate, so the analysis was repeated using an alternate scenario in which the pond temperature was modeled to be the average of the maximum and minimum historical averages for that location. That is, rather than using the average T_{max} value to model the pond temperature, $(T_{max}+T_{min})\cdot 0.5$ was used. The same historical average temperature

data source was used [15] . Figure A1.19 illustrates how such an assumption affects the average annual yield and Table 3 illustrates the bearing on total national production potential. The true value is somewhere within this reported range. The average annual yield results used to project the upper limit, however, appear more consistent with other literature and therefore present a more likely scenario.

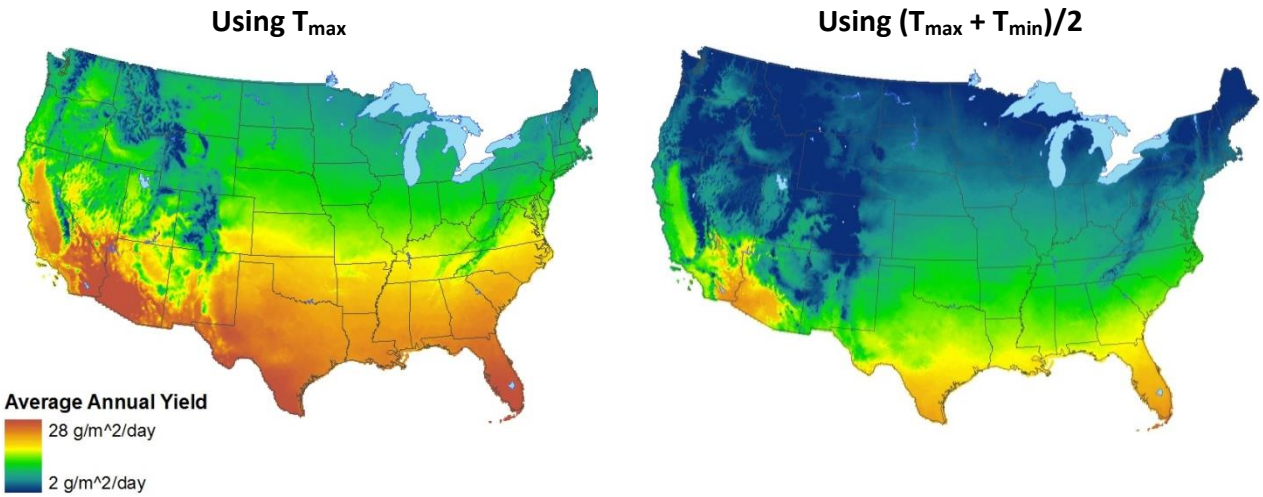

Figure A1.19 - A comparison of the average annual algae yield growth simulation results based on different pond temperature algae growth model assumptions.

Table A1.4 - A comparison of national production potential results based on different pond temperature algae growth model assumptions.

	Using T_{max}	Using $(T_{max} + T_{min})/2$
Pond Area Required (ha)	83,000	29,000
Liters of bio-oil (billions)	1.68	0.54

A1.7 References

(1) Maurer, M.; Schwegler, P.; Larsen, T. A. Nutrients in urine: energetic aspects of removal and recovery. *Water Science and Technology* **2003**, *48*, 37–46.

(2) Grobbelaar, J. U. *Richmond A (ed) Handbook of Microalgal Culture: Biotechnology and Applied Phycology*; Richmond, A., Ed.; Blackwell Science, 2004; Vol. 40, p. 577.

(3) Lardon, L.; Hélias, A.; Sialve, B.; Steyer, J.-P.; Bernard, O. Life-Cycle Assessment of Biodiesel Production from Microalgae. *Environmental Science & Technology* **2009**, *43*, 6475–6481.

(4) Nielsen, P. H.; Jorgensen, K. R. Municipal wastewater treatment http://www.lcafood.dk/processes/wastetreatment/wastewatertreatment.htm (accessed May 5, 2011).

(5) Lundquist, T. J.; Woertz, I. C.; Quinn, N. W. T.; Benemann, J. R. A Realistic Technology and Engineering Assessment of Algae Biofuel Production. *Assessment* **2010**, *October*, 1.

(6) Crites, R. W.; Tchobanoglous, G. *Small and decentralized wastewater management systems*; Tchobanoglous, G., Ed.; McGraw-Hill, 1998; p. 1084.

(7) Scheehle, E. A. Improvements to the U . S . Wastewater Methane and Nitrous Oxide Emissions Estimates. *Water* **1997**.

(8) Benemann, J. R. Utilization of carbon dioxide from fossil fuel-burning power plants with biological systems. *Energy Conversion and Management* **1993**, *34*, 999–1004.

(9) Tamiya, H.; Hase, E.; Shibata, K.; Mituya, A.; Iwamura, T.; Nihei, T.; Sasa, T. Kinetics of Growth of Chlorella, with Special Reference to its Dependence on Quantity of Available Light and on Temperature. In *Algal Culture From Laboratory to Pilot Plant, John S. Burlew Ed.*; Carnegie Institution of Washington, 1953; p. 357.

(10) Atkins, W. R. G.; Poole, H. H. Photoelectric measurements of the luminous efficiency of daylight. *Soc Lond B Bio* **1936**, *121*, 1–17.

(11) Myers, J. Growth Characteristics of Algae in Relation to the Problems of Mass Culture. In *Algal Culture From Laboratory to Pilot Plant, John S. Burlew Ed.*; Carnegie Institution of Washington, 1953; p. 357.

(12) United States Census 2000 http://www.census.gov/main/www/cen2000.htm.

(13) Gurney, K. R.; Mendoza, D. L.; Zhou, Y.; Fischer, M. L.; Miller, C. C.; Geethakumar, S.; De La Rue Du Can, S. High resolution fossil fuel combustion CO2 emission fluxes for the United States. *Environmental science technology* **2009**, *43*, 5535–5541.

(14) *The 2002 Financial Survey: A National Survey of Municipal Wastewater Management Financing and Trends*; 2002.

(15) PRISM Climate Group - 1981-2010 U.S. Climatology Normals http://www.prism.oregonstate.edu/ (accessed May 13, 2010).

(16) Frank, E. D.; Han, J.; Palou-Rivera, I.; Elgowainy, A.; Wang, M. Q. *Life-Cycle Analysis of Algal Lipid Fuels with the GREET Model*; 2011.

(17) Renouf, M. A.; Wegener, M. K.; Nielsen, L. K. An environmental life cycle assessment comparing Australian sugarcane with US corn and UK sugar beet as producers of sugars for fermentation. *Biomass and Bioenergy* **2008**, *32*, 1144–1155.

(18) Farnsworth, R. K.; Thompson, E. S. *Mean Monthly, Seasonal, and Annual Pan Evaporation for the United States*; Washington, D.C., 1982.

(19) Bolstad, P. *GIS Fundamentals: A first text on geographic information systems*; Third Edit.; Eider Press: White Bear Lake, MN, 2008; p. 620.

(20) Usda National Agricultural Statistics Service http://www.nass.usda.gov/.

(21) NREL US Life Cycle Inventory Database http://www.nrel.gov/lci/.

(22) MACEDO, I.; SEABRA, J.; SILVA, J. Green house gases emissions in the production and use of ethanol from sugarcane in Brazil: The 2005/2006 averages and a prediction for 2020. *Biomass and Bioenergy* **2008**, *32*, 582–595.

(23) Frischknecht, R.; Jungbluth, N.; Althaus, H.-J.; Doka, G.; Dones, R.; Heck, T.; Hellweg, S.; Hischier, R.; Nemecek, T.; Rebitzer, G.; Spielmann, M. The ecoinvent Database: Overview and Methodological Framework (7 pp). *The International Journal of Life Cycle Assessment* **2004**, *10*, 3–9.

(24) Ipcc, I. P. O. C. C. *IPCC Fourth Assessment Report: Climate Change 2007*; Solomon, S.; Qin, D.; Manning, M.; Chen, Z.; Marquis, M.; Averyt, K. B.; Tignor, M.; Miller, H. L., Eds.; Intergovernmental Panel on Climate Change, 2007; Vol. 4, pp. 213–252.

(25) Torcellini, P.; Long, N.; Judkoff, R. Consumptive Water Use for U.S. Power Production. *Contract* **2003**, *110*, 18.

APPENDIX 2. SUPPORTING INFORMATION FOR CHAPTER 3

A2.1 Carbon Accounting

As with all biofuels, the life cycle assessment of algal biodiesel requires close attention to both the biogenic carbon exchanges (i.e. sequestration and natural emissions in fermenters, anaerobic digesters, and farming emissions) and anthropogenic carbon emissions (i.e. from combusting natural gas for process heat or the emissions from the electrical grid and life cycle of other inputs). The waterfall plots shown in Figure A2.1 illustrate this carbon accounting.

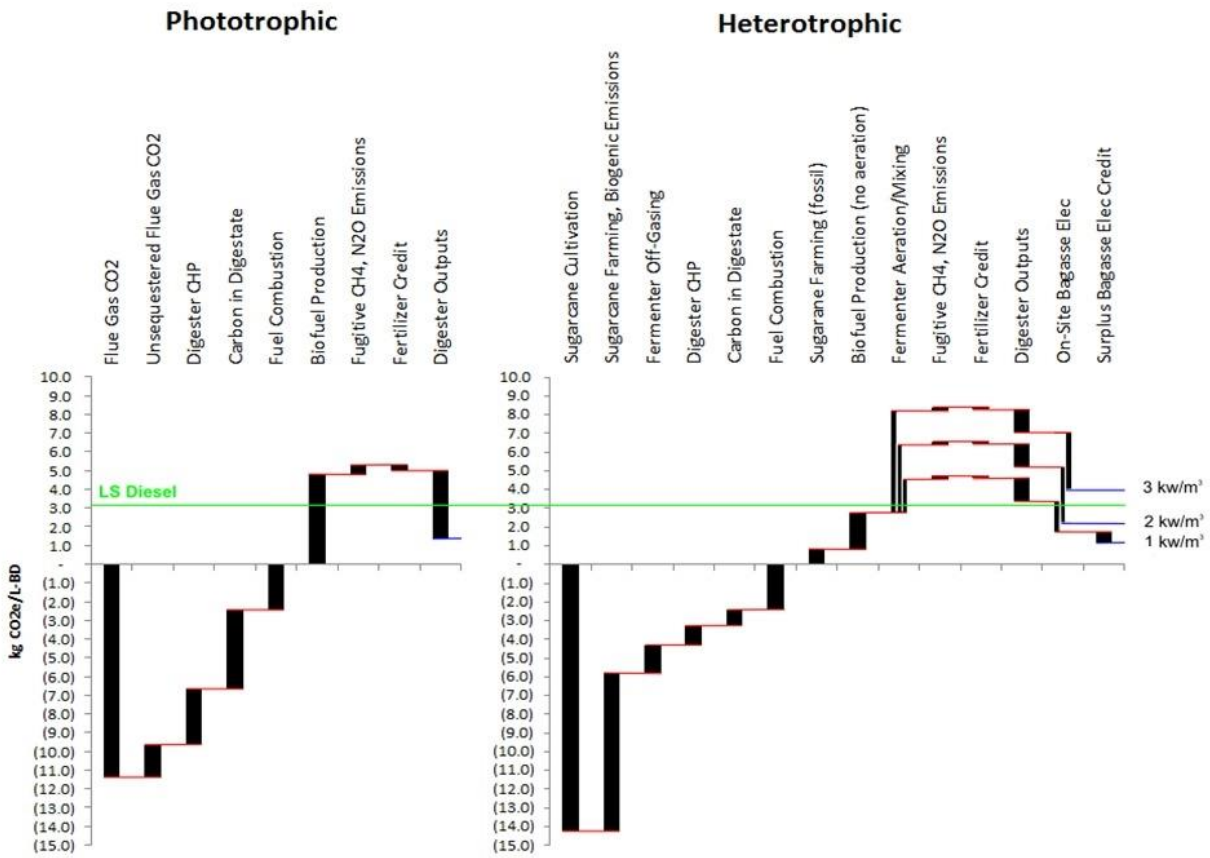

Figure A2.1 - The contributions to the global warming potential (GWP) for two of the three pathways are illustrated in the above waterfall plot. Bars shown in the negative portion of the plots indicate biogenic carbon emissions, which balance to zero upon combustion of the fuel. Bars shown in the positive portion of the plots represent the anthropogenic emissions that contribute to the fuel's net carbon footprint. Three fermenter technology scenarios (1, 2, & 3 kW/m^3 for aeration/mixing) are illustrated for the heterotrophic pathway (right), illustrating the significance of these assumptions on the results. These plots do not include impacts from indirect land use change (ILUC).

A2.2 Elemental Biomass Composition

The composition of the algal biomass is important for a number of reasons. Most importantly, the lipid fraction of the algae determines how much biomass must be cultivated to produce the functional unit of algal biodiesel. A higher lipid fraction therefore implies that less nutrients and infrastructure is required (and hence less upstream embodied and operational energy). Another consequence, however, is that

after the lipid has been extracted there is less lipid extracted algae (LEA) leftover for energy recovery via anaerobic digestion.

The distribution of the macromolecules (protein, carbohydrates, and lipids) was based on Frank et al. (2011) for the phototrophic and heterotrophic biomass (or the "baseline" and "high lipid" scenarios, respectively)[16]. The hybrid scenario, which contains 55% lipid rather than the 50% lipid selected for the heterotrophic biomass, was approximated by keeping the same 1:1 protein to carbohydrate ratio for the non-lipid portion. The macromolecule approximations of $C_{40}H_{74}O_5$ for lipid, $C_{4.43}H_7O_{1.44}N_{1.16}$ for protein, and $C_6H_{12}O_6$ for carbohydrate were based on Lardon et al. (2009)[3]. Although phosphorus is not represented in these formulae, a 10:1 ratio (by mass) of N:P was assumed, as recommended by the authors. A summary of these results is shown in Table A2.1 and Figure A2.2.

Table A2.1 - Biomass composition assumptions for the three pathways.

		Phototrophic	Heterotrophic	Hybrid
Macromolecule Composition				
Lipid:	$C_{40}H_{74}O_5$	25.0%	50.0%	55.0%
Protein:	$C_{4.43}H_7O_{1.44}N_{1.16}$	50.0%	25.0%	22.5%
Carbohydrate:	$C_6H_{12}O_6$	25.0%	25.0%	22.5%
Elemental Composition				
C		54.68%	60.69%	62.18%
H		7.96%	9.18%	9.43%
O		27.59%	25.21%	23.96%
N		7.99%	4.03%	3.63%
P		1.77%	0.89%	0.80%
Total:		**100.00%**	**100.00%**	**100.00%**

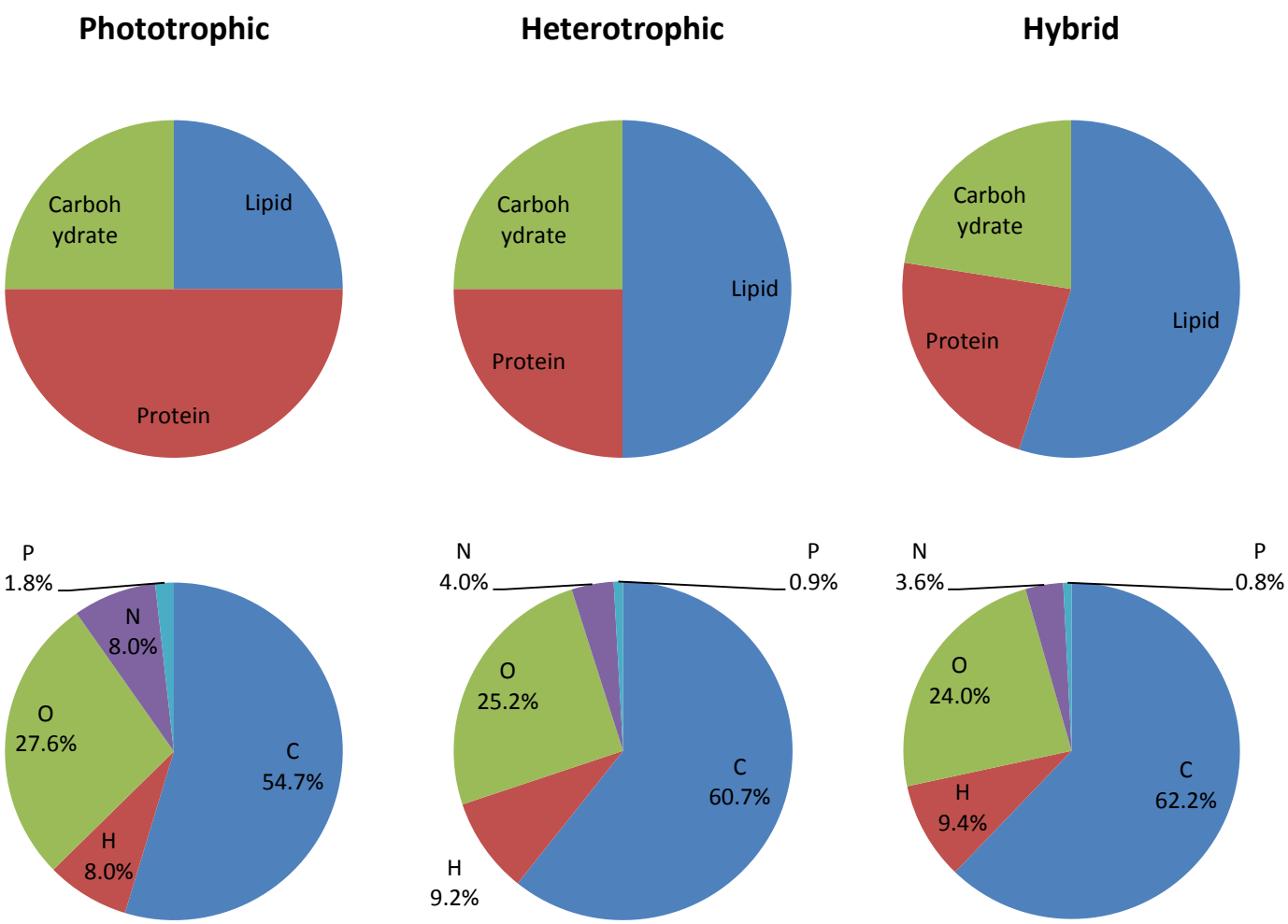

Figure A2.2 - Biomass composition assumptions for the three pathways.

A2.3 Fossil Energy Ratio (FER) Results with Sugar from Sugar Beet

Due to limited space, the primary article content did not display the FER results featuring Sugar Beet at the sugar source. In none of the fermenter aeration/mixing energy requirement scenarios do the heterotrophic or hybrid pathways provide a FER greater than one, as shown in Figure A2.3. Cultivation of sugarcane yields an abundance of bagasse which can be combusted to provide a substantial amount of energy on site; Sugar beet, conversely, does not. It is possible that an animal feed co-product could be

produced from sugar beet residuals, but this possibility was not explored in this analysis [17].

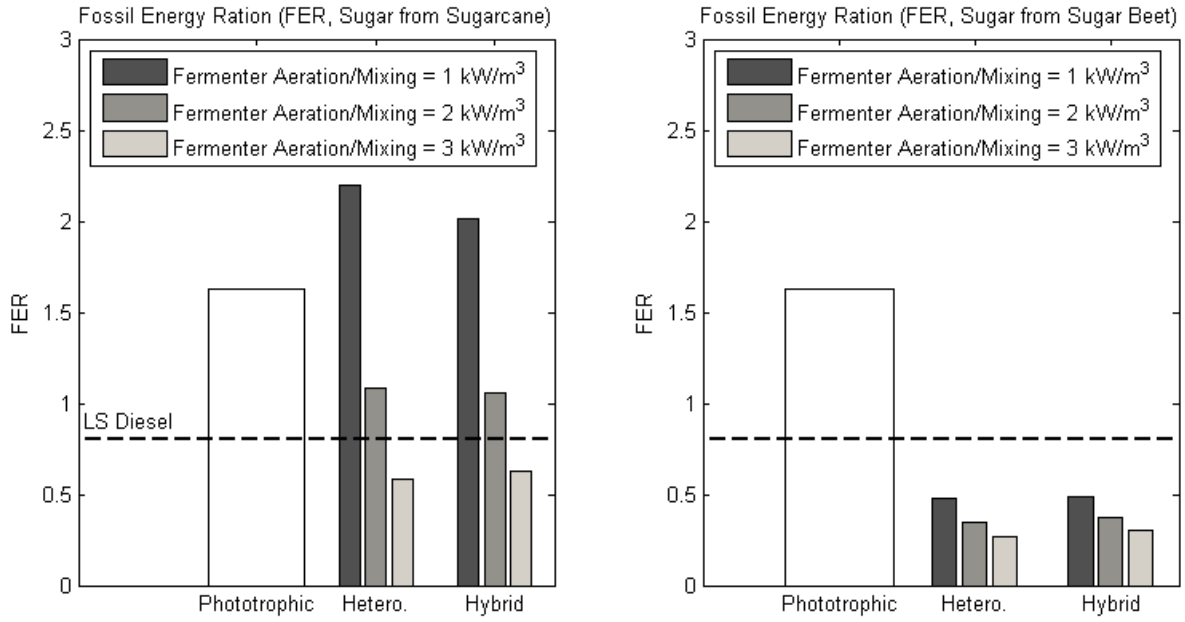

Figure A2.3 - Fossil Energy Ratio (FER) results comparing sugar from sugarcane and sugar beet.

A2.4 Weighting Factors for Phototrophic Pathway

One of the key variables used to determine the water stress impact of the phototrophic pathway is the rate of evaporation, as this determines the amount of make-up water that must be pumped into the pond to maintain the appropriate volume. The national data set used in this analysis was produced by the National Oceanic and Atmospheric Administration[18]. The agency did not provide a continuous coverage layer with predicted evaporation rates but rather reported empirical evaporation data recorded at several hundred weather stations across the country. The locations of these sites were not established systematically, however, and therefore

averaging the results from each of the locations would skew the results toward locations where the concentration of sites is higher. The sites are much closer together on the west coast, for example, than in the southeastern United States. To compensate for this non-uniform distribution, results from each of the sites were weighted according to the area of its Thiessen polygon. This approach assigns a polygon to each evaporation data site such that any location within that polygon is nearer to its associated point than to that of any other polygon[19]. These polygons are shown in Figure A2.4. The sites that are highlighted in red are those that meet the minimum average annual productivity of 20 $g \cdot m^{-2} \cdot day^{-1}$.

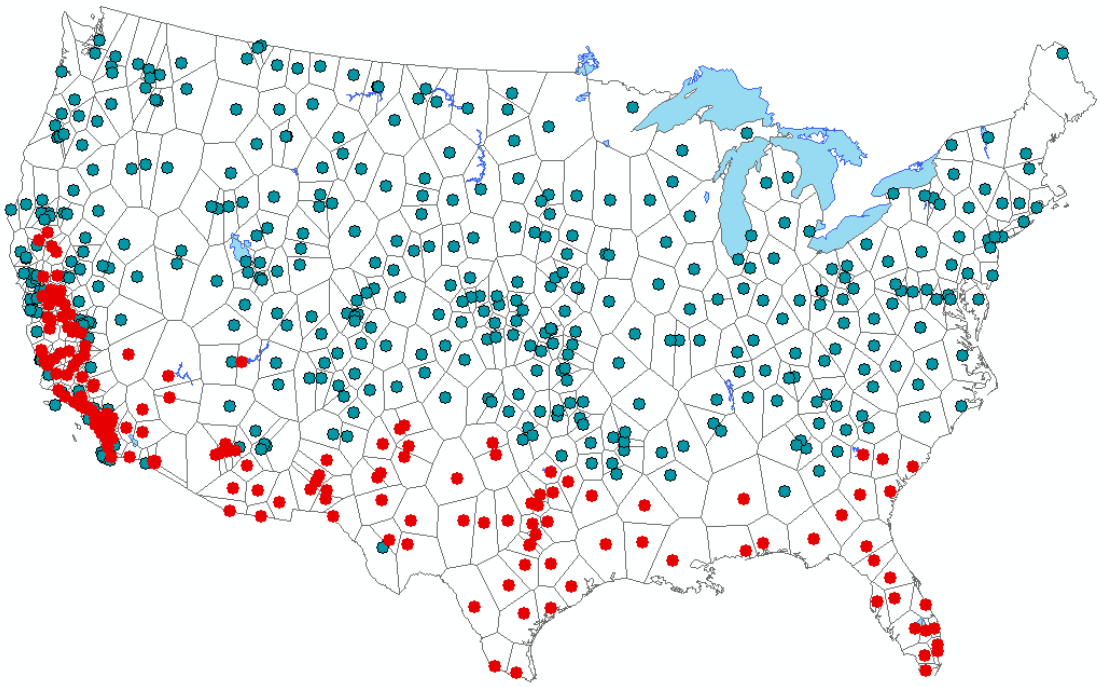

Figure A2.4 - The Thiessen polygons associated with the NOAA evaporation data sites are outlined above, trimmed by the perimeter of the contiguous United States. Locations highlighted in red are those that meet the minimum average annual productivity cut-off of 20 $g \cdot m^{-2} \cdot day^{-1}$.

A2.5 Impact Factors

A summary of the impact factors used in the analysis is included in Table A2.2. Recall that a geographic information systems (GIS) approach was used to explore the regional variations for the land use and water stress impact calculations based on yield data from the National Agricultural Statistics Service [20].

Table A2.2 - Impact factors applied to the inventory of material and energy flows for the three pathways.

Process/Input	Value	Units	Reference
Global Warming Potential			
Electricity, US Grid Average	0.216	Kg CO_2e/MJ	[21]
Sugar, from sugarcane	0.222[α]	Kg CO_2e/kg	[22]
Sugar, from sugar beet	0.505[β]	Kg CO_2e/kg	[23]
N Fertilizer (urea, as N)	3.3	Kg CO_2e/kg	[23]
P Fertilizer for cultivation, (diammonia phosphate, per mass P_2O_5)	1.57	Kg CO_2e/kg	[23]
Methanol	0.556	Kg CO_2e/kg	[21]
Hexane	0.898	Kg CO_2e/kg	[23]
Natural Gas, combusted in industrial equipment	2.4	Kg CO_2e/m^3	[21]
Methane emissions (fugitive), CH_4	25	Kg CO_2e/kg	[24]
Nitrous Oxide emissions (field), N_2O (as N)	298	Kg CO_2e/kg	[24]
Fossil Energy			
Electricity, US Grid Average	3.03	MJ/MJ	[21]
Sugar, from cane	1.834[α]	MJ/kg	[22]
Sugar, from beet	6.49[β]	MJ/kg	[23]
N Fertilizer (urea, as N)	65.4	MJ/kg	[23]
P Fertilizer for cultivation, (diammonia phosphate, per mass P_2O_5)	22.12	MJ/kg	[23]
Methanol	35.44	MJ/kg	[21]
Hexane	60.89	MJ/kg	[23]
Natural Gas, combusted in industrial equipment	42.1	MJ/m_3	[21]
Land Use			
N Fertilizer (urea, as N)	0.0856	m^2/kg	[23]
P Fertilizer for cultivation, (diammonia phosphate, per mass P_2O_5)	0.115	m^2/kg	[23]
Water Use			
Water consumption for electricity generation.	2.1[γ]	L/MJ	[25]

[α]Adapted from the year 2020 scenario.

[β]Sugar from sugar beet was modeled based on a refinery in Switzerland.

[γ]National weighted average for thermoelectric and hydroelectric power in the United States.

A2.6 Inventory Tables

Table A2.3 - A summary of the inventory of inputs required for the three pathways to produce 5 million liters of algal biodiesel annually. This table reflects the 1 kW/m^3 fermenter aeration/mixing scenario with sugarcane as the feedstock. Recall that water inputs and land requirements were calculated independently based on a GIS analysis.

		Units	Seed Train	Pond Growth	Dewatering	Fermenter Growth	Cell Separation	Oil Conversion	Digester Operation	Digester Output	Excess Bagasse Cogeneration Used Onsite	Total
PHOTOTROPHIC	Electrical Energy	MJ	-	21,772,622	21,719,608	-	14,711,782	470,725	13,948,774	(60,657,624)	-	11,965,886
	Heat Energy	MJ	-	-	-	-	48,989,207	9,087,036	15,597,104	(79,038,722)	-	-
	Sugar	kg	-	-	-	-	-	-	-	-	-	-
	N Fertilizer (Urea, as N)	kg	-	462,357	-	-	-	-	-	-	-	462,357
	P Fertilizer	kg P2O5	-	488,753	-	-	-	-	-	-	-	488,753
	Methanol	kg	-	-	-	-	-	440,392	-	-	-	440,392
	Hexane	kg	-	-	-	-	22,900	-	-	-	-	22,900
	Natural Gas	m3	-	-	-	-	1,628,089	301,995	518,348	(2,232,732)	-	215,701
HETEROTROPHIC	Electrical Energy	MJ	8,902,872	-	3,708,564	33,388,668	7,902,858	470,725	4,177,304	(20,698,088)	(37,852,902)	-
	Heat Energy	MJ	-	-	-	-	48,989,207	9,087,036	4,670,937	(26,970,236)	-	35,776,943
	Sugar	kg	5,150,784	-	-	15,452,351	-	-	-	-	-	20,603,135
	N Fertilizer (Urea, as N)	kg	24,887	-	-	99,548	-	-	-	-	-	124,435
	P Fertilizer	kg P2O5	26,308	-	-	105,232	-	-	-	-	-	131,539
	Methanol	kg	-	-	-	-	-	440,392	-	-	-	440,392
	Hexane	kg	-	-	-	-	22,900	-	-	-	-	22,900
	Natural Gas	m3	-	-	-	-	1,628,089	301,995	155,232	(761,871)	-	1,323,446
MIXOTROPHIC	Electrical Energy	MJ	-	2,410,049	13,895,527	33,388,668	7,902,858	470,725	4,177,304	(20,698,088)	(41,547,041)	-
	Heat Energy	MJ	-	-	-	-	48,989,207	9,087,036	4,670,937	(26,970,236)	-	35,776,943
	Sugar	kg	-	-	-	18,027,743	-	-	-	-	-	18,027,743
	N Fertilizer (Urea, as N)	kg	-	89,659	-	-	-	-	-	-	-	89,659
	P Fertilizer	kg P2O5	-	94,777	-	-	-	-	-	-	-	94,777
	Methanol	kg	-	-	-	-	-	440,392	-	-	-	440,392
	Hexane	kg	-	-	-	-	22,900	-	-	-	-	22,900
	Natural Gas	m3	-	-	-	-	1,628,089	301,995	155,232	(761,871)	-	1,323,446

Table A2.4 A summary of the inventory of inputs required for the three pathways to produce 5 million liters of algal biodiesel annually. This table reflects the 2 kW/m^3 fermenter aeration/mixing scenario with sugarcane as the feedstock. Recall that water inputs and land requirements were calculated independently based on a GIS analysis.

		Units	Seed Train	Pond Growth	Dewatering	Fermenter Growth	Cell Separation	Oil Conversion	Digester Operation	Digester Output	Excess Bagasse Cogeneration Used Onsite	Total
PHOTOTROPHIC	Electrical Energy	MJ	-	21,772,622	21,719,608	-	14,711,782	470,725	13,948,774	(60,657,624)	-	11,965,886
	Heat Energy	MJ	-	-	-	-	48,989,207	9,087,036	15,597,104	(79,038,722)	-	-
	Sugar	kg	-	-	-	-	-	-	-	-	-	-
	N Fertilizer (Urea, as N)	kg	-	462,357	-	-	-	-	-	-	-	462,357
	P Fertilizer	kg P2O5	-	488,753	-	-	-	-	-	-	-	488,753
	Methanol	kg	-	-	-	-	-	440,392	-	-	-	440,392
	Hexane	kg	-	-	-	-	22,900	-	-	-	-	22,900
	Natural Gas	m3	-	-	-	-	1,628,089	301,995	518,348	(2,232,732)	-	215,701
HETEROTROPHIC	Electrical Energy	MJ	17,803,426	-	3,708,564	66,765,746	7,902,858	470,725	4,177,304	(20,698,088)	(70,158,322)	9,972,212
	Heat Energy	MJ	-	-	-	-	48,989,207	9,087,036	4,670,937	(26,970,236)	-	35,776,943
	Sugar	kg	5,150,784	-	-	15,452,351	-	-	-	-	-	20,603,135
	N Fertilizer (Urea, as N)	kg	24,887	-	-	99,548	-	-	-	-	-	124,435
	P Fertilizer	kg P2O5	26,308	-	-	105,232	-	-	-	-	-	131,539
	Methanol	kg	-	-	-	-	-	440,392	-	-	-	440,392
	Hexane	kg	-	-	-	-	22,900	-	-	-	-	22,900
	Natural Gas	m3	-	-	-	-	1,628,089	301,995	155,232	(761,871)	-	1,323,446
MIXOTROPHIC	Electrical Energy	MJ	-	2,410,049	13,895,527	66,765,746	7,902,858	470,725	4,177,304	(20,698,088)	(61,388,532)	13,535,588
	Heat Energy	MJ	-	-	-	-	48,989,207	9,087,036	4,670,937	(26,970,236)	-	35,776,943
	Sugar	kg	-	-	-	18,027,743	-	-	-	-	-	18,027,743
	N Fertilizer (Urea, as N)	kg	-	89,659	-	-	-	-	-	-	-	89,659
	P Fertilizer	kg P2O5	-	94,777	-	-	-	-	-	-	-	94,777
	Methanol	kg	-	-	-	-	-	440,392	-	-	-	440,392
	Hexane	kg	-	-	-	-	22,900	-	-	-	-	22,900
	Natural Gas	m3	-	-	-	-	1,628,089	301,995	155,232	(761,871)	-	1,323,446

Table A2.5 - A summary of the inventory of inputs required for the three pathways to produce 5 million liters of algal biodiesel annually. This table reflects the 3 kW/m^3 fermenter aeration/mixing scenario with sugarcane as the feedstock. Recall that water inputs and land requirements were calculated independently based on a GIS analysis.

		Units	Seed Train	Pond Growth	Dewatering	Fermenter Growth	Cell Separation	Oil Conversion	Digester Operation	Digester Output	Excess Bagasse Cogeneration Used Onsite	Total
PHOTOTROPHIC	Electrical Energy	MJ	-	21,772,622	21,719,608	-	14,711,782	470,725	13,948,774	(60,657,624)	-	11,965,886
	Heat Energy	MJ	-	-	-	-	48,989,207	9,087,036	15,597,104	(79,038,722)	-	-
	Sugar	kg	-	-	-	-	-	-	-	-	-	-
	N Fertilizer (Urea, as N)	kg	-	462,357	-	-	-	-	-	-	-	462,357
	P Fertilizer	kg P2O5	-	488,753	-	-	-	-	-	-	-	488,753
	Methanol	kg	-	-	-	-	-	440,392	-	-	-	440,392
	Hexane	kg	-	-	-	-	22,900	-	-	-	-	22,900
	Natural Gas	m3	-	-	-	-	1,628,089	301,995	518,348	(2,232,732)	-	215,701
HETEROTROPHIC	Electrical Energy	MJ	26,703,980	-	3,708,564	100,142,824	7,902,858	470,725	4,177,304	(20,698,088)	(70,158,322)	52,249,845
	Heat Energy	MJ	-	-	-	-	48,989,207	9,087,036	4,670,937	(26,970,236)	-	35,776,943
	Sugar	kg	5,150,784	-	-	15,452,351	-	-	-	-	-	20,603,135
	N Fertilizer (Urea, as N)	kg	24,887	-	-	99,548	-	-	-	-	-	124,435
	P Fertilizer	kg P2O5	26,308	-	-	105,232	-	-	-	-	-	131,539
	Methanol	kg	-	-	-	-	-	440,392	-	-	-	440,392
	Hexane	kg	-	-	-	-	22,900	-	-	-	-	22,900
	Natural Gas	m3	-	-	-	-	1,628,089	301,995	155,232	(761,871)	-	1,323,446
MIXOTROPHIC	Electrical Energy	MJ	-	2,410,049	13,895,527	100,142,824	7,902,858	470,725	4,177,304	(20,698,088)	(61,388,532)	46,912,666
	Heat Energy	MJ	-	-	-	-	48,989,207	9,087,036	4,670,937	(26,970,236)	-	35,776,943
	Sugar	kg	-	-	-	18,027,743	-	-	-	-	-	18,027,743
	N Fertilizer (Urea, as N)	kg	-	89,659	-	-	-	-	-	-	-	89,659
	P Fertilizer	kg P2O5	-	94,777	-	-	-	-	-	-	-	94,777
	Methanol	kg	-	-	-	-	-	440,392	-	-	-	440,392
	Hexane	kg	-	-	-	-	22,900	-	-	-	-	22,900
	Natural Gas	m3	-	-	-	-	1,628,089	301,995	155,232	(761,871)	-	1,323,446

Table A2.6 - A summary of the annual outputs for the three pathways assuming sugarcane is the feedstock.

			Aeration/Mixing Energy Scenario:		
		Units	**1 kW/m3**	**2 kW/m3**	**3 kW/m3**
PHOTOTROPHIC	Fugitive Methane	kg CH4	73,524	73,524	73,524
	Fugitive N2O	kg N2O-N	1,228	1,228	1,228
	Biodiesel	Liters	**5,000,000**	**5,000,000**	**5,000,000**
	N Fertilizer from Residue	kg N	122,831	122,831	122,831
	P2O5 Fertilizer from Residue	kg P2O5	396,440	396,440	396,440
	CO2 from biogas combustion	kg CO2	15,157,619	15,157,619	15,157,619
	CO2 from fermenter	kg CO2	-	-	-
	Bagasse Elec Generation (consumed on site)	MJ	-	-	-
	Surplus Bagasse Elec Generation	MJ	-	-	-
HETEROTROPHIC	Fugitive Methane	kg CH4	25,089	25,089	25,089
	Fugitive N2O	kg N2O-N	419	419	419
	Biodiesel	Liters	**5,000,000**	**5,000,000**	**5,000,000**
	N Fertilizer from Residue	kg N	41,913	41,913	41,913
	P2O5 Fertilizer from Residue	kg P2O5	135,276	135,276	135,276
	CO2 from biogas combustion	kg CO2	5,172,206	5,172,206	5,172,206
	CO2 from fermenter	kg CO2	7,292,813	7,292,813	7,292,813
	Bagasse Elec Generation (consumed on site)	MJ	70,158,322	70,158,322	70,158,322
	Surplus Bagasse Elec Generation	MJ	32,305,420	-	-
MIXOTROPHIC	Fugitive Methane	kg CH4	25,089	25,089	25,089
	Fugitive N2O	kg N2O-N	419	419	419
	Biodiesel	Liters	**5,000,000**	**5,000,000**	**5,000,000**
	N Fertilizer from Residue	kg N	41,913	41,913	41,913
	P2O5 Fertilizer from Residue	kg P2O5	135,276	135,276	135,276
	CO2 from biogas combustion	kg CO2	5,172,206	5,172,206	5,172,206
	CO2 from fermenter	kg CO2	8,117,543	8,117,543	8,117,543
	Bagasse Elec Generation (consumed on site)	MJ	61,388,532	61,388,532	61,388,532
	Surplus Bagasse Elec Generation	MJ	19,841,490	-	-

Table A2.7 – Sensitivity of net energy ratio (NER) results to open pond algae yield and heterotrophic cultivation batch length. Results are unitless.

Scenario	Yield (pond growth)	Batch Length (fermenter growth)	Photo.	Heterotrophic			Hybrid		
				1 $kw \cdot m^{-3}$	2 $kw \cdot m^{-3}$	3 $kw \cdot m^{-3}$	1 $kw \cdot m^{-3}$	2 $kw \cdot m^{-3}$	3 $kw \cdot m^{-3}$
Low	12.5 $g \cdot m^{-2} \cdot day^{-1}$	4 days	1.05	1.66	1.48	0.95	1.69	1.55	1.10
Baseline	25 $g \cdot m^{-2} \cdot day^{-1}$	3 days	1.54	1.59	1.12	0.60	1.62	1.09	0.66
High	37.5 $g \cdot m^{-2} \cdot day^{-1}$	2 days	1.82	1.53	0.77	0.44	1.53	0.74	0.46

Table A2.8 – Sensitivity of global warming potential (GWP) results to open pond algae yield and heterotrophic cultivation batch length. Results are in units of kg $CO_2e \cdot L^{-1}$.

Scenario	Yield (pond growth)	Batch Length (fermenter growth)	Photo.	Heterotrophic			Hybrid		
				1 $kw \cdot m^{-3}$	2 $kw \cdot m^{-3}$	3 $kw \cdot m^{-3}$	1 $kw \cdot m^{-3}$	2 $kw \cdot m^{-3}$	3 $kw \cdot m^{-3}$
Low	12.5 $g \cdot m^{-2} \cdot day^{-1}$	4 days	2.14	1.42	1.63	2.50	1.38	1.53	2.13
Baseline	25 $g \cdot m^{-2} \cdot day^{-1}$	3 days	1.46	1.48	2.14	3.86	1.45	2.16	3.52
High	37.5 $g \cdot m^{-2} \cdot day^{-1}$	2 days	1.23	1.56	3.05	5.22	1.54	3.14	4.95

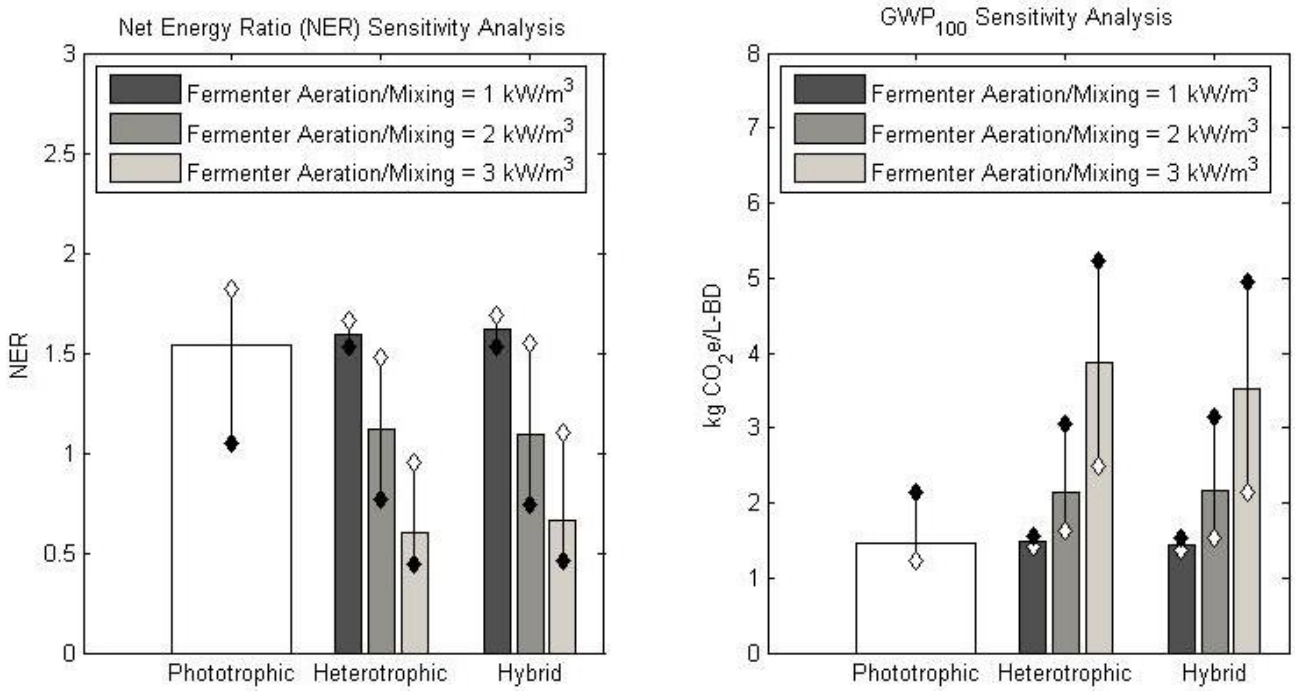

Figure A2.5 - Results of additional sensitivity analyses. The high performance scenario is marked with a white diamond, while the low performance scenario is marked with a black diamond.

A2.7 Works Cited

[1] Frank, E. D.; Han, J.; Palou-Rivera, I.; Elgowainy, A.; Wang, M. Q. Life-Cycle Analysis of Algal Lipid Fuels with the GREET Model. *Center for Transportation Research, Energy Systems Division, Argonne National Laboratory, Oak Ridge*, **2011**.

[2] Lardon, L.; Hélias, A.; Sialve, B.; Steyer, J.-P.; Bernard, O. Life-Cycle Assessment of Biodiesel Production from Microalgae. *Environ. Sci. Technol.* **2009**, *43*(17), 6475-6481.

[3] Renouf, M. A.;Wegener, M. K.;Nielsen, L. K. An environmental life cycle assessment comparing Australian sugarcane with US corn and UK sugar beet as producers of sugars for fermentation, *Biomass Bioenergy* **2008**, *32*(12), 1144–1155.

[4] Farnsworth, R. K.; Thompson, E. S. Mean Monthly, Seasonal, and Annual Pan Evaporation for the United States. US Department of Commerce, National Oceanic and Atmospheric Administration, National Weather Service, 1982.

[5] Bolstad,P . *GIS Fundamentals: A first text on geographic information systems, Third Edit.* Eider Press: White Bear Lake, MN, 2008.

[6] NASS, USDA. "National Agricultural Statistics Service." US and State Level Crop Production Historical Data (2005).

[7] NREL, *US Life Cycle Inventory Database*, National Renewable Energy Laboratory: Golden CO, 2011, http://www.nrel.gov/lci/.

[8] Macedo, I.; Seabra, J.; Silva, J. Greenhouse gases emissions in the production and use of ethanol from sugarcane in Brazil: The 2005/2006 averages and a prediction for 2020. *Biomass Bioenergy* **2008**, *32*(7), 582-595.

[9] Frischknecht, R.;Jungbluth, N.;Althaus,H.J.; Doka, G.;Dones, R.; Heck, T.; Hellweg, S.; Hischier, R.; Nemecek, T.; Rebitzer, G.; Spielmann, M. The ecoinvent Database: Overview and Methodological Framework . *The International Journal of Life Cycle Assessment* **2005**, *10*(1), 3-9.

[10] Solomon, S. Ed. *Climate change 2007-the physical science basis: Working group I contribution to the fourth assessment report of the IPCC (Vol. 4).* Cambridge University Press, 2007.

[11] Torcellini, P.; Long, N.; Judkoff, R.Consumptive Water Use for U.S. Power Production, 2003.

APPENDIX 3. SUPPORTING INFORMATION FOR CHAPTER 4

Table A3.1 - A summary of the financial model implemented in the analysis, adapted from Davis et al. (2012) to distinguish costs that scale based on algal biomass, pond size, and oil produced.

Table Data Adapted from Davis et al. (2012) - Numbers are based on a 10.4 million gallons oil/year facility			Derivative Values Implemented in Model		
DIRECT CAPITAL COSTS	**Cost ($MM)**	Note	**$/kg algal biomass**	**$/ha**	**$/L-Oil**
Ponds & paddle wheels	$ 138.6			$ 3,178	
Pond liners	$ 205.2			$ 4,705	
Flue gas delivery & distribution	$ 38.7		$ 0.018		
Water delivery & distribution	$ 3.7			$ 85	
Primary harvesting (settling)	$ 47.0			$ 1,078	
Secondary harvesting (DAF)	$ 1.7		$ 0.001		
Tertiary harvesting (centrifuge)	$ 4.4		$ 0.002		
HTL reactor - Adapted from: Kasteren et al. (2007)	$ 4.1	1	$ 0.002		
Solvent extraction (LLE column, centrifuge, solvent stripper)	n/a				
Land costs	$ 35.9			$ 192	
Gasification - Adapted from Santosa et al. (2009)	$ 16.5	2	$ 0.003		
Gen-Set - Using equation in Peters et al. (1968)	$ 6.2	3	$ 0.001		
Inoculum production system	$ 50.2		$ 0.024		
Steam boiler	$ 1.0		$ 0.000		
Water pumps	$ 13.2		$ 0.006		
Initial water charge	$ -		$ -		
Total Installed Depreciable Capital	**$ 530.5**				
Total Installed Non-Depreciable Capital	**$ 35.9**				
Total Installed Capital	**$ 566.4**				
INDIRECT CAPITAL COSTS	**Cost ($MM)**				
Site development	$ 12.9			$ 296	
Warehouse	$ 4.9		$ 0.002		
Total Direct Costs	**$ 548.3**				
Pro-rateable costs	$ 56.0		$ 0.006		
Field expenses	$ 56.0		$ 0.026		
Home office and construction	$ 56.0		$ 0.026		
Contingency	$ 112.0		$ 0.012		
Other costs	$ 28.0		$ 0.003		
Total Indirect Costs	**$ 308.0**				
Fixed Capital Investment	**$ 856.3**				
Working Capital	$ 43.4		$ 0.020		
Total Capital Investment	**$ 935.6**				
OPERATING COSTS	**Cost ($MM/year)**				
Power	calc. separately				
Nutrients (N,P)	calc. separately				
Flocculant	$ 8.3		$ 0.027		
Solvent (extraction)	n/a				
Waste disposal	$ -		$ -		
Utilities	$ -		$ -		
Labor and overhead	$ 8.2			$ 1,316	
Maintenance, tax, insurance	$ 19.2		$ 0.063		
Net Operating Costs	**$ 35.7**				
HYDROTREATING UPGRADING COSTS	**Cost ($/gallon)**				
Hydrotreating total cost per gallon of oil	$ 1.382				$ 0.365
Total Upgrading Costs	**$ 1.382**				

1 - Van Kasteren, J. M. N., & Nisworo, A. P. (2007). A process model to estimate the cost of industrial scale biodiesel production from waste cooking oil by supercritical transesterification. Resources, Conservation and Recycling, 50(4), 442-458.

2 - Santosa, D. M., Valkenburg, C., Jones, S. B., & Tjokro Rahardjo, S. A. (2009). Catalytic hydrothermal gasification of lignin-rich biorefinery residues and algae. Richland, WA: Pacific Northwest National Laboratory.

3 - Peters, M. S., Timmerhaus, K. D., West, R. E., Timmerhaus, K., & West, R. (1968). Plant design and economics for chemical engineers (Vol. 4). New York: McGraw-Hill.

Adapted From:

Davis, R.; Fishman, D.; Frank, E. D.; Wigmosta, M. S.; Aden, A.; Coleman, A. M.; Pienkos, P. T.; Skaggs, R. J.; Venteris, E. R.; Wang, M. Q. Renewable Diesel from Algal Lipids: An Integrated Baseline for Cost, Emissions, and Resource Potential from a Harmonized Model; Argonne, IL, 2012; p. 85.

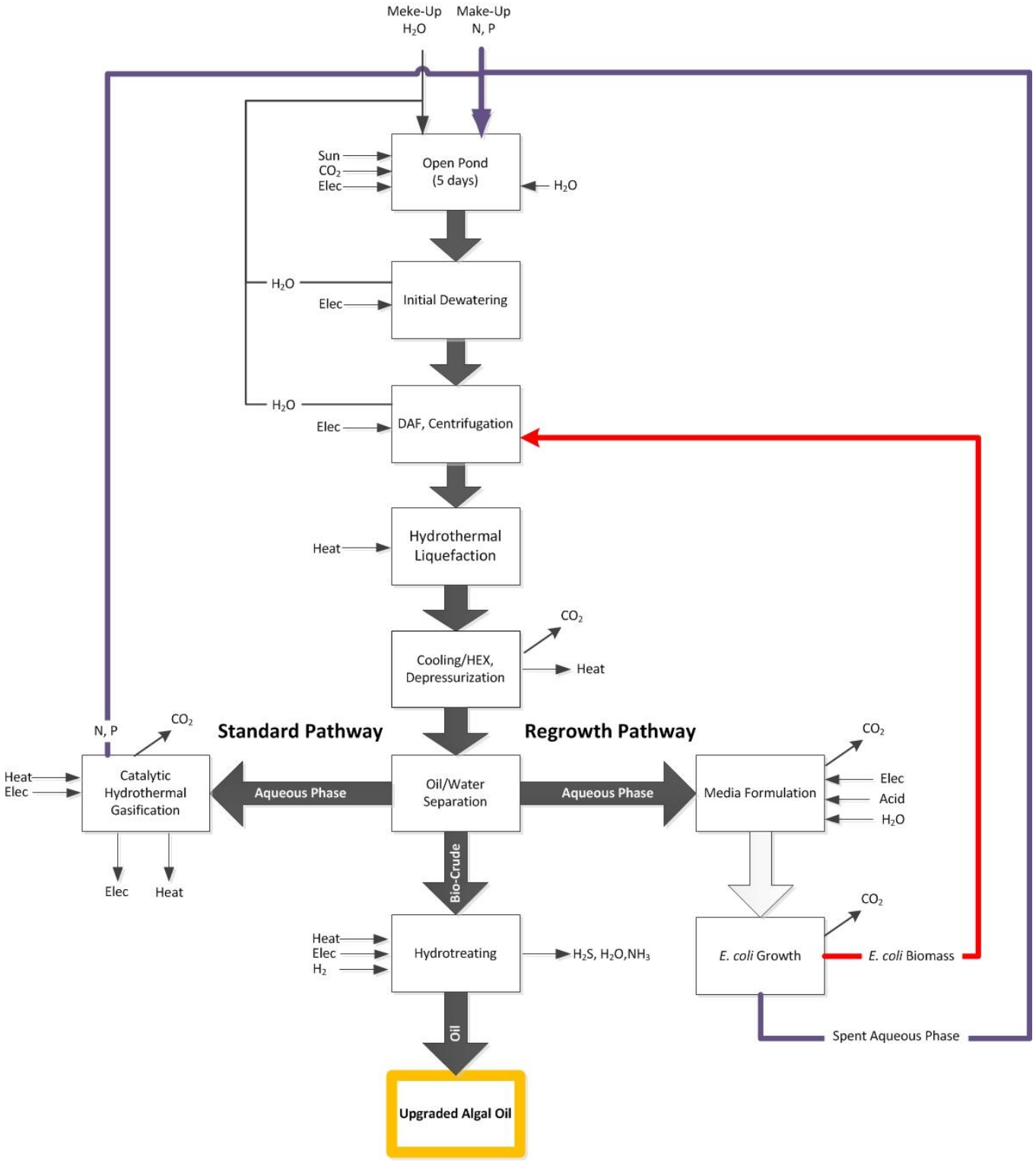

Figure A3.1 - A summary of the processes and inputs/outputs considered for the standard and regrowth pathway.

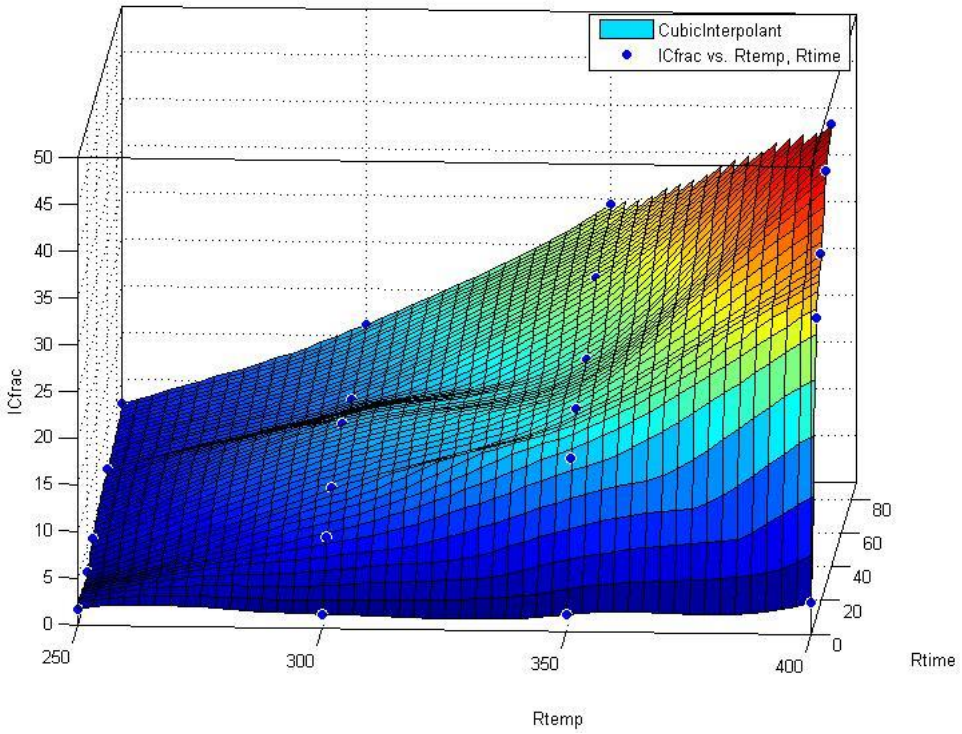

Figure A3.2 - The cubic interpolant curve that was fit to the experimental data using MATLAB© to predict the fraction of organic vs. inorganic carbon across the design space.

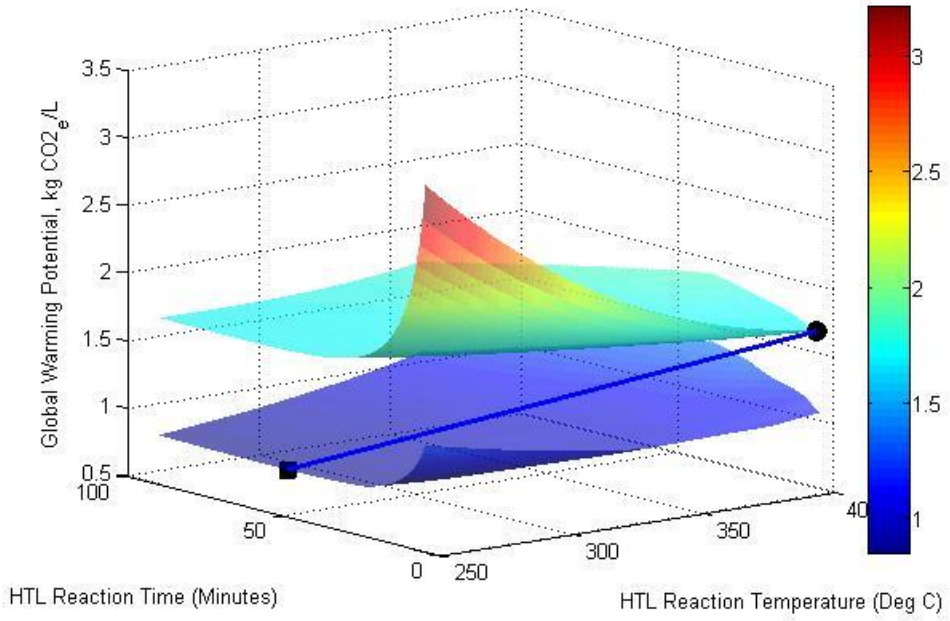

Figure A3.3 - A comparison of Global Warming Potential (GWP) results for the standard pathway (the surface marked with a square at the optimal conditions) to the regrowth pathway (marked with a circle) across the full range of reaction conditions considered in the analysis. A line connects the optimal points on both surfaces for clarity.

Monte Carlo Sensitivity Analysis Parameters

Table A3.2 - A list of the low, high, and median values used in the 10,000 trial Monte Carlo Simulation.

Low	Median	High	Parameter	Unit	Sources
25	48	83	Paddle Energy	kWh/ha/day	1
0.75	0.85	0.95	CO2 Uptake Eff	%	1
0.06	0.21	0.36	Make-Up H2O	m^3/kg	2
0	0.000123	0.000246	To-Site Pumping	kWh/L	3
0	2.12E-05	4.24E-05	CO2 transport	kWh/g CO2	1
6.2	13.2	50	Biomass Yield	g/m^2/day	3,4
0	0.000025	0.00005	Pumping Energy (on site)	kWh/L	3
0	0.0193	0.0386	Centrifugation	kWh/kg algae	3
0	0.133	0.266	DAF Energy	kWh/kg algae	3
250	330	350	Days of Operation	days/year	3
0.009273	0.03175	0.056	H2 Demand	g H2/g biocrude	5-7
0.8	0.95	0.99	Organic Carbon Utilized by CHG	%	8-10
0.28	0.33	0.38	CHP Electricity Efficiency	%	1

(1) Frank, E. D.; Han, J.; Palou-Rivera, I.; Elgowainy, A.; Wang, M. Q. Life-Cycle Analysis of Algal Lipid Fuels with the GREET Model; 2011.

(2) Orfield, N.; Keoleian, G.; Love, N. A GIS based national assessment of algal biofuel production potential through flue gas and wastewater co-utilization. Biomass and Bioenergy 2013.

(3) Davis, R.; Fishman, D.; Frank, E. D.; Wigmosta, M. S.; Aden, A.; Coleman, A. M.; Pienkos, P. T.; Skaggs, R. J.; Venteris, E. R.; Wang, M. Q. Renewable Diesel from Algal Lipids: An Integrated Baseline for Cost, Emissions, and Resource Potential from a Harmonized Model; Argonne, IL, 2012; p. 85.

(4) Davis, R.; Aden, A.; Pienkos, P. T. Techno-economic analysis of autotrophic microalgae for fuel production. Applied Energy 2011, 88, 3524–3531.

(5) Duan, P.; Savage, P. E. Upgrading of crude algal bio-oil in supercritical water. Bioresource Technology 2011, 102, 1899–906.

(6) Li, Z.; Savage, P. E. Feedstocks for fuels and chemicals from algae: Treatment of crude bio-oil over HZSM-5. Algal Research 2013, 2, 154–163.

(7) Frank, E. D.; Elgowainy, A.; Han, J.; Wang, Z. Life cycle comparison of hydrothermal liquefaction and lipid extraction pathways to renewable diesel from algae. Mitigation and Adaptation Strategies for Global Change 2012.

(8) Boukis, N.; Diem, V.; Dinjus, E.; Galla, U.; Kruse, A. Biomass Gasification in Supercritical Water. In 12th European Conference on Biomass for Energy, Industry, and Climate Protection; Amsterdam, The Netherlands, 2002.

(9) Kruse, A. Hydrothermal biomass gasification. J Supercrit Fluids 2009, 47, 391–399.

(10) Genifuel Corporation http://www.genifuel.com.